Spring 2015

Biophysical effects of ultrasound therapy for cartilage regeneration and microbubble mediated shock waves and drug release control for cancer treatment

Kee Woong Jang
University of Iowa

BIOPHYSICAL EFFECTS OF ULTRASOUND THERAPY FOR CARTILAGE REGENERATION AND MICROBUBBLE MEDIATED SHOCK WAVES AND DRUG RELEASE CONTROL FOR CANCER TREATMENT

by

Kee Woong Jang

A thesis submitted in partial fulfillment of the
requirements for the Doctor of Philosophy
degree in Biomedical Engineering
in the Graduate College of
The University of Iowa

May 2015

Thesis Supervisor: Associate professor James A. Martin

Graduate College
The University of Iowa
Iowa City, Iowa

CERTIFICATE OF APPROVAL

PH.D. THESIS

This is to certify that the Ph.D. thesis of

Kee Woong Jang

has been approved by the Examining Committee for the thesis requirement for the Doctor of Philosophy degree in Biomedical Engineering at the May 2015 graduation.

Thesis Committee:

James A. Martin, Thesis Supervisor

Tae-Hong Lim

Edwin L. Dove

Joseph M. Reinhardt

Edward Sander

To my wife, Ah-young

ACKNOWLEDGEMENTS

My experiences in graduate studies have been challenging and valuable venture at the University of Iowa. A lot of people have provided me with indispensable support, guidance and encouragement over the years and now I would like to show my appreciation to them.

I would first like to express my gratitude to Dr. James A. Martin who was my research supervisor providing me a valuable opportunity to study at the Ponseti Biochemistry and Cell Biology lab. in the Department of Orthopaedics and Rehabilitation and indispensable continuous encouragement and motivation for my study. I would also like to show my gratitude to Dr. Tae-hong Lim, who was my academic advisor, providing me critical advices and guidance of my study. I would also like to show my gratitude to other members of my thesis committee, Drs. Edwin L. Dove, Joseph M. Reinhardt and Edward Sander for their guidance and perspectives.

My research could not be completed without laboratory colleagues. I would like to thank Lei Ding, Dongrim Seol, Babara J. Laughlin, Hyounghun Choe, Abigail D. Smith, Yin Yu, Cheng Zhou, John F. Bierman, Gail L. Kurriger, Hongjun Zheng, Marc J. Brouillette and other lab members.

Last but not least, I would like to thank to my parents and families praying for me with incredible love and supports. Most importantly, I would like to show my deepest appreciation to my wife, Ah-young Shin, and my son, Yoon Ho Jang, with my never ending love.

ABSTRACT

Articular cartilage is a complex soft tissue covering the end of moving bones in joints which provide pressure load distribution over the joint surface and smooth lubrication with little friction for establishing movement. Articular cartilage has an intrinsically limited capacity for self-repair when injured due to the lack of nerve and blood supply. Considered that injured cartilage is left untreated, it is likely to undergo progressive cartilage degeneration without pain which may lead to posttraumatic osteoarthritis. Therefore functional and physiologic restoration of injured cartilage back to a normal condition has long been in demand, yet current available repairing methods in clinics have met with limited success. Mechanically applied loads to articular cartilage is necessary for chondrocytes, cartilage cells, since they are responsible for cartilage matrix turnover by synthesizing extracellular matrix (ECM) molecules in response to bio- chemical and mechanical changes in ECM.

Ultrasound has emerged as an anabolic stimulator over the past few decades and a number of studies have proven that ultrasound therapy is beneficial for cartilage repair by synthesizing cartilage ECM components such as type II collagen and proteoglycan. Ultrasound therapy has also proven its potential for the attenuation of progressive cartilage degradation and induction of chondrogenic differentiation of mesenchymal stem cells. The use of ultrasound as an anabolic stimulator would be valuable with respect to cartilage repair since ultrasound as a form of mechanical energy can be non-invasively transferred into

a human body. However, understanding the underlying mechanisms has been slow and the mechanisms have been roughly classified into thermal and non-thermal effects. Biologically detailed underlying mechanisms have not been sufficiently studied. That might be the reason why the application of ultrasound as a therapeutic tool has been limitedly available in clinics. In this study, mechanism involved biophysical effects of low intensity ultrasound has been studied for cartilage regeneration. First of all, the effect of ultrasound therapy as a mechanical stimulator on chondrogenic progenitor cell homing toward injured sites in cartilage was investigated with underlying biologic mechanisms. And the feasibility of ultrasound therapy for reactive oxygen species production mediated cartilage energy modulation was evaluated.

There have been extensive preclinical studies about the effects of microbubble mediated ultrasound therapy on the targeted drugs or gene delivery into tissues of interest. Mechanical shock waves are released during ultrasound mediated microbubble destruction and the waves facilitate drug delivery into target tissues through transient blood vessel disruption. However, the clinical use of this technique has been limited through vascular system. In this study, the effects of microbubble mediated low intensity ultrasound therapy on directly delivered mechanical shock waves and controlled drug release were investigated.

In conclusion, low intensity ultrasound therapy accelerates the homing of chondrogeic progenitor cells toward injured sites in cartilage *via* triggering mechanotransductive cell signaling pathways. This may result in speed up the return to normal cellularity and cartilage integrity by accelerating cartilage

matrix repair. Low intensity ultrasound therapy was investigated as an energy modulator for chondrocytes *via* reactive oxygen species production in articular cartilage; however, little effects of ultrasound therapy driven cartilage energy modulation were found. The strong relationship between microbubbles mediated low intensity ultrasound therapy and the controlled release of drugs and mechanical shock waves was found. This strongly suggests that low intensity ultrasound therapy can play a role as a non-invasive controller for the release of drugs and lethal shock waves upon request.

PUBLIC ABSTRACT

Ultrasound is a form of mechanical waves that can be non-invasively transferred into the human body. Ultrasound has extended its application from medical ultrasonography into a variety of fields. In this study, ultrasound was evaluated as a multi-functional therapeutic tool for the orthopaedic rehabilitation. First the low intensity ultrasound therapy was investigated as an anabolic stimulator for cartilage regeneration and as a delivery controller for targeted drugs and mechanical shock waves.

Over the past few decades, ultrasound has been emerged as an anabolic stimulator for the cartilage regeneration; however, understanding of the underlying mechanisms has been slow. In this study, mechanism involved beneficial effects of ultrasound therapy on cartilage regeneration was investigated. We found that low intensity ultrasound stimulates the homing of chondrogenic progenitor cells toward injured sites in cartilage by triggering mechanotransductive cell signaling pathways that may result in faster cartilage regeneration.

Microbubble mediated ultrasound therapy has been frequently studied as a way to enhance the delivery efficiency of intravascular administered drugs or genes to targeted tissues. In this study, the effects of microbubble mediated low intensity ultrasound therapy on the intratumorally delivered lethal shock waves for tumor treatments and the controlled drug release were investigated. We found that ultrasound power dependent release of mechanical shock waves has

significant effects on the suppression of tumor growth and controlled drug release.

TABLE OF CONTENTS

LIST OF FIGURES

CHAPTER 1

INTRODUCTION

Articular cartilage is a complex soft tissue covering the end of moving bones in joints which provides pressure load distribution over the joint surface and smooth lubrication with little friction for establishing movement. Chondrocytes, the specialized cartilage cells, play a role in maintaining the extracellular matrix (ECM) integrity by producing structural molecules such as collagen, proteoglycan and other glycoproteins.(1) Physically applied compressional forces are necessary for chondrocyte metabolism; however, repetitive overloading or acute injurious loading in cartilage often results in chondrocyte dysfunction or death.(2-8) Osteoarthritis (OA) is often considered as primarily aging-related degenerative joint disease characterized by progressive loss of cartilage which results in pain, stiffness and restricted motion; however, recent evidences suggest that massive chondrocyte death caused by joint injury may contribute to the development of posttraumatic osteoarthritis (PTOA) if injured cartilage is being untreated.(1, 9-13)

Functional and physiologic restoration of damaged cartilage has long been in demand and some repairing methods are available for patients in clinic such as abrasion arthorplasty, arthroscopic lavage and debridement, subchondral drilling, micro-fracture, osteochondral grafting, and autologous- or allogeneic-osteochondral explants or chondrocyte implantation.(14-23) However, these methods are limitedly successful for patients with their intrinsic limitations. To

make things worse, articular cartilage is avascular and aneural, a lack of nerve and blood supply, so it has limited capacity for self-repair and mild cartilage injuries often undergo progressive degeneration without pain.(5, 24) Current evidence suggests that mechanical insults in cartilage result in massive chondrocyte death *via* instant chondrocyte necrosis followed by apoptosis triggered by intracellular signaling cascades.(25-28) It has been demonstrated that the production of reactive oxygen species (ROS) released from mitochondria is closely related to progressive chondrocyte apoptosis following a cartilage injury.(29, 30)

Hypocellularity caused by cartilage injury may play a role in prevention of cartilage repair. Recent findings demonstrated that superficial zone specific chondrogenic progenitor cells (CPCs) emerged following cartilage injury and they were highly clonogenic, motile and chemotactic. After 7 to 10 days of cartilage injury, a large number of CPCs was found in injured sites in cartilage.(31) This may indicate that enhanced homing of CPCs into injured sites in cartilage may play a critical role in faster recovery of cartilage back to normal condition.

Since ultrasound is a form of mechanical waves that can be non-invasively transferred into the human body, there have been frequent attempts to use of ultrasound as an anabolic stimulator for the repair of injured cartilage. It is likely that ultrasound can trigger mechanotransductive cellular signaling pathways which may be the result of stimulating chondrocytes to produce type II collagen and proteoglycan (PG) or chondrogeneis of mesenchymal stem cells (MSCs).(32-

43) However, the underlying mechanisms have been largely veiled, but a few detailed mechanisms include hyperthermal effect, cavitational effect or triggering mechanotransduction pathways.(44-48) Nevertheless, these known mechanisms may not be enough to fully utilize ultrasound as an anabolic stimulator. In this study, the effects of low intensity ultrasound therapy on the homing of CPCs toward injured sites in cartilage were first investigated as a integrin associated cellular mechanotransductive pathway trigger.

In order for chondrocytes to maintain cartilage integrity or turnover of ECM components, cellular metabolic energy such as ATP is supposed to be sufficiently provided. However, the ATP supply is always needed and limited in cartilage due to a low oxygen level which restricts cellular respiration. Recently, it was suggested that a moderate level of reactive oxygen species (ROS) produced by mechanically applied loads on cartilage was turned out to be beneficial for cartilage since induced ROS are consumed for the synthesis of ATP *via* glycolytic activity. In this study, the use of low intensity ultrasound therapy was investigated as a mechanical energy transporter for the production of ROS in chondrocytes which may result in the energy modulation in articular cartilage.

Microbubble mediated ultrasound therapy has been frequently studied as a way to enhance the efficiency of the delivery of intravascular injected drugs or genes to target tissues. Microbubbles, as a form of tiny gas- or air-filled bubbles, have become popular in medical ultrasound imaging field as contrast agents due to their dynamic behavior in the field of ultrasound. Under the lower peak

negative pressure of ultrasound, they linearly oscillate by changing their shape and size inversely proportional to ultrasound pressure amplitude. However, microbubbles in the higher peak negative pressure of ultrasound non-linearly oscillate which may result in complete destruction. Fragmented microbubbles are likely to be a source of inertial cavitation that may produce shock waves, hyperthermia and formation of free radicals.(49-51) There have been extensive preclinical studies about the effects of microbubble mediated ultrasound therapy for the targeted drug or gene delivery into tumors. Mechanical shock waves, released during ultrasound mediated microbubble destruction, is likely to be lethal by rupturing adjacent cell membrane and the shock waves can be used for facilitating drug delivery into target tumors through transient blood vessel disruption. Unfortunately, the clinical use of this technique has been limited through systemic circulation. However, musculoskeletal tumors can arise from anywhere in tissues or bones without specificity to age, gender and race. Treatment options are often limited to direct excision with risk of undesirable normal tissue damage, but tumors sometimes could not be treated due to a surgical inaccessibility. Most importantly, it would be always favorable for patients with non- or minimally- invasive tumor treatment method. In this study, the effects of microbubble mediated low intensity ultrasound therapy on the direct delivery of lethal shock waves into tumors and ultrasound power dependent drug release control was investigated.

CHAPTER 2

BACKGROUND

2.1 Articular cartilage

Articular cartilage is highly specialized smooth and white connective tissue covering joints at the end of moving bones. The main function of articular cartilage is to allow bones to glide over each other with smooth lubrication in addition to facilitation of the transmission of weight loads(1, 52). Articular cartilage has very limited capacity for self-repair when it is injured due to a lack of blood and nerve supply as well as hypo-cellularity.

2.1.1 Anatomy of articular cartilage in knee joints

The major structures of the knee joint are composed of articular cartilage, menisci, ligaments, synovial membranes, muscles and tendons (Fig. 2.1). Articular cartilage, also referred to hyaline cartilage, covers three bones (patella, femur and tibia) in knee joint and enables them to withstand applied load during daily activities (Fig. 2.2).

2.1.2 Structures of articular cartilage

Depending on morphology and cellularity of chondrocytes and the alignment of collagen fibers and proteoglycans, articular cartilage can be classified into three different zones; superficial, middle and deep zones (Fig. 2.3A). Articular cartilage is composed of mostly water (70%), collagen and PG (30%) and a small portion of chondrocytes (less than 1%). Chondrocytes behave

differently in each zone in cartilage providing for unique bio- chemical and mechanical properties in response to external stimuli.(53-55)

2.1.2.1 Superficial zone

The superficial zone is the thinnest zone among all zones in articular cartilage and is covered by lubricin that provides for facilitating joint lubrication. The superficial zone contains the most abundant amount of collagen fibers that are aligned in parallel with cartilage surface that provides high tensile strength and resistance to shear forces (Fig. 2.3B). The content of proteoglycan is relatively low and water content is the highest among all zones in cartilage. The cellularity of chondrocytes in the superficial zone is the most abundant and they are morphologically flat in shape.(56) The mechanical properties of articular cartilage may be rapidly degraded under the disruption of the superficial zone, which could result in initiation of osteoarthritis.

2.1.2.2 Middle zone

The middle zone shows great resistance to compressive forces that transferred from cartilage surface and works as a functional bridge between the superficial and deep zone in cartilage. This zone takes up 40-60% of cartilage in total volume and the chondrocytes are morphologically spherical with low cellularity. Alignment of collagen fibers in this zone is randomly distributed (Fig. 2.3B).

2.1.2.3 Deep zone

The cartilage in the deep zone takes up 30% of total cartilage volume and PG contents are the most abundant with the lowest water content. The diameter

of collagen fibers is the largest and aligned perpendicular to the cartilage surface. Collagens and chondrocytes are morphologically aligned perpendicular to the cartilage surface providing the greatest resistance to compressive forces (Fig. 2.3B).

2.1.2.4 Calcified zone

The calcified zone is located in between the deep zone and the subchondral bone. Cellularity and metabolic activity of chondrocytes in this zone are very low and chondrocytes produce type X collagen that provides structural integrity and shock absorber along with the subchondral bone.(55, 57)

2.1.3 Physiologic functions of articular cartilage

Articular cartilage primarily functions for absorption of compressively applied forces and lubrication for articulating movements in the knee joints. When mechanical load is applied in knee joints, a physiologic and functional role of articular cartilage is to distribute applied pressure along with cartilage to minimize peak stress on subchondral bones and to reduce friction between moving bones for smooth articulation.(58)

2.1.4 Chondrocytes

Chondrocytes are highly specialized and differentiated cells entrapped by extracellular matrix and are known as a single type of cells in cartilage. Chondrocytes take only a small portion (approximately 1 to 5% of the total volume) in articular cartilage even though cellularity and portion depend on species.(59, 60) Although the size, morphology, metabolism of chondrocytes differ depending on each zone in articular cartilage, the primary role of

chondrocytes is to maintain cartilage integrity by producing matrix molecules such as type II collagen, proteoglycan and other glycoproteins.(1, 53, 54, 61) When compressive forces are applied toward articular cartilage which result in bio- chemical and mechanical changes in extracellular matrix, chondrocytes start carrying out maintenance for the homeostatic balances between cartilage anabolism and catabolism.

2.1.5 Cartilage injury

Cartilage injuries can be characterized by extracellular matrix tear which may result in massive chondrocyte death or hypocellularity in cartilage. The massive chondrocyte death could initiate progressive cartilage degeneration which may lead to serious functional or physiologic problems in joints and fail to protect bones underneath cartilage from compressive loading. The initiation of cartilage degeneration may be caused by traumas such as car accidents, fall or spot-associated activities and the cartilage degeneration could be accelerated by injury responded cytokines or alarmins release such as tumor necrosis factors (TNF), interleukin (IL) families and matrix metalloproteinase (MMP) families.(25, 62-64) Damaged cartilage may end up with osteoarthritis (OA) in late stage which is the most common type of arthritis if injured cartilage is left untreated.

2.1.6 Osteoarthritis and posttraumatic osteoarthritis

Osteoarthritis (OA) can be characterized as a degenerative disease of synovial joints as a result of progressive loss of cartilage with symptoms including pain, stiffness and restricted motion (Fig. 2.4). Although the

pathogenesis of OA is still unclear, risk factors include aging, obesity, joint injury and joint overuse.(1, 9, 11, 65, 66) The world health organization (WHO) estimates that 10% of people in the world and over 27 million people in the US suffer from OA. The medical cost for OA is approximately 128 billion dollars per year and is over $2,600 per year per person with OA.(67-71)

Current understanding suggests that massive chondrocyte death caused by joint injuries also plays a role in development of posttraumatic osteoarthritis (PTOA).(1, 5, 30) In traumatized cartilage, chondrocytes produce and release inflammatory signals or cytokines such as tumor necrosis factor (TNF) families, interleukin (IL) families and other proteases which are closely involved in deterioration of cartilage.(62, 63, 72) Recent studies demonstrated that production of reactive oxygen species (ROS) in mitochondria is significantly enhanced following a cartilage injury which resulted in progressive chondrocyte death over time. The production of ROS immediately after cartilage injury was suppressed by anti-oxidants resulting in prevention of progressive chondrocyte death.(29, 30) In addition, informational blocks between chondrocytes and bio-chemical or mechanical changes in ECM, such as inhibition of focal adhesion or cytoskeletal dissolution, significantly prevented chondrocyte death following cartilage injury which suggests that informational blockages of integrin associated mechanotransduction pathways could rescue chondrocytes from instant necrosis as well as progressive apoptosis.(73, 74)

2.1.7 Cartilage repair

Articular cartilage can be degenerated by accidental trauma or fall-associated joint injuries as well as spontaneous degradation as a result of aging or joint overuse. Since articular cartilage has very limited capacity for self-repair due to a lack of blood supply and a nervous system, mild cartilage damage may often lead to development of posttraumatic osteoarthritis without symptoms such as pain.(5, 11-13, 24) For this reason, successful cartilage repairing strategies have been in demand for a long time and some techniques are available in clinics such as microfracture, arthroscopic lavage, autologous chondrocyte or mesenchymal stem cells (MSCs) implantation, and auto- or allo-graft osteochondral transplantation. However, these methods have met with limited success due to their intrinsic limitations and most importantly, patients are always in favor with non- or minimal- invasive treatment methods.

2.1.7.1 Microfracture

Microfracture is a direct surgery technique that creates holes in between cartilage and subchondral bone to make paths for the supply of blood and bone marrow (Fig. 2.5). Fibrin clot fills out cartilage defects and infiltrated bone marrow derived MSCs start making cartilage matrix.(75) Microfracture technique is especially beneficial when patients have a small size of lesion in cartilage.(76, 77) However, this technique is partially successful with respect to functional restoration of articular cartilage since newly formed cartilage by infiltrated MSCs is made of type I collagen which is not a right type for articular cartilage.

2.1.7.2 Arthroscopic lavage

Arthroscopic lavage is the procedure for cleaning or debriding out blood, inflammatory mediators or degenerative cartilage debris in joints which could result in pain relief, recovery of restricted motion and suppressed inflammation for patients. Typically this technique would be effective for patients suffering from relatively minor cartilage defects or in earlier stage of arthritis; however, the efficacy has been debated for patients who are already diagnosed with or in late stage of OA.(18)

2.1.7.3 Cell implantation techniques

Chondrocyte implantation is also one of the cell-based cartilage repairing methods and the procedure requires three steps. In a first stage, articular cartilage biopsy is taken arthroscopically from a non-injured area from the patients and then the cartilage pieces are enzymatically digested for chondrocyte isolation. The isolated chondrocytes are cultured *in vitro* in a laboratory to get a sufficient number of chondrocytes and then injected into defect area in cartilage with or without combination of scaffold matrix.(78-80) Instead of cartilage tissue harvested from the patients, MSCs isolated from bone marrow can be used for implantation after culturing and chondrogenic differentiation.(81, 82) However, the efficiency for cartilage repair by cell implantation techniques has not been reached at a satisfactory level and potential infections or undesirable immune responses may cause problems (Fig. 2.6).

2.1.7.4 Osteochondral transplantation

Osteochondral transplantation is a technique that replaces injured cartilage regions in patient joints with healthy cartilage including subchondral bone harvested from donor sites (Fig. 2.7). The source of osteochondral explants is typically from healthy non-loaded area in patients or from a cadaver donor after being sterilized.(83) Osteochondral transplantation has been reported as a promising technique for the functional restoration of cartilage in joints; however, it is risky for potential disease transmission or undesirable immune response.

2.2 Ultrasound therapy for articular cartilage repair

In 1880, the effect of piezoelectricity was discovered that high frequency of sound waves, the upper limit of human hearing, can be produced and received. The biophysical effects of ultrasound have started to be unveiled since ultrasound was found to be absorbed in the human skin. The beneficial effects of ultrasound clinically were first clinically proven in 1970, that ultrasound stimulated bone fracture healing. Since then ultrasound has extended its application to a number of medical fields such as soft tissue healing, lithotripsy and tumor treatment. A number of studies have found that ultrasound therapy is beneficial for the repair of biologic soft tissues including articular cartilage; however, its underlying mechanisms have been mostly still veiled.

2.2.1 Mechanisms of ultrasound therapy

Studies have suggested that the underlying mechanisms of ultrasound therapy can be classified into thermal and non-thermal effects. Thermal effects can be achieved by using a continuous mode of ultrasound waves that may result

in increased metabolic rate or blood circulation (Fig. 2.8A). Non-thermal effects are more like mechanical interactions which can be achieved by using a pulsed mode of ultrasound waves, resulting in modulation of inflammatory responses, drug sonophoration and calcium signaling (Fig. 2.8B).(84, 85) However, regardless of either continuous or pulsed ultrasound type, thermal and non-thermal effects always take place at the same time in practice and neither of them can be neglected. Therefore, the reality of unveiling the underlying mechanisms of the benefits of ultrasound therapy is complicated.

2.2.1.1 Thermal effects of ultrasound therapy

When ultrasound travels into the human body, ultrasound can be absorbed or attenuated depending on types or properties of tissues, and energy conversion takes place from absorbed ultrasonic energy to heat energy.(86) The conversion efficiency of ultrasonic energy to heat highly depends on compositional tissue structures, tissue attenuation coefficient, a mode of ultrasound waves either pulsed or continuous, ultrasound duration and ultrasound frequency. Studies have shown that low intensity continuous ultrasound, 1MHz in frequency, 225mW/cm^2 in intensity and 5 minutes in duration, elevated temperatures in articular cartilage from 36 ^{o}C to 42 ^{o}C.(87)

2.2.1.2 Non-thermal effects of ultrasound therapy

Acoustic cavitation is one of the key mechanisms of the non-thermal effects of ultrasound therapy (Fig. 2.9). A cavitational effect is the formation of tiny air bubbles as a result of pressure fluctuation that produced by positive and negative pressure oscillation as ultrasound travels.(88) Under the lower peak

negative ultrasound pressure, the air bubbles are forced to linearly oscillate by changing their size and shape in a process, which is called stable cavitation. However, under the higher peak positive ultrasound pressure, the air bubbles no longer linearly oscillate and finally undergo complete destruction by producing shock waves with high local heat and acoustic streaming. Evidences suggest that beneficial effects of ultrasound are likely due to non-thermal interactions of ultrasound with tissue rather than ultrasound associated hyperthermia.(88) However, others have suggested that the formation of acoustic cavitation is not produced within the power ranges of therapeutic ultrasound.(89-92)

2.2.2 Acoustic properties of articular cartilage

The propagation of ultrasound in articular cartilage depends on the compositional properties of cartilage such as maturity and zonal layers. Studies have shown that, in mature cartilage of rat patellae, the speed of ultrasound is approximately 1,690 m/s and attenuation coefficient is 0.41 dB/MHz/mm. However, in immature cartilage, the properties are somewhat different; the speed of ultrasound with 1,640 m/s and the attenuation coefficient with 0.25 dB/MHz/mm. Acoustic properties also depend on zonal layers in cartilage; ultrasound speed and attenuation are lower in deeper zone compared to superficial zone in cartilage suggesting that compositional differences in each layers such as cellularity, collagen and PG play a role in ultrasound propagation.(93) Attenuation or absorption of ultrasound in cartilage is most likely to result in hyperthermia which is closely associated with ultrasound frequency, intensity and duration.(94)

2.2.3 Cartilage anabolism in response to ultrasound therapy

In the past few decades, there have been frequent attempts to use ultrasound as a mechanical stimulator for the repair of articular cartilage. A number of studies have shown that low intensity ultrasound stimulates cartilage anabolism by increasing extracellular matrix molecule production such as type II collagen and proteoglycan.(32-37, 42, 95, 96) Low intensity ultrasound therapy also has proven to be an effective for chondrogenic differentiation of mesenchymal stem cells.(38-41, 43) The initiation of mechanotransductive signaling pathways of chondrocytes has been also suggested as one of the underlying mechanism candidates of the beneficial effects of low intensity ultrasound therapy for cartilage repair.(44, 45, 97, 98) However, the unveiled mechanisms would not be enough to fully understand and utilize the ultrasound therapy as an anabolic stimulator for cartilage repair.

2.3 Acoustic behaviors of microbubbles in ultrasound fields

Microbubbles, as a form of tiny gas- or air- filled bubbles, have become popular in medical ultrasound research fields due to their dynamic behavior in ultrasound fields. Intravenously administered microbubbles as contrast agents systemically circulate and produce high degree of echogenicity in response to ultrasound waves. Microbubbles are typically made of biocompatible materials in order for intravenous administration and the shell of microbubbles can be made of albumin, lipid or synthetic polymer with either air or heavy gases in the core depending on desired bubble characteristics such as size, stability, diffusion and surface tension.(99, 100)

The behavior of microbubbles in the field of ultrasound is exceptionally dynamic. Under the lower peak negative pressure of ultrasound, approximately less than 0.05 of mechanical index (MI), microbubbles linearly oscillate by changing their shape and size inversely proportional to ultrasound pressure amplitude that may produce microstreaming. However, microbubbles in the higher peak negative pressure of ultrasound, approximately 1 or higher of MI, non-linearly oscillate which may result in complete destruction. Fragmented microbubbles are likely to be a source of inertial cavitation that may produce shock waves, hyperthermia and formation of free radicals (Fig. 2.9).(49-51)

2.3.1 Microbubbles as contrast agents

The first use of microbubbles as ultrasound contrast agents was in 1968.(101) The first generation of contrast agents was the air containing microbubbles in the core; however, the microbubbles were not stable enough in the blood stream because they are almost all disappeared a few seconds after intravenous administration. The later generation of contrast agents overcame this limitation by making heavy gas filled microbubbles with smaller diameters, which increase stability in the blood stream.(102) Since then, microbubbles with diverse acoustic characteristics have been developed depending on the purposes of use. Beyond the use of microbubbles as contrast agents, recent studies have proven that microbubbles has potential to be used as a vehicle for drug and gene delivery as well as for thrombolysis and tumor treatment (Fig. 2.10).(103-115)

2.3.2 Microbubble mediated ultrasound therapy for the cancer treatment

The use of microbubbles has extended and proven its application from serving as contrast agents to the treatment of tumors. Mechanical shock waves can be produced during ultrasound mediated microbubble destruction, and the shock waves have also proven to be effective in anti-cancer drug delivery into tumors. At the moment of complete destruction of the microbubbles as a result of non-linear oscillation in higher negative peak pressure of ultrasound, released shock waves themselves are lethal by rupturing adjacently located cell membranes.(102, 116-119) Recent attempts have shown that targeting area-specific drug or gene delivery is possible by combining the use of ultrasound exposure and functional microbubbles, that are conjugated with anti-cancer drugs, genes, specific ligands and antibodies.(120-124) Tumor specific anti-cancer drug delivery by ultrasound mediated microbubble destruction has proven to be effective in suppression of tumor growth that may have a potential to be considered as a novel non-invasive tumor treatment method.(49, 112-115) However, the clinical use of this technique has been limited through vascular system that may result in low efficiency of drug delivery.(125)

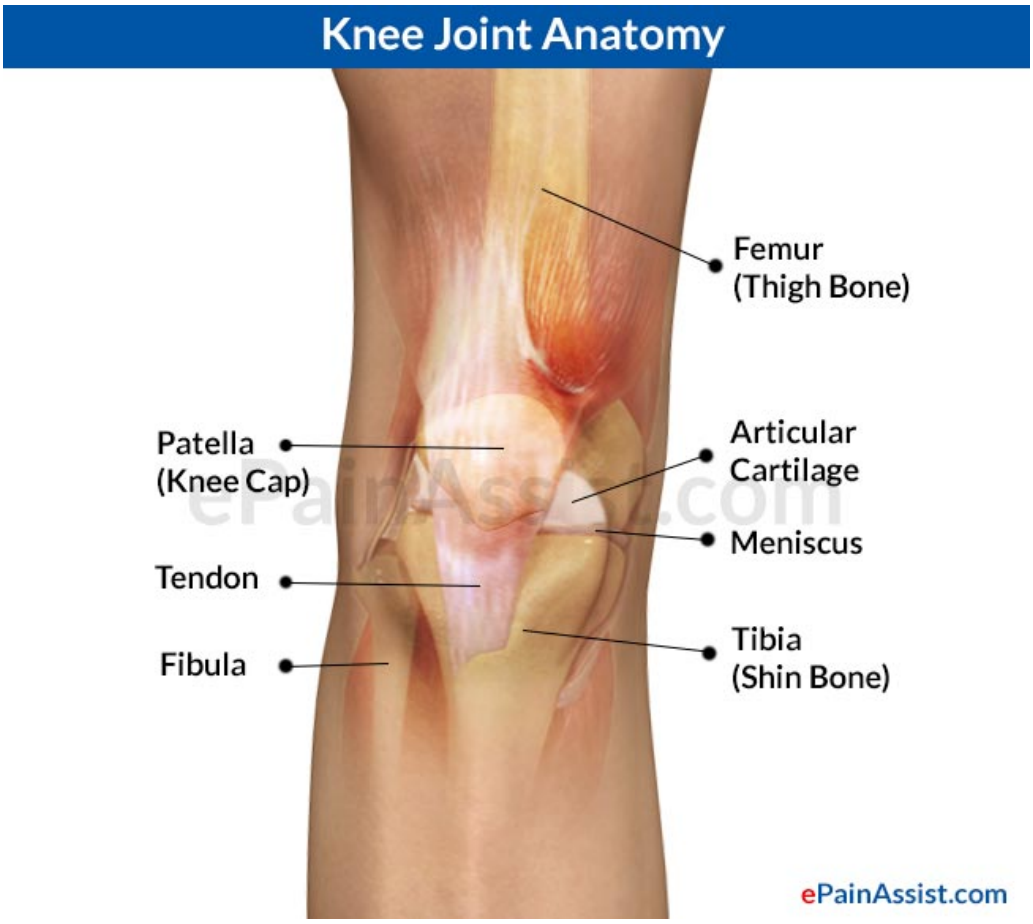

Figure 2.1 Anatomy of knee joints. The major structures of the knee joints are composed of articular cartilage in both side of femur and tibia, menisci, ligaments, synovial membranes, patella and tendons.(126)

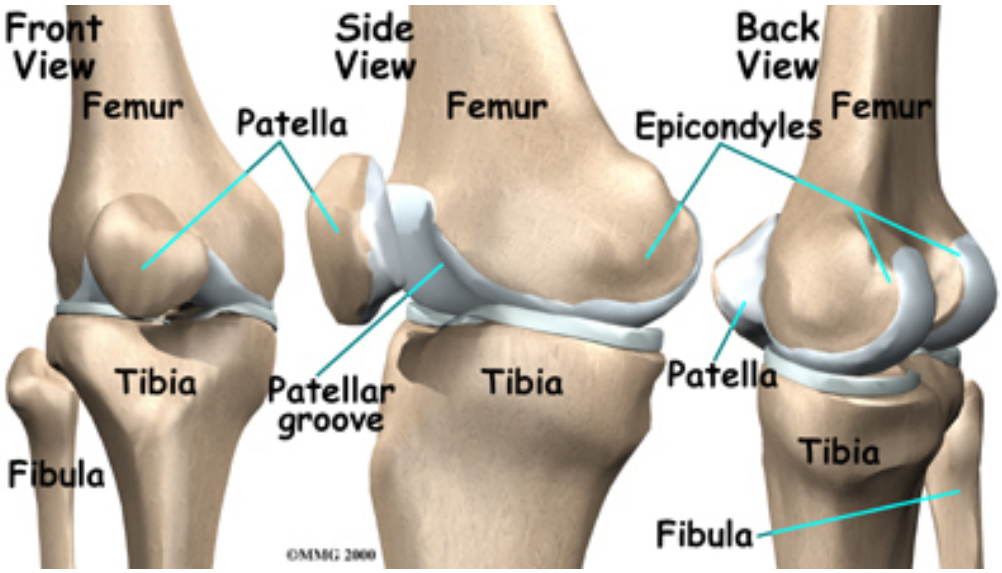

Figure 2.2 Articular cartilage in knee joints. Articular cartilage, also referred to hyaline cartilage, covers three bones (patella, femur and tibia) in knee joint and enables them to withstand applied load during daily activities.(127)

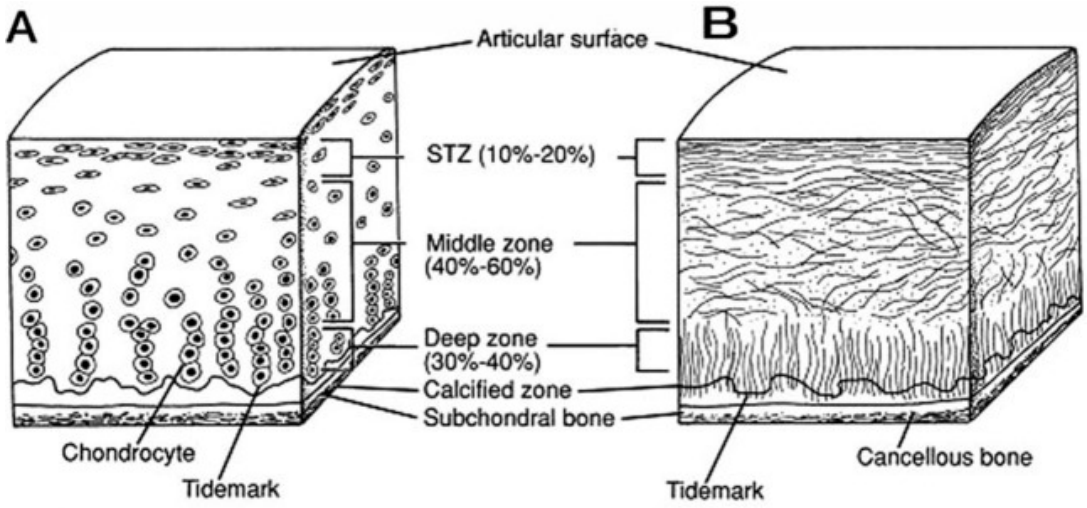

Figure 2.3 The structure of articular cartilage. Articular cartilage can be classified into three different zones; superficial, middle and deep zones depending on morphology and cellularity of chondrocytes and the alignment of collagen fibers and proteoglycans(52)

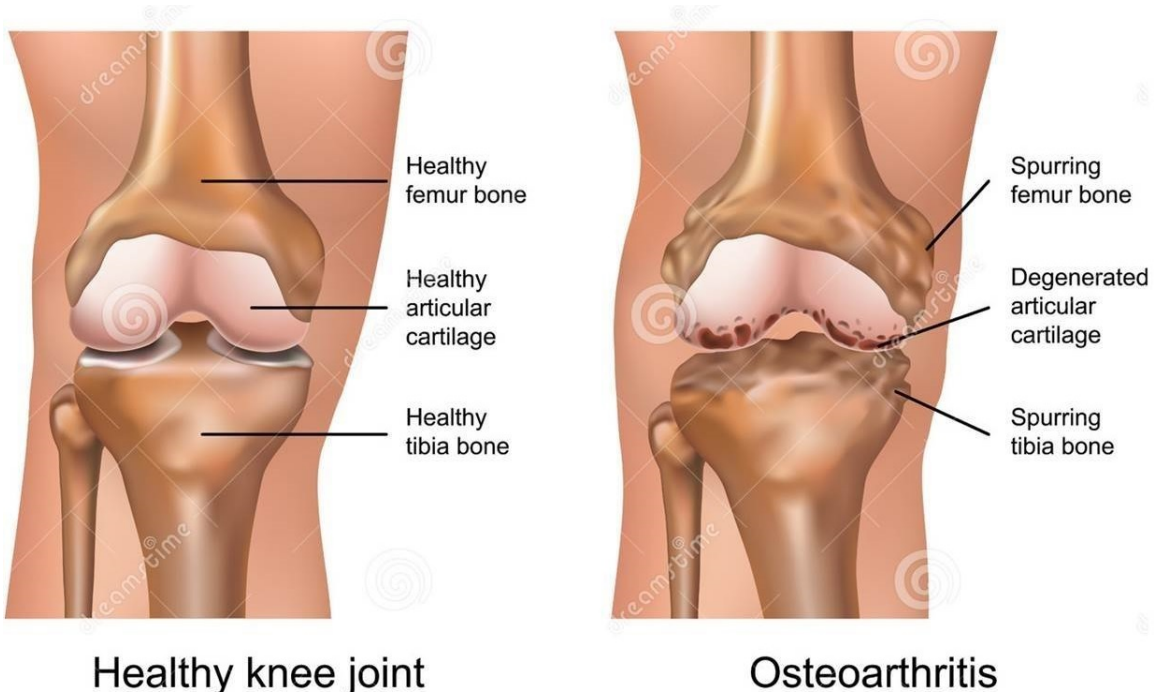

Figure 2.4 Osteoarthritis (OA). OA can be characterized as a degenerative disease of synovial joints as a result of progressive loss of articular cartilage with symptoms including pain, stiffness and restricted motion.(128)

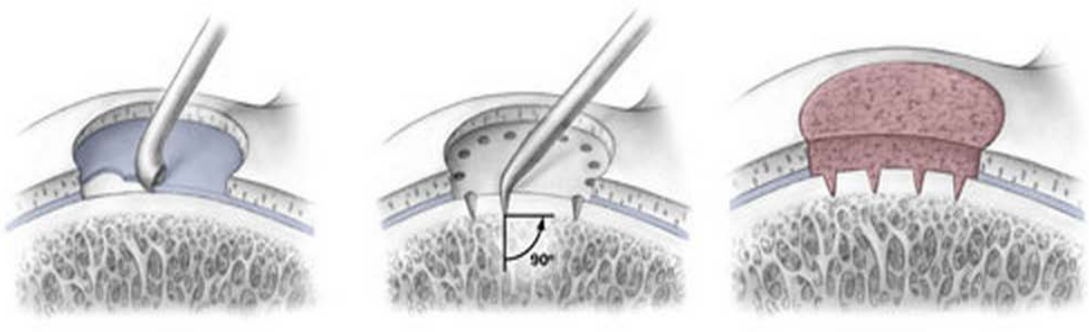

Figure 2.5 The microfracture surgery for cartilage repair. Microfracture is a one-step direct surgery technique that creates cracks in between cartilage and subchondral bone to make paths for the blood supply and bone marrow. Fibrin clot fills out cartilage defects and infiltrated bone marrow derived MSCs start making cartilage matrix.(129)

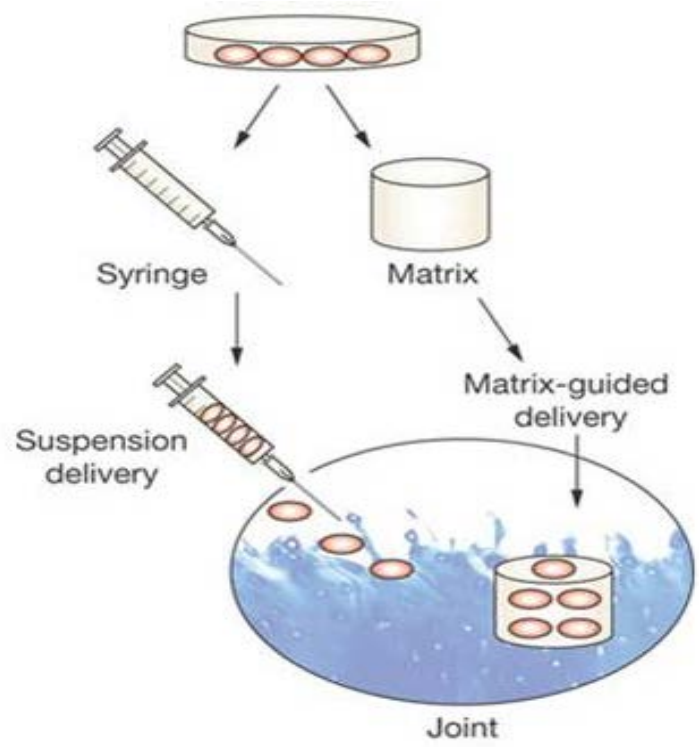

Figure 2.6 Cell transplantation techniques for cartilage repair. Chondrocyte or MCSs implantation as one of the promising cell-based cartilage repairing methods has been considered as one of the promising cartilage repairing methods. This requires three surgical steps. In a first stage, cells were harvested in a non-injured area from the patients and then cultured *in vitro* in a laboratory to get a sufficient number of chondrocytes. The cells then injected into defects in cartilage with or without combination of scaffold matrix.(130)

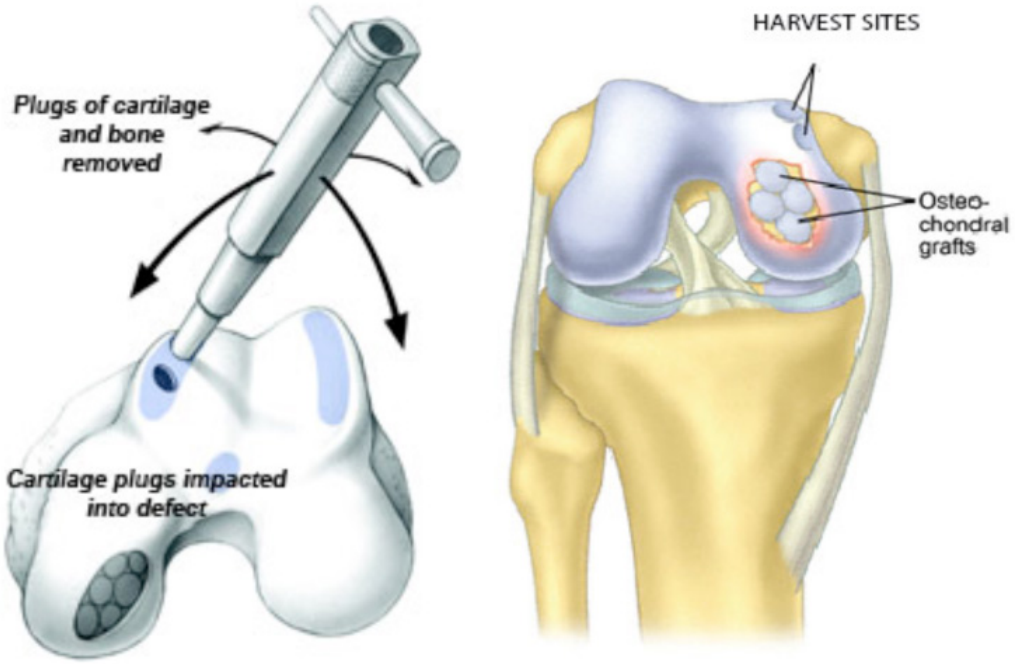

Figure 2.7 Osteochondral transplantation for cartilage repair. Osteochondral transplantation is a technique that replaces damaged articular cartilage in patient joints with healthy cartilage including subchondral bone harvested from donor sites.(131)

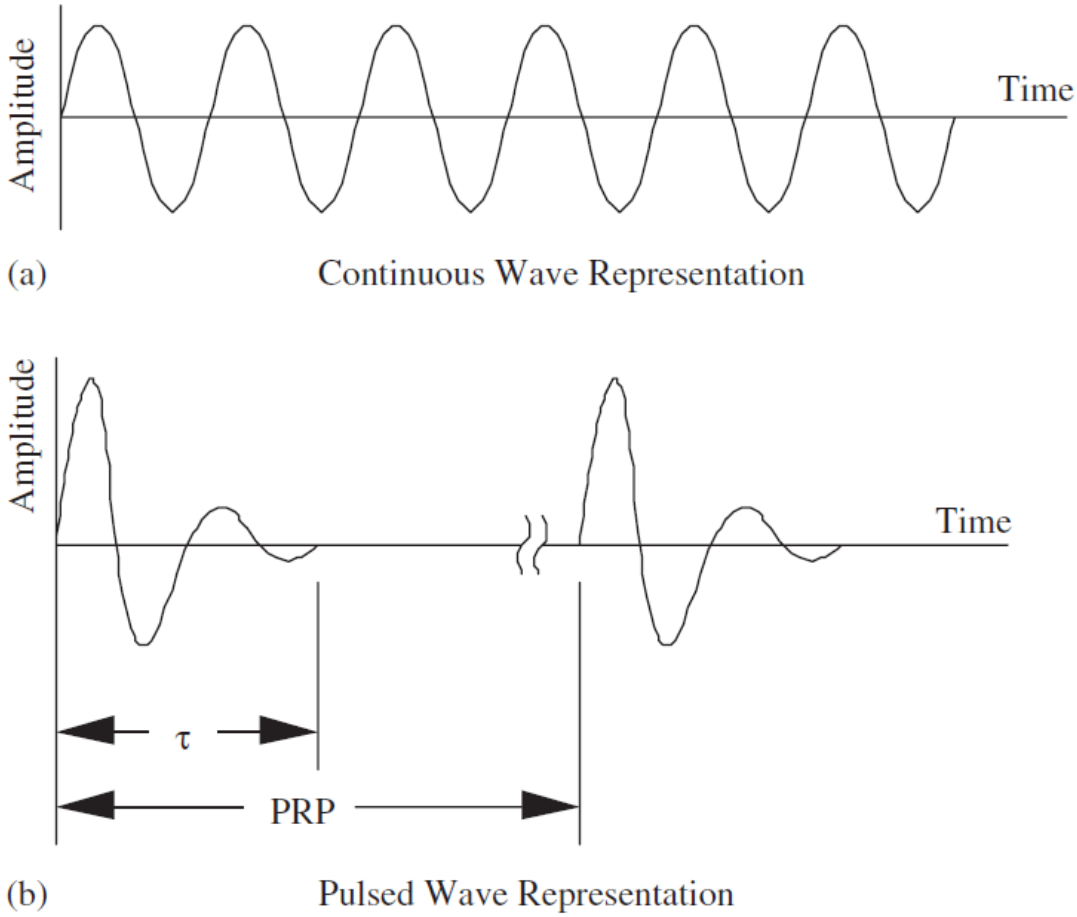

Figure 2.8 Schematic representations of continuous and pulsed mode of ultrasound waveforms. Continuous mode of ultrasound can be achieved by using continuous waveforms as an input and pulsed mode of ultrasound can be achieved by using pulsed waveforms as an input.(46)

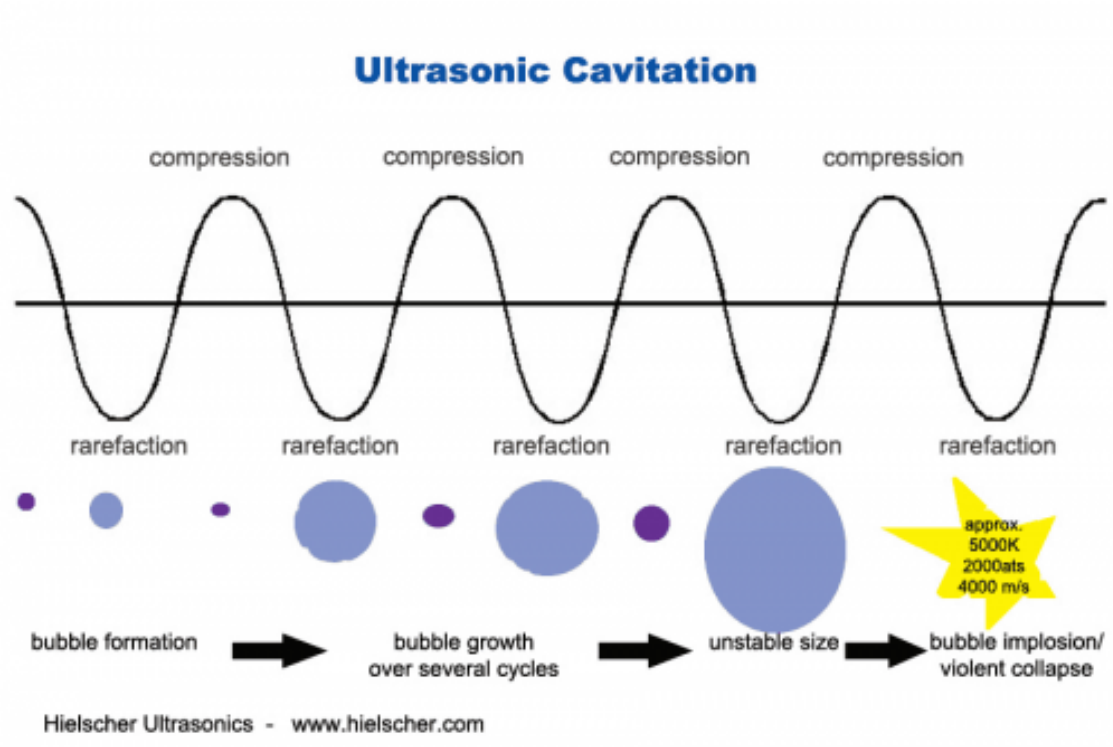

Figure 2.9 Ultrasonic cavitation. Cavitation is the formation of tiny gas- or air-filled bubbles in response to changes of ultrasound pressures. Microbubbles linearly oscillate in a low intensity of ultrasound while microbubbles non-linearly oscillate which may result in complete destruction in a higher intensity of ultrasound. Fragmented microbubbles are likely to be a source of inertial cavitation which may produce shock waves, hyperthermia and formation of free radicals.(46)

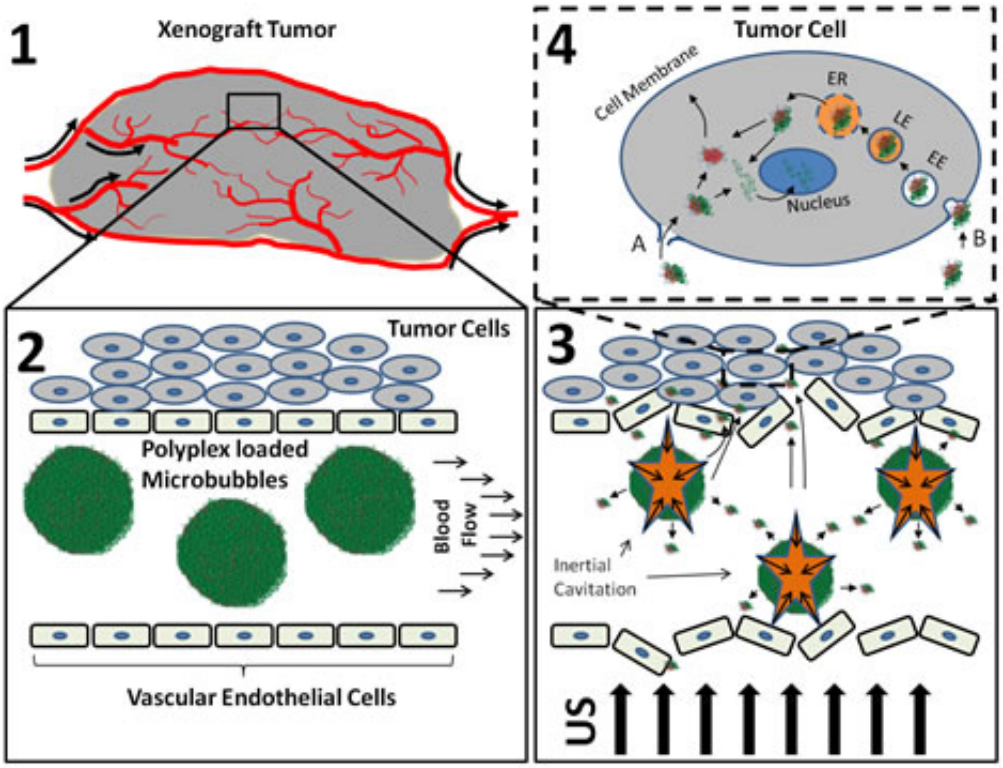

Figure 2.10 Ultrasound targeted microbubble destruction for drug delivery into tumors. Drugs or genes conjugated microbubbles has the potential for the targeted tumor treatment.(132)

CHAPTER 3

MECHANISM INVOLVED BIOPHYSICAL EFFECTS OF ULTRASOUND THERAPY FOR ARTICULAR CARTILAGE REPAIR

3.1 Background and significance

Articular cartilage is a soft tissue covering the joint surfaces and serves as a shock absorber allowing joints to withstand daily activity such as walking and running with little friction. Articular cartilage is composed of mostly water (80%), type II collagen and proteoglycan (10-20%) and a few portions of chondrocytes (less than 1%). Articular cartilage can be typically classified into superficial, middle and deep zone depending on the morphology of chondrocytes and composition of extracellular matrix (ECM) components. Due to the unique characteristics such as aneural and avascular, articular cartilage has a very limited capacity for self-repair when injured. Current evidence suggests that massive chondrocyte death caused by cartilage injury is likely to develop to the posttraumatic osteoarthritis (PTOA) over time if it is left untreated.(133)

It was found that stem cell-like progenitor cells, chondrogenic progenitor cells (CPCs), emerged following a cartilage injury and they exhibit distinctly different characteristics compared to normal chondrocytes. Following 7 to 10 days of post cartilage injury, the CPCs start repopulating in injured sites where massive chondrocytes death was found. The current understanding suggests that the CPCs are expected to have the potential for cartilage repair since it showed stem cell-like characteristics such as higher colony formation, motility,

clonogenicity, chemotaxis and multipotency. An examination of the gene expression of CPCs by microarray analysis revealed that the CPCs are closer to mesenchymal stem cells (MSCs) rather than normal chondrocytes.(31) Thus it is reasonable to assume that expedited CPC homing into an injured site following a cartilage injury may play a crucial role in cartilage repair.

In the past few decades, there have been frequent attempts to use low-intensity ultrasound as an anabolic stimulator for injured cartilage repair. It has been proven that low intensity ultrasound therapy enhanced ECM macromolecule production such as type II collagen and proteoglycan.(32, 33, 35-37, 134) Low intensity ultrasound therapy also proved to be effective in the attenuation of progressive cartilage degradation and the enhancement of chondrogenesis of MSCs.(39, 42) However, progress in understanding its mechanism has been slow, and few detailed underlying mechanisms are available now. The initiation of integrin clustering associated mechanotransductive signaling pathways has been suggested as one of the beneficial effects of low intensity ultrasound therapy since ultrasound is a form of mechanical waves that can be transferred non-invasive ways.(44, 45, 97) Integrins, a class of trans-membrane receptors, cluster in response to mechanical or chemical changes in ECM which triggers signal transduction pathway *via* focal adhesion complexes and integrin clustering is essential phenomena for cell survival such as migration, proliferation and differentiation.(135-140) Focal adhesion kinase (FAK) is a major player in relaying extracellular signals through integrins to downstream factors *via* tyrosine phosphorylation.(141-145) FAK and Src family kinases (SFKs) are members of focal adhesion complex that

play a critical role in the cell-signaling hub. Current understanding suggests that FAK phosphorylation at kinase domain at tyrosine 576/577 is closely involved in cell migration signaling pathways as upstream factors and the suppression of the kinase domain in FAK by SFK inhibitor resulted in significant suppression of cell motility.(146-148)

Reactive oxygen species (ROS) are a group of intermediate molecules or ions containing oxygen by the incomplete electron reduction such as superoxides, peroxides, hydroxyl radical and hypochlorous acid. ROS can be produced exogenously as a result of ionizing radiation, xenobiotics or drugs. ROS can be also produced endogenously as a natural byproduct of cellular respiration, and they play a role in microbicidal activity, the regulation of signal transduction and gene expression. However, an imbalanced level of ROS may result in oxidative damages to DNA, proteins and lipids. In articular cartilage, mitochondrial function is impaired due to limited oxygen supply, less than 5%, which in turn adenosine triphosphate (ATP) contents are always low and demanding. Recent studies showed that ROS production is considerably enhanced after cartilage injury followed by massive apoptotic chondrocyte death within 24 hours. Suppression of the ROS production by rotenone, an electron transport chain inhibitor, or N-acetylcysteine, a free radical scavenger, could prevent progressive chondrocyte death suggesting that chondrocytes led to progressive death by oxidative stress following a cartilage injury.(29, 74) Due to low levels of oxygen, the metabolism of articular cartilage dominantly relies on the glycolytic pathway for ATP supply rather than by oxidative phosphorylation.(149-153) Recent

findings demonstrate that moderately produced ROS in articular cartilage as a result of mechanical loading supports chondrocyte metabolism by increasing ATP synthesis suggesting that induced ROS production supports glycolysis to produce ATP.(154, 155)

For these reasons, low intensity ultrasound was considered as a mechanical stimulator and mechanism involved its biophysical effects in articular cartilage were investigated in this study. First, the effect of low intensity ultrasound therapy on the homing of CPCs toward injured site in cartilage and their mechanotransductive signaling pathways was investigated following a cartilage injury. Second, the effects of low intensity ultrasound therapy on metabolic energy modulation in cartilage was investigated which may account for others' finding that low intensity ultrasound stimulates extracellular matrix molecule synthesis because such anabolism requires metabolic energy like ATP.

3.2 Specific aims and hypotheses

A number of studies have reported that low intensity ultrasound therapy is beneficial for cartilage repair by stimulating the production of extracellular matrix macromolecules; however, detailed underlying mechanisms have been unveiled only in part. In this study, the biophysical effects of low intensity ultrasound therapy on injured cartilage were examined with underlying mechanisms. Previously, the emergence of CPCs following a cartilage injury were discovered and the CPCs exhibited homing ability toward injured sites in cartilage suggesting that the repopulation of CPCs in injured site plays a critical role in initiation of cartilage repair. Thus, we investigated the effect of

mechanical stimulation by low intensity ultrasound therapy on the homing ability of CPC with specific aims and hypotheses as follows.

Specific Aim 1: Determine the effect of low intensity ultrasound therapy on CPC homing following a cartilage injury.

Hypothesis 1: Ultrasound therapy accelerates CPC homing toward injured site in cartilage

Hypothesis 2: Ultrasound therapy triggers mechanotransductive signaling pathways of CPCs *via* focal adhesion kinase phosphorylation.

Specific Aim 2: Determine the pre-stimulatory effect of low intensity ultrasound therapy and chondrocytes-extracellular matrix (ECM) adhesions on cell mortality following a cartilage injury.

Hypothesis 1: Ultrasound therapy induced FAK activation between chondrocytes and ECM results in greater cell mortality following a blunt impact induced cartilage injury.

Hypothesis 2: Inhibition of chondrocyte-ECM adhesions by chemical inhibitors prevents massive chondrocyte death following a blunt impact induced cartilage injury.

In the past few decades, a number of studies have shown that low intensity ultrasound stimulates ECM molecule production such as type II collagen and proteoglycan. Chondrocytes are obviously required metabolic energy such as ATP for maintaining cartilage integrity by replenishing those ECM molecules. However, the level of ATPs is always low and in demand as a result of low level of O_2 in cartilage. Recent findings suggest that the production of ATP was enhanced by non-injurious cyclic mechanical loading in articular cartilage *via* moderately increased ROS levels suggesting elevated ROS are used for glycolysis in chondrocytes.

Thus, the effect of low intensity ultrasound therapy on modulation of chondrocyte energy metabolism by examining ROS induced ATP production was investigated with the following specific aims and hypotheses.

Specific Aim 3: Determine the effect of ultrasound therapy on reactive oxygen species (ROS) production in articular cartilage.

Hypothesis 1: Low intensity ultrasound therapy suppresses ROS production following a cartilage injury that may prevent oxidative stress associated progressive chondrocyte death.

Hypothesis 2: Low intensity ultrasound therapy can be used for a mechanical stimulator for increase in sub-lethal levels of ROS in articular cartilage.

Specific Aim 4: Determine the effect of ultrasound therapy on ATP synthesis *via* induced ROS production in articular cartilage.

Hypothesis 1: Low intensity ultrasound therapy enhances ATP production in articular cartilage *via* beneficial ROS production.

3.3 Materials and methods

3.3.1 Preparation of osteochondral explants

Osteochondral explants, 2.5 x 2.5 cm^2 including the central loaded area, were manually prepared by sawing from mature bovine stifle joints obtained from a local abattoir (Bud's Custom Meats, Riverside, IA). The explants were gently rinsed in Hank's Balanced Salt Solution (HBSS) (Invitrogen Life Technologies, Carlsbad, CA, USA) and pre-equilibrated in conditioned medium with 45% Dulbecco's modified Eagle medium (DMEM) and 45% Ham's F-12 (F12) supplemented with 10% fetal bovine serum (FBS) (Invitrogen Life Technologies), 100 U/ml penicillin, 100 µg/ml streptomycin, and 2.5 µg/ml amphotericin B at 37°C, 5% O_2 and 5% CO_2 for 2 days.

3.3.2 Articular cartilage defect models.

After 2 days of pre-equilibration of the osteochondral explants, partial-thickness cartilage defects, approximately 0.5 mm in depth, were aseptically created using a 22 gauge sterilized needle by scratching cartilage surface with X-shapes. To make full-thickness cartilage defects in osteochondral explants, a biopsy punch (Miltex Inc., York, PA, USA), 2 mm in diameter, was used and the defects were filled with commercial TISSEEL^{TM} fibrin hydrogel (Baxter Healthcare Corp, Westlake Village, CA, USA).

To mimic traumatized joint injuries, osteochondral explants were rigidly fixed in a customized drop-tower device and subjected to a 7 J/cm^2 single blunt impact.

3.3.3 Confocal microscopic analysis

Osteochondral explants were stained with 1 μM Calcein-AM, a live cell indicator, and either 1 μM ethidium-homodimer-2, a dead cell indicator, or 5 μM dihydroethidium (DHE), an ROS indicator, (Invitrogen^{TM} Life Technologies) for 30 minutes. A confocal laser scanning microscope (Fluoview 1000, Olympus, Center Valley, PA, USA) was used to scan cartilage with an average of 200 μm at 20 μm intervals both impact sites and remote sites. The percentage of cell viability was evaluated as [(live chondrocytes)/(live + dead chondrocytes)] x100 [%] and the percentage of ROS production was evaluated as [(DHE positive chondrocytes)/(live + DHE positive chondrocytes)] x100 [%]. For the purpose of visualization, scanned images were stacked for Z-axis projection using ImageJ (rsb.info.nih.gov/ij).

3.3.4 Chondrogenic progenitor cell isolation

Following a blunt impact-induced cartilage injury, the explants were returned to culture. After seven to ten days, cartilage part in the explants was

incubated with 0.25% trypsin-EDTA (Invitrogen Life Technologies) for 20 minutes after being gently rinsed with HBSS. The chondrogenic progenitor cells were then isolated from trypsin suspension by centrifugation.

3.3.5 Configuration of the ultrasound therapy system

The versatile sweep function generator (4040B, BK Precision, Yorba Linda, CA, USA) was used to modulate input sinusoidal waveforms, either continuous or pulsed, a burst rate fixed at 1kHz. Input pulses with various duty cycles at 0, 1, 10, 30, 50 and 100% were tested by adjusting the number of pulse cycles per each burst; 0% and 100% duty cycles are equivalent to non-ultrasound control and continuous ultrasound respectively. The input pulses are amplified by radio frequency power amplifier (ENI310L, Electronic Navigation Industries Inc., Rochester, NY, USA) and amplified pulses are transferred to non-focused ultrasonic transducers (Ultrasonic S-Lab, Concord, CA, USA). The ultrasound power was estimated by radiation force balance and calculated ultrasound intensity was assumed as spatial averaged and temporal averaged (SATA).(156-158) An acoustic absorber was placed during ultrasound exposure on sample in order to prevent undesired standing wave interruptions.

3.3.6 Western blot analysis for phosphor-proteins detection

To analyze phosphorylated protein activation by western blot, cells in cartilage or in a monolayer culture were lysed using cold lysis buffer containing protease and phosphatase inhibitor (CalBiochem, San Diego, CA, USA). Total protein concentration was determined using a BCA Protein Assay kit (Thermo Fisher Scientific Inc., Rockford, IL, USA) and then denatured with 2x sample buffer reduced with 0.05 M dithiothreitol (DTT). 2.5 µg proteins were resolved in 10% sodium dodecyl sulfate polyacrylamide gel

electrophoresis (SDS-PAGE gels) and blotted onto nitrocellulose membranes. After blocking with 5% non-fat dried milk in tris buffered saline (20 mM Tris buffer containing 140 mM NaCl, pH 7.4) containing 0.1% Tween-20 (TBST) for 1 hour, the blot was then incubated with total-, phosphor- target proteins with a loading control of either anti-beta actin or anti-glyceraldehyde 3-phosphate dehydrogenase (GAPDH) antibodies in a 1:1000 dilution in 5% BSA in TBST overnight at 4ºC. The blots were then washed with TBST and incubated with horseradish peroxidase (HRP) conjugated goat anti-rabbit IgG in a 1:2000 dilution in 5% BSA in TBST for 1 hour. The target proteins were reacted with SuperSignal West Dura Chemiluminescent Substrate (Thermo Fisher Scientific Inc.) and the chmiluminescent signals were detected with Kodak Biomax Xar film (Sigma-Aldrich®, Rochester, NY, USA). The integrated density of bands was quantified by ImageJ and the relative fold increase was estimated.

3.3.7 Statistical analysis

Statistical analysis was performed using software package SPSS (IBM, Armonk, NY, USA). One-way analysis of variance (ANOVA) with the Tukey *post hoc* test was used to test all possible pairwise comparisons. The level of significance was set at $p < 0.05$.

3.4 Results

3.4.1 Configuration and validation of ultrasound therapy system.

Input waveforms, either continuous or pulsed waves with duty cycle adjustments, were produced using a function generator, and the waveforms were then amplified by a radio frequency power amplifier (Fig. 3.1). Then amplified waveforms were transferred to ultrasonic transducers that convert electric signals to ultrasound waves. The ultrasound

power was estimated by a radiation force balance which converts applied ultrasonic radiation force into ultrasonic power using an acoustic absorber and a high-resolution balance (Fig. 3.2).

3.4.2 Emergence of CPCs in response to cartilage injury and its isolation

Seven to ten days following a cartilage injury, a number of chondrogenic progenitor cells (CPCs) were observed in a superficial zone in cartilage. The CPCs were morphologically elongated in shape, in contrast to the normal chondrocytes (NCs) which remained round in shape (Fig. 3.3 A1 and A2; higher magnification). The superficial zone specific CPCs were isolated by trypsinization for 20 minutes (Fig. 3.3 B1 and B2, before and after trypsinization). Yet, NCs were not isolated by trypsinization in non-injured cartilage and no considerable morphological changes were observed before and after trypsinization (Fig. 3.3 C1 and C2, before and after trypsinization).

3.4.3 Intrinsic CPC homing ability in injured cartilage and its acceleration by ultrasound stimulation

Fourteen days following a partial thickness cartilage injury, the effect of consecutive low intensity ultrasound stimulation for 20 minutes daily was significant. At day 0, immediately after cartilage defects creation, no CPCs were found in defect sites (Fig. 3.4 A1 and B1). After 14 days very few CPCs were found in the defect sites of the untreated control (Fig. 3.4 A2). However, consecutive 14 days of ultrasound stimulated cartilage showed significantly higher numbers of CPCs was observed and repopulated in defect sites (Fig. 3.4 B2). Similarly, in the partial thickness cartilage defect model, obviously few CPCs were found immediately after full cartilage defects creation (Fig. 3.4 C1 and D1). Low intensity ultrasound applied for cartilage for 7 consecutive days and

significantly higher numbers of CPCs was found in fibrin-hydrogel injected defect sites (fig. 3.4. D2). However, no meaningful difference was found in ultrasound untreated control group (Fig. 3.4 2).

3.4.4 Ultrasound therapy triggered mechanotransductive pathways in CPCs

When cells are received extracellular bio- mechanical and chemical changes, integrins cluster each other and proteins underneath the integrins start forming focal adhesion complex. Focal adhesion kinase (FAK) is activated and relay signals to its downstream factors including Src family kinases (SFKs), Ras family of GTPases, Phosphoinositide3 kinase, Cell division control protein 42 homolog (CDC42) and Ras-related C3 botulinum substrate (RAC) to modulate cytoskeletal alterations or gene transcription (Fig. 3.5).(159)

3.4.4.1 FAK phosphorylation in CPCs by ultrasound stimulation

Phospho-protein analysis by western blot revealed that FAK phosphorylation showed ultrasound parameter dependent activation. FAK activation was compared by adjusting ultrasound parameters; frequencies were set at 1, 3.5 and 5 MHz, intensities were set at approximately 15 or 30 mW/cm^2, and duration of either 5 or 20 minutes (Fig. 3.6 A). The statistic analysis of quantified integrated density revealed that FAK phosphorylation was significantly enhanced by ultrasound stimulation and the FAK activation was maximized at 3.5 MHz and 27.5 mW/cm^2 ($p=0.045$, Fig. 3.6 B).

3.4.4.2 Time course of FAK activation in response to ultrasound therapy and its combined effect with chemoattractants.

Time course of FAK activation was examined at post 0, 5 and 30 minutes following ultrasound stimulation. The results indicate that FAK phosphorylation

increased a little immediately after ultrasound stimulation and this became apparent at post 5 minutes and significant at post 30 minutes, compared to untreated control group (Fig. 3.7 A) To compare FAK activation in response to ultrasound stimulation and the combined effect with chemoattractants, 100 nM HMGB1 or 10 nM fMLF was added immediately after ultrasound stimulation. The results showed that ultrasound alone ($p=0.004$) and 10 nM fMLF with ($p=0.003$) or without ultrasound stimulation ($p=0.005$) significantly enhanced phosphorylation of FAK respectively, while HMGB1 had no effect (Fig. 3.7 B and C).

3.4.4.3 Downstream factors of FAK and ultrasound therapy triggered mechanotransductive pathways in NCs and CPCs

Activation of Rho family of GTPases was targeted as downstream factors of FAK since this protein family is often likely to be activated with integrins associated FAK signaling pathway. The results indicated that ultrasound stimulation activated Rho proteins as well as phosphorylation of rac1 and cdc42, which are known to be closely associated with actin polymerization and cellular directional movement. The pattern of the protein family activation in response to ultrasound is somewhat different between CPCs and NCs. It was found that ultrasound stimulation was little more sensitive in CPCs than NCs that FAK and Rho family of GTPases in CPCs was noticeable activated while it failed to activate them in NCs (Fig. 3.8).

3.4.5 Suppression of CPC motility by focal adhesion inhibition

Western blot results showed that Src family kinases (SFKs) inhibitors reduced FAK phosphorylation at Tyr 576/577 in a dose dependent manner (Fig. 3.9 A). To

examine the effect of CPC motility in response to FAK blockage by SFK inhibitor treatment, a monolayer wound healing assay and a cell invasion assay kit were performed. Monolayer wound healing assay results showed that the motility of CPCs was reduced by the SFKs inhibitor in a dose dependent manner (Fig. 3.9 B and C). Three dimensional cell invasion assay kit results confirmed that CPC motility was enhanced by ultrasound stimulation ($p=0.004$) and abolished by 10 μM SFKs inhibitor ($p=0.001$) (Fig. 3.9 D).

3.4.6 The effects of focal adhesion activation or inhibition on chondrocyte mortality following an impact induced cartilage injury.

The effect of ultrasound stimulation on FAK activation was first examined for whether increased FAK phosphorylation leads to chondrocyte mortality following a blunt impact induced cartilage injury. Secondly, inhibition of focal adhesion by treating the cartilage with either FAK or SFK inhibitor was evaluated to see if focal adhesion blocks reduce chondrocyte death. Cell viability in intact cartilage was approximately 100%; however, the viability dropped to approximately 60% following an impact induced cartilage injury. FAK activation induced by ultrasound pre-stimulation resulted in no effect with respect to cell viability following an impact induced cartilage injury. However, focal adhesion blocks induced by treatment with FAK or SFK inhibitors significantly prevented injury induced massive chondrocyte death; cartilage treated with 10 μM SFK inhibitor, 10 or 100 μM FAK inhibitor all recovered up to 80% of cell viability (Fig. 3.10).

Cell viability was examined in all tested groups at post 24 hours following an impact induced cartilage injury and the results showed that overall viability declined approximately 30% more in each groups. However, non-impact induced cartilage

maintained its viability almost 100%. All of other tested groups showed higher cell viability compared to injured control cartilage. Statistical analysis revealed that only 100μM FAK inhibitor treated cartilage was the only treatment that had a statistically significant effect (Fig. 3.11).

3.4.7 Kinetics of FAK and SFK inhibition

To confirm the dose-response inhibitory effects of focal adhesion complex member proteins, FAK and SFKs, by chemical inhibitors, FAK and SFK inhibitors, kinetics of FAK and SFK inhibition were examined. First, SFK phosphorylation was induced by treatment with IL-1β and TNF-α and 0.1, 1 and then 10 μM SFK inhibitor was treated. The results demonstrated that 10 ng/mL IL-1β and 100 ng/mL TNF-α considerably enhanced SFK activation while SFK inhibitor suppressed it in dose-dependent manner (Fig. 3.12 A and B). To activate FAK phosphorylation at auto-phosphorylation site, tyrosine 397, 100 nM fMLF was treated. However, no noticeable FAK activation was observed and both 1 and 10 μM FAK inhibitor treatment showed no effect with respect to FAK suppression. Only 100uM of FAK inhibitor treatment significantly suppressed FAK phosphorylation (Fig. 3.12 C and D).

3.4.8 The effects of ultrasound therapy on ROS production in articular cartilage

3.4.8.1 The enhancement of ROS production by LIPUS following an impact induced cartilage injury.

Immediately after cartilage injury, low intensity pulsed ultrasound (LIPUS) was applied for 60 minutes and cartilage tissue was stained with 1 μM of Calcein-AM, a live cell indicator, and 5 μM dihydroethidium (DHE), a superoxide indicator. Confocal microscopy was performed to quantify ROS production in articular cartilage and the

results revealed that percentage of ROS production was around 2% in non-injured cartilage with or without LIPUS stimulation. Impact induced cartilage injury significantly enhanced ROS levels up to 10% and this was further increased by LIPUS stimulation for 60 minutes up to 20% (Fig. 3.13).

3.4.8.2 LIPUS duration dependent ROS production following an impact induced cartilage injury

In the absence of LIPUS stimulation, there was no noticeable correlation between ROS production and the time post impact induced cartilage injury. However, LIPUS stimulation following an impact induced cartilage injury showed that the overall levels of ROS production were higher than impact induced control group. The duration of LIPUS stimulation explains 68% of variance in superoxide production when fitting a linear regression (Fig. 3.14).

3.4.8.3 Cytotoxicity of produced ROS by LIPUS stimulation following an impact induced cartilage injury

Cell viability was examined after 24 hours in both center and edge of impact sites following an impact induced cartilage injury. The results indicated that there was no considerable cell viability difference between impact-control and impact with LIPUS stimulated groups (Fig. 3.15).

3.4.8.4 Source of ROS enhancement by LIPUS stimulation in injured cartilage

To understand the role of increased ROS by LIPUS stimulation in chondrocytes, the source of ROS was examined by discriminating either intracellular or extracellular in chondrocytes by counting ROS that are

overlapped with chondrocytes that stained with live cell indicator. The results demonstrated that LIPUS stimulated intracellular ROS production, which was up to 60 minutes of duration, compared to control group. However, this effect was diminished with 90 minutes of LIPUS stimulation (Fig. 3.16A). Extracellular ROS were not considerably different in cartilage exposed to LIPUS up to 60 minutes but the difference became noticeable with LIPUS stimulation for 90 minutes (Fig. 3.16B). However, no statistical significance was found (Fig. 3.16).

3.4.8.5 Enhanced ROS production by LIUS stimulation following an impact induced cartilage injury

Low intensity continuous ultrasound (LIUS) stimulation was also applied for 5 minutes following an impact induced cartilage injury and cartilage tissue was stained with 1 μM of Calcein-AM, a live cell indicator, and 5 μM dihydroethidium (DHE), a superoxide indicator. Confocal microscopy was performed to quantify ROS production in articular cartilage and the results revealed that percentage of ROS production was around 2% in non-injured cartilage and LIUS stimulation alone did not increase ROS production without cartilage injury. However, similarly to LIPUS stimulation, LIUS stimulation significantly increased ROS production following a cartilage injury; ROS levels were over 20% in LIUS stimulation and 10% in control group (Fig. 3.17). However, no considerable difference between control and LIUS stimulated cartilage without impact injury was observed (Fig. 3.17).

3.4.8.6 Induced ROS production by ultrasound therapy in intact cartilage

Since no ROS production was found in intact cartilage by low intensity pulsed and continuous ultrasound stimulation, the effects of higher ranges of ultrasound intensities up to 10W/cm^2 on ROS production with respect to the intensity of DHE stain were investigated. Confocal microscopy results showed that 10 W/cm^2 of pulsed ultrasound therapy significantly enhanced intracellular ROS intensity compared to untreated control (Fig. 3.18). Post 24 hours of cell viability examination revealed that the ultrasound therapy induced ROS production had no cytotoxic effect on the cartilage (Fig. 3.19).

3.4.8.7 Suppression of ROS production by ultrasound therapy by anti-oxidant treatment

To confirm that the enhancement of intracellular ROS intensity was as a result of oxidants production, cartilage was treated with 20μM or 2mM of N-acetylcysteine (NAC) during ultrasound therapy. The results showed that NAC treatment significantly suppressed ultrasound therapy induced ROS intensity while no noticeable effects of NAC treatment was found without ultrasound therapy.

3.4.9 The effects of ultrasound therapy induced ROS production on ATP synthesis

Since ultrasound therapy induced ROS production did not lead to chondrocyte death in cartilage, the relationship between ultrasound induced ROS production and ATP synthesis was investigated. First, relatively higher intensity of ultrasound, 2.5 or 10 W/cm^2, was applied to intact cartilage as enhancement of

ROS was observed at this range. However, the results showed that no noticeable difference of ATP synthesis in response to the ultrasound exposure was found compared to control group. And the effects of lower intensity of ultrasound, below 1 W/cm^2 with adjustment of ultrasound parameters such as duty cycle, ultrasound duration and pulse repetition frequency on ATP synthesis were investigated. However, the results indicated that ultrasound had no significant effects on ATP synthesis regardless of pulse duty cycle, pulse repeat, duration or a number of stimulation per day (Fig. 3.22).

Articular cartilage origin-dependent ATP production in response to ultrasound therapy was investigated to see if there was the sensitivity of ultrasound therapy depending on physical location of articular cartilage. The results showed no significant difference of ATP production in cartilage harvested from lateral tibia plateau in response to ultrasound stimulation was found. However, a noticeable ATP production in cartilage from medial tibia plateau in response to ultrasound stimulation was found while this was not statistically significant (Fig. 3.23).

To verify the sensitivity of ATP production in response to ultrasound stimulation in cartilage, PG contents in cartilage originated from the lateral or medial tibia plateau were compared. The results showed similar patterns to ATP synthesis was found that the PG amount was slightly higher in the medial tibia plateau after ultrasound stimulation, there was no noticeable PG amount difference was observed in cartilage from lateral tibia plateau. However, no statistical significance was found (Fig. 3.24).

3.5 Discussion and conclusions

There have been frequent attempts to use low intensity ultrasound therapy to stimulate cartilage repair and studies have shown that ultrasound stimulates cartilage anabolism by enhancing the production of matrix molecules including proteoglycan and collagen.(32, 34-37, 134) Ultrasound therapy has also been proven to be effective in attenuating the progression of cartilage degradation *in vivo* and proposed as a tool for chondrogenesis of mesenchymal stem cells (MSCs) for cartilage repair.(38-43) However, progress in understanding the mechanism of these effects has been slow and a few detailed biologic mechanisms have been unveiled including hyperthermal effect, cavitational effect or triggering mechanotransduction pathways.(44-48) However, these known mechanisms are unable to fully explain how ultrasound acts as an anabolic stimulator. Therefore, low intensity ultrasound therapy was further investigated as a mechanical stimulator that can trigger mechanotransductive signaling pathways by transporting a form of mechanical energy non-invasively in articular cartilage.

Previous studies have demonstrated that chondrogenic progenitor cells (CPCs) are emerged following a cartilage injury and they are highly clonogenic, motile and chemotactic. In response to cartilage injury CPCs tend to migrate toward the injured site from nearby healthy cartilage, which leads to repopulation of the matrix within 7-14 days. The CPCs exhibit significantly higher expression of cell motility involved genes and their chemotaxis by chemo-attractants was remarkably higher than normal chondrocytes. Thus it was presumable that enhanced CPC homing into injured sites could be responsible for initiating the repair of injured cartilage by replenishing extracellular matrix (ECM)

macromolecules such as proteoglycans, collagen fibers.(31) Therefore, it has been hypothesized that mechanical stimulation by low intensity ultrasound therapy promotes the homing ability of CPCs toward injured sites in articular cartilage *via* triggering mechanotransductive cell signaling pathways. This may speed up the return to normal cellularity in injured cartilage by accelerating cartilage matrix repair and opposing the progression of OA.(35-39, 95)

Dynamically regulated adhesion between cells and ECM is critical for cell motility as well as proliferation, differentiation and survival.(139, 140) The formation and turnover of integrin-associated focal adhesion complexes is regulated not only by cytoskeleton-linked proteins such as talin, vinculin, α-actinin and paxilin, but also by intracellular signaling proteins such as focal adhesion kinase (FAK), c-Src, protein kinase C (PKC), phosphatidylinositol 3 kinase (PI3K) and Rho kinase (ROCK).(135, 160-166) Integrins trigger signal transduction *via* tyrosine phosphorylation and there is substantial evidence showing that FAK is a major player in relaying signals from integrins to downstream factors, which in turn causes cell motility.(137, 138, 141-145, 167-169) Focal adhesion associated protein tyrosine kinases such as FAK and Src family kinases (SFKs) play significant role in cell motility.(170, 171) Directional cell migration is critical instance for living organisms to maintain homeostasis or immune response. N-formyl-methionyl-leucyl-phenylalanine (fMLF) and High-mobility group protein B1 (HMGB1) are well known chemo-attractants involved in directional cell migration toward target location.(172-175)

In this study, CPCs were harvested from injured cartilage and the effect of FAK activation on their motility was investigated in response to low intensity ultrasound

stimulation. Among the tested combinations of intensity and frequency, ultrasound delivered at 3.5 MHz and 27.5 mW/cm^2 was optimal in terms of inducing FAK activation. Considered that only 30 % of CPCs were within the field of ultrasound stimulation due to the difference between the effective area of transducers and the area of 6-well cell culture plate, it is expected that FAK activation in CPCs by ultrasound would be greater if all CPCs were stimulated. FAK was also significantly activated by treatment with fMLF, a mitochondrial alarmin ($p=0.003$).(172-174) In the explant model, fMLF and other factors released from dead chondrocytes appear to initiate CPC migration in the immediate aftermath of impact; however, this effect is unlikely to be sustained for more than 48 hours due to spontaneous degradation of the factors.(30) In contrast, ultrasound stimulation was repeated daily throughout the experiment. Thus, it seems probable that the greater number of migrating CPCs found on ultrasound-treated explants was due to continued stimulation of FAK phosphorylation after peptide chemotactic factors had cleared.

In partial thickness cartilage injuries, increased numbers of CPCs in the ultrasound stimulated half of cartilage tissue were observed, while few CPCs migrated in the ultrasound blocked half.(98) This result suggests that optimized ultrasound stimulation enhances FAK phosphorylation of CPCs in cartilage, resulting in increased migratory activity. Cell migration assay results confirmed that ultrasound stimulation significantly enhanced CPC migration compared to ultrasound un-stimulated control group ($p=0.004$). SFKs inhibitor has been well studied for its inhibitory effect on phosphorylation and activation of FAK at Tyr 576/577. Current understanding suggests that inhibited recruitment of SFKs leads to block FAK phosphorylation at Tyr 576/577

which triggers signaling pathway for cell migration.(146-148, 176, 177) SFKs inhibitor also blocked ultrasound-induced increases in chemotaxis in transwell assays where migrating cells were required to invade a 3-dimensional collagen matrix, and in monolayer scratch assays where migration was unhindered by matrix. Recent evidence suggests that triggering integrin mediated mechano-transduction pathways is regarded as one of the mechanisms of therapeutic ultrasound. The findings in this study can support that enhanced migratory activity of CPCs *via* FAK activation in response to low intensity ultrasound therapy is closely associated with mechano-trasduction pathways. However, the effect of thermal, cavitation and standing waves during ultrasound stimulation cannot be excluded even though they are unlikely associated.(44, 45, 97) Whether repopulation improves cartilage repair depends on the ability of CPCs to re-establish a functional cartilage matrix *in situ*, which remains unproven. It may be advantageous to follow pro-migratory ultrasound treatment with treatments designed to encourage chondrogenic differentiation and discourage chondrolytic activity. In any event, the findings described here justify further research to determine the potential for ultrasound to oppose the initiation and progression of OA.

Considerable clinical and experimental evidence shows that acute severe joint injuries and excessive repetitive mechanical loading due to post-injury joint incongruity and instability cause post-traumatic osteoarthritis, and that excessive repetitive loading in uninjured joints causes osteoarthritis.(178, 179) Since chondrocytes are responsible for maintaining the ECM by producing collagens, proteoglycans and glycoproteins, and the cells have limited ability to replace themselves in adults, significant chondrocyte death from cartilage mechanical injury is likely to initiate cartilage degradation which could

lead to osteoarthritis. Moreover, recent work suggests that chondrolytic factors such as matrix metalloproteinases (MMPs), tumor necrosis factor (TNF) and a disintegrin and metalloproteinase with thrombospondin motifs 5 (ADAMTS-5) are highly up-regulated in cartilage injury sites *via* activating mitogen-activated protein kinases (MAP kinases) such as p-38 and ERK 1/2 which are closely associated with propagation of chondrocyte death.(64) Also it was suggested that mechanical insults to articular cartilage result in massive chondrocyte death through necrosis or progressive intracellular signaling cascades that lead to apoptosis.(25-28) Other studies have shown that rapid production of reactive oxygen species (ROS) immediately after cartilage mechanical injury leads directly to massive chondrocyte death. Immediate or delayed treatment with N-acetylcysteine, a free radical scavenger, and rotenone, an electron transport chain inhibitor, significantly reduce the level of ROS, which result in increased chondrocyte survival. These findings demonstrate that mitochondria may be responsible for the injury induced ROS production that leads to chondrocyte death following mechanical injury due to oxidative stress.(29, 30) In addition, pre-treatment with cytochalasin-B or nocodazole, which block formation of contractile microfilaments and microtubules, significantly decreased chondrocyte death suggests that relief of cytoskeletal tension enhanced the survivability of chondrocytes in impact-injured cartilage.(74) Taken together, these previous works show that cartilage injury releases mediators that cause chondrocyte death and ECM degradation and suggest that immediate intervention to stop progressive chondrocyte death after cartilage injury may prevent articular cartilage from progressive degradation that can lead to osteoarthritis.

Focal adhesions, a protein complex underneath of cellular attachment to ECM, play a role in not only for providing a biochemical signaling hub *via* tyrosine phosphorylation, but also for carrying out cellular activities such as migration, proliferation and gene expression.(139, 140, 160, 163, 166, 180-182) Integrins are a class of transmembrane receptors that cluster in response to mechanical and chemical changes in the ECM to form adhesions which involve multiple intracellular kinases and structural proteins, some of which link integrin complexes to the cytoskeleton.(135-138, 167) Therefore, it has been hypothesized that treatment with FAK and SFK inhibitors would significantly reduce chondrocyte death induced by impact injury, which causes excessive strain.(125, 183-186)

Cell viability without injury remained at almost 100% during experiments while it declined approximately 60% following an impact induced cartilage injury and further reduced to 40% after 24 hours. First, the effect of FAK activation by low intensity ultrasound stimulation on cell viability following cartilage injury was examined. The results showed that no considerable cell viability difference between impact-control group and low intensity ultrasound stimulated group was found at either time points. To examine the inhibitory effect of focal adhesions on cell death following cartilage injury, articular cartilage was treated with FAK inhibitor at concentrations of 10μM and 100μM and SFK inhibitor at a concentration of 10μM since the concentrations have been shown to diminish the activation of FAK and SFKs by blocking tyrosine phosphorylation.(187-190) Phosphoprotein analysis confirmed that tyrosine phosphorylation was diminished by pre-treatment of inhibitors for FAK or SFK, supporting the conclusion that inhibiting the

formation of focal adhesions by blocking phosphorylation of FAK or SFKs decreased massive cell death following an impact induced cartilage injury.

The decrease in cell viability over the 24 hours following impact is striking: from 59% to 34% in untreated control samples ($p<0.001$), from 80% to 48% in 10μM SFKi treated samples ($p<0.001$), from 77% to 45% in 10μM FAKi treated samples ($p<0.001$), and from 82% to 56% in 100μM treated samples ($p<0.001$). The decrease in viability 24 hours after impact was also found in previous studies and suggests that mechanical insults to cartilage cause acute chondrocyte necrosis and subacute apoptosis.(30) Although it did not appear that the FAK inhibitor blocked FAK activation in a clear dose-dependent manner, FAK activation was significantly reduced at a concentration of 100μM. This suggests that the autophosphorylation of FAK at Tyr 397 was activated by some other unknown factors and that 100nM fMLF failed to stably stimulate its phosphorylation. However, of the tested doses only 100μM FAKi significantly blocked its activation. Although the data suggest that acute inhibition of focal adhesions might decrease progressive cell death, only 100μM FAKi rescued significantly more chondrocytes 24 hours after impact. These data are consistent with the previous observation that cytoskeletal dissolution reduced impact-associated cell death and support the hypothesis that joint surface impact causes chondrocyte death by inducing the activation of a mechanotransduction pathway that transmits extracellular strains to intracellular organelles *via* integrins and the cytoskeleton. Further advances in understanding the mechanisms by which mechanical forces cause cartilage loss would have the potential to lead to new treatments of injured joints that could decrease the risk of OA following joint injuries.

Although detailed biologic mechanisms of low intensity ultrasound therapy have not been yet fully elucidated, a number of studies have suggested that ultrasound stimulates cartilage repair by enhancing the production of matrix molecules including proteoglycan and collagen.(32, 34-37, 134) Chondrocytes obviously require ATP, an energy-bearing molecule, to maintain cartilage matrix integrity or turnover. However, the levels of ATP in cartilage are always low and in demand since chondrocytes run their metabolism dominantly *via* a glycolytic pathway for ATP supply rather than through oxidative phosphorylation to maintain cartilage matrix integrity as a result of low level of oxygen supply.(149-153) Thus, the phenomenon of ultrasound driven cartilage repair could be explained by energy modulation of chondrocytes in response to low intensity ultrasound stimulation. Recent findings demonstrated that ROS can be a double-edged sword in articular cartilage. Excessive production of ROS following a cartilage injury resulted in progressive chondrocyte death due to oxidative stress. In contrast, moderate levels of ROS production in articular cartilage in response to mild levels of mechanical stimulation supports chondrocyte metabolism by enhancing ATP synthesis, which suggests that induced ROS supports glycolysis by producing ATP.(154, 155) Thus, all things considered, low intensity ultrasound stimulation may have the potential to be used as a mechanical stimulator to induce modest ROS production and stimulating ATP synthesis *via* a glycolytic pathway in chondrocytes. On the other hand, ultrasound stimulation may suppress excessive ROS production following a cartilage injury which could prevent progressive chondrocyte death. For these reasons, the effect of low intensity ultrasound therapy on the level of ROS production was first

examined following an impact induced cartilage injury and then the effects of low intensity ultrasound therapy as a mechanical stimulator which modulates energy production was investigated in intact articular cartilage.

LIPUS stimulation at 25 mW/cm^2 of intensity for 60 minutes, no considerable ROS production was observed in intact articular cartilage. However, LIPUS stimulation at 25mW/cm^2 of intensity for 60 minutes, following a blunt impact induced cartilage injury, produced almost 2 fold increase in ROS production compared to the control group. Cell viability 24 hours after LIPUS stimulation revealed that the enhanced ROS was not toxic for chondrocytes following a cartilage injury; no noticeable cell viability difference between the LIPUS non-treated control group and LIPUS stimulated group was found. Following a cartilage injury, ROS production was gradually increased over time in the untreated control group; however, LIPUS stimulation accelerated overall levels of ROS production. The duration of exposure to LIPUS explains 68% of the variance in ROS production when this result was fitted to a linear regression. To examine a functional role of the enhanced ROS levels after LIPUS stimulation following a cartilage injury, the origin of ROS was examined to see if they were intracellular or extracellular. This was done by counting ROS that overlapped with chondrocytes that stained with live cell indicator since intracellular ROS may have close correlations with ATP synthesis *via* glycolysis. Further analysis revealed that LIPUS stimulation increased intracellular ROS production compared to the untreated control group. The difference was apparent at 30 and 60 minutes of LIPUS; however, this was diminished at 90 minutes of LIPUS. Although these results have no statistical significance, it may suggest that LIPUS stimulation has the potential to attenuate cartilage degeneration following a

cartilage injury by modulating energy production such as ATP *via* ROS consumption in glycolysis.

In non-injured intact cartilage, LIPUS less than 50 mWcm^2 had no effect on ROS production. Thus intact cartilage was exposed to higher intensity of ultrasound therapy, above 1 W/cm^2, to see if there was an induced ROS production which may result in cartilage energy modulation.

All of the ultrasound parameters tested was safe with respect chondrocyte viability after 24 hours. First, ultrasound therapy with 10 W/cm^2 of intensity was applied for 1 minute in intact cartilage and the results showed that the intensity of ROS in live chondrocytes was significantly higher than untreated control group. The ultrasound therapy induced ROS production was suppressed by treatment with NAC suggesting that ultrasound exposure induced the production of intracellular ROS in chondrocytes. Since ROS production was significantly increased by ultrasound stimulation without considerable cell death, ATP production was evaluated to see if enhanced ROS production was related to a glycolysis pathway in chondrocytes. However, no noticeable changes in ATP were found in response to intensities of 2.5 and 10 W/cm^2. Further investigation continued with a lower intensity of ultrasound (below 1 W/cm^2), adjusted duty cycle of pulse, duration of ultrasound, different time points after ultrasound and ultrasound exposure for a week. However, no meaningful ATP production changes were found. Although ultrasound stimulation with the 5% duty cycle for 20 minutes increased ATP production compared to untreated control group, this was not statistically significance. Further analysis of cartilage origin-dependent ATP production was investigated to see if ATP synthesis in

response to ultrasound stimulation may depend on physical origins of a cartilage, such as lateral and medial tibia plateau. The results indicated that ultrasound stimulation had no effect on ATP synthesis in cartilage from the lateral tibia plateau whereas there was a noticeable increase in ATP synthesis in cartilage from medial tibia plateau. However, this was not statistically significant. PG contents in cartilage from both lateral and medial tibia plateau were evaluated and the amount of PG was higher in ultrasound stimulated cartilage from medial tibia plateau compared to control group; however, there was not noticeable difference in cartilage from lateral tibia plateau. The pattern of PG and ATP production seems to be similar; however, the increase was not statistically significant. It is unclear yet ultrasound increased PG synthesis in medial cartilage or ATP production was enhanced by higher amount of PG. In either case, these data suggest that biologic effect of ultrasound stimulation may depend on the thickness of cartilage or ultrasound properties such as wavelength or duty cycles.

In conclusion, the beneficial effects of ultrasound therapy for cartilage repair were investigated to identify the underlying mechanisms with a little different point of view compared to others. Low intensity ultrasound therapy following cartilage injuries accelerates the homing of chondrogenic progenitor cells toward injured sites *via* triggering mechanotransductive cell signaling pathways. Integrins associated focal adhesion complexes are activated by low intensity ultrasound therapy as well as downstream factor activation such as actin polymerization and directional movement related proteins. The low intensity

ultrasound therapy was evaluated with respect to an induction of beneficial ROS production that may result in enhancement of ATP production *via* a glycolytic pathway. However, no significant effects of low intensity ultrasound therapy on the energy modulation in articular cartilage were found in this study.

Figure 3.1 Configuration of ultrasound therapy system. (A) Versatile sweep function generator produces either continuous or pulsed waveforms. (B) Generated signal waves are amplified by a radio frequency power amplifier. (C) Various sizes, types and frequencies of ultrasonic transducers. Generated and amplified electrical signal waves are converted into mechanical ultrasound waves by ultrasonic transducers.

Figure 3.2. Ultrasound power measurement by a radiation force balance. An acoustic absorber placed on the balance absorbs almost 100% of ultrasound waves and the balance measures the weight caused by ultrasound power. http://www.npl.co.uk/

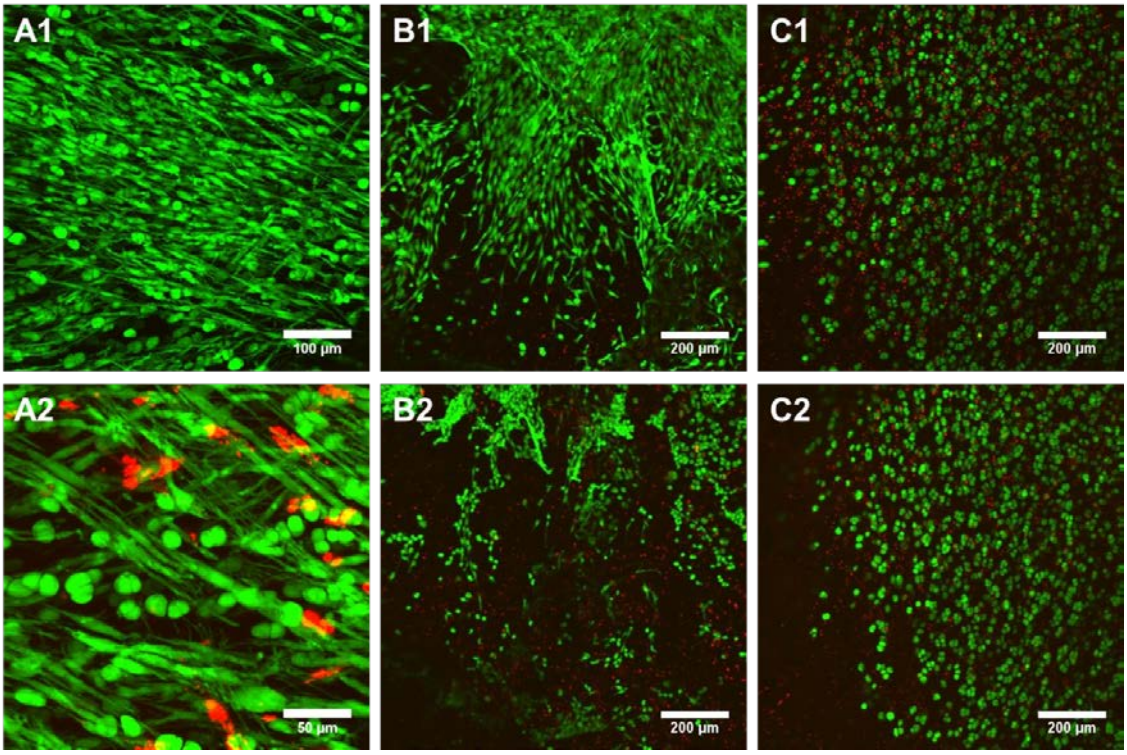

Figure 3.3. Morphology of CPCs in cartilage injury and isolation. (A) CPCs are elongated in shape (A1) and have morphologically different compared to normal chondrocytes which are round in shape (A2). (B) CPCs are isolated by trypsinization. Before trypsinization, abundant CPCs are populated in injured sites in cartilage (B1), however, immediately after trypsinization they are all isolated from cartilage surface (B2). (C) NCs are not isolated by trypsinization. Before trypsinization in non-injured sites in cartilage, NCs are the most cell type seen in cartilage (C1) and trypsinization did not isolated the NCs (C2). Bars in A1 = 100 µm, in A2 = 50 µm, in B and C = 200 µm.

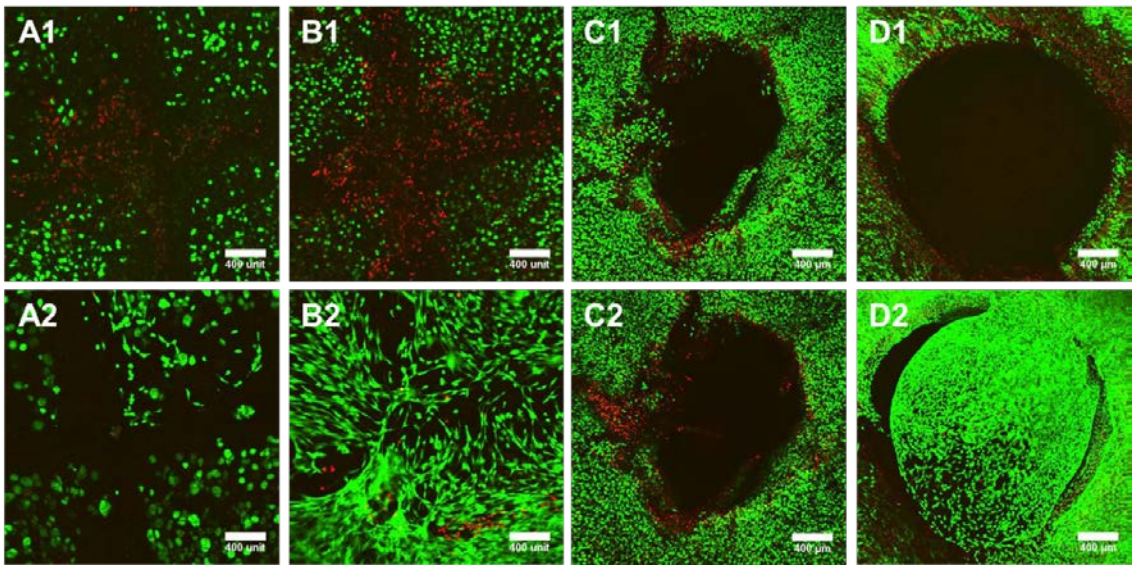

Figure 3.4. The effects of LIPUS stimulation on CPC homing ability toward injured sites in cartilage in partial and full thickness cartilage defect models. Confocal microscopy images showing live cells (green) and dead cells (red) in cartilage defects. (A and B) Partial thickness cartilage defect model. Massive chondrocyte death was found at day 0 immediately after partial cartilage defect creation (A1 and B1). After 14 days of un-treated control group, little CPCs were found in injured site in cartilage while significantly higher number of CPCs were migrated into injured sites in ultrasound stimulated cartilage (A2 and B2). (C and D) Full thickness cartilage defect filled with fibrin hydrogel model. No considerable CPC migration was observed in untreated control group at day 0 and 7. (C1 and C2) while significantly higher number of migrated CPCs into fibrin-injected cartilage defects observed in 7 consecutive ultrasound stimulated group at day 0 and 7 (D1 and D2). Bars = 400 µm.

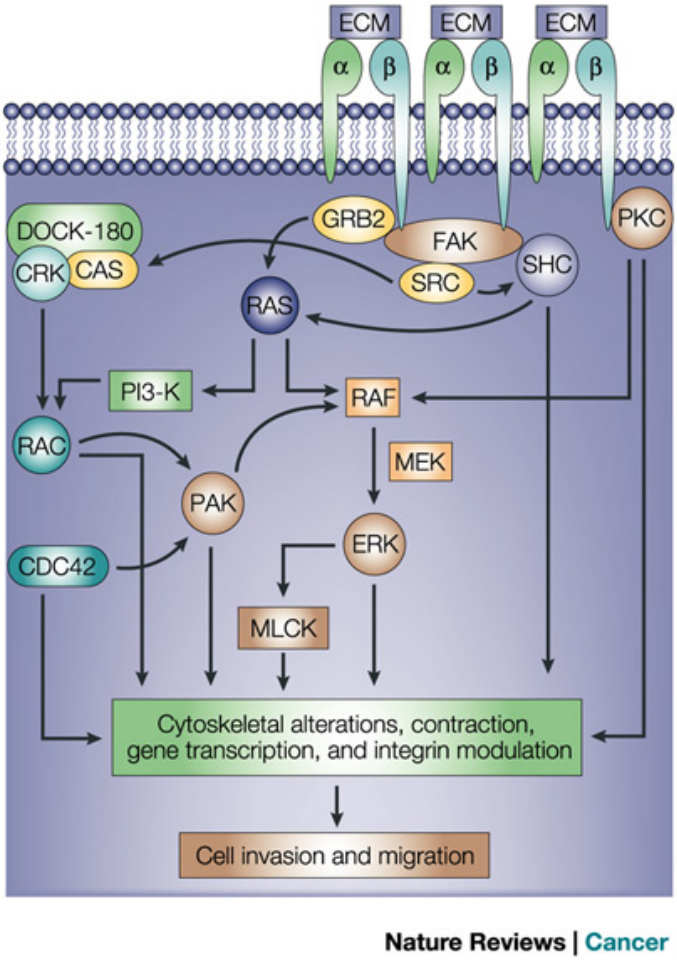

Figure. 3.5 Integrins triggered intracellular signaling regulation.(159) Integrin clustering by extracellular matrix changes activates downstream signaling factors such as foal adhesion kinase (FAK), growth facto receptor bound proteins 2 (GBR2), SRC, RAS, MEK, ERK and etc..

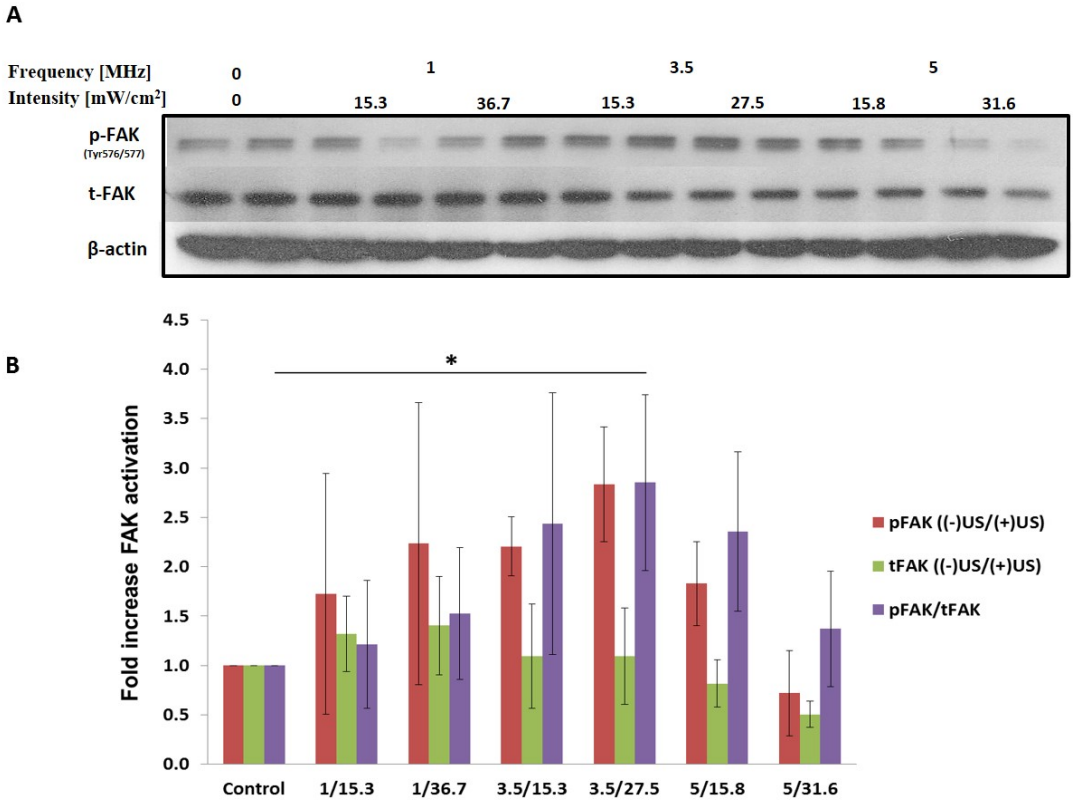

Figure 3.6. Ultrasound dose-dependent FAK phosphorylation in CPCs. (A and B) Western blot and its quantitated integrated density showing that FAK is activated depending on ultrasound dose. Comparing integrated density dependent on ultrasound dose, frequencies at 1, 3.5 and 5 MHz and intensities at approximately 15 or 30 mW/cm^2, FAK phosphorylation was maximized at 3.5 MHz and 27.5 mW/cm^2 (p=0.045). Row at the bottom represents LIPUS frequency [MHz]/intensity [mW/cm^2] as shown in Figure 3.6 B. Asterisk represents statistically significant (*p< 0.05).

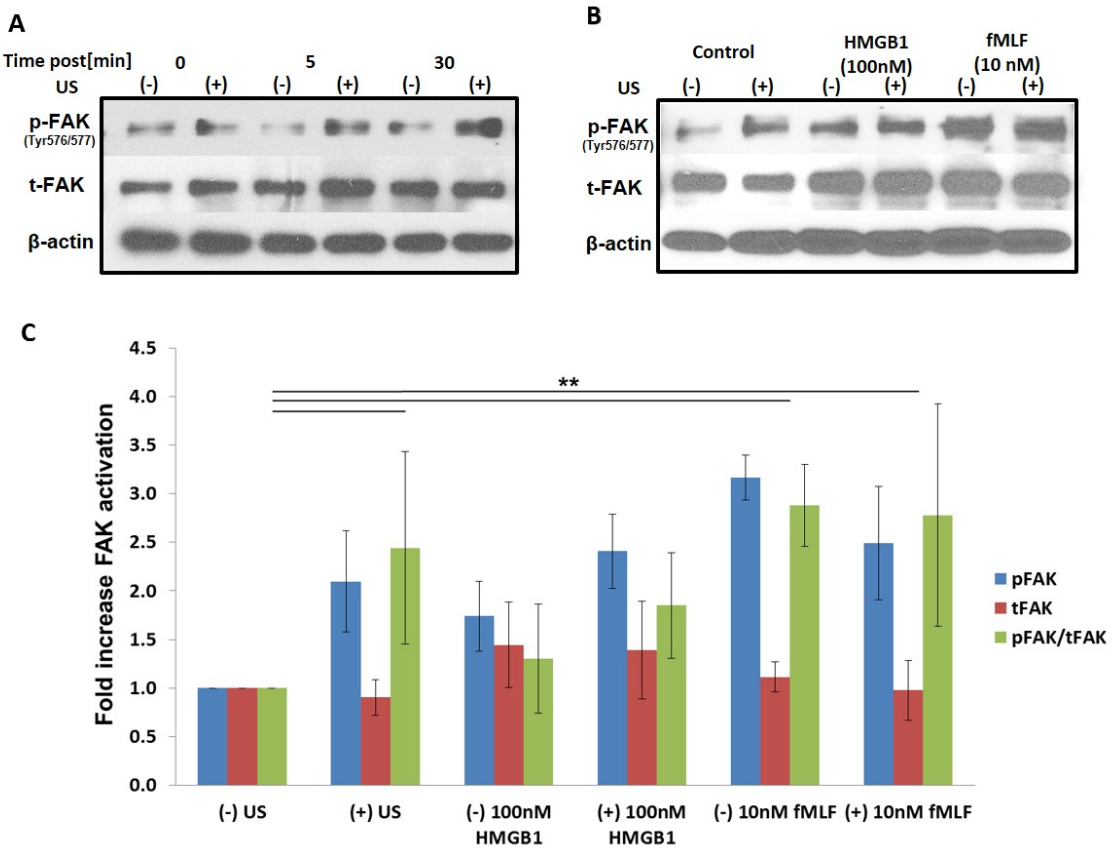

Figure 3.7. FAK phosphorylation in CPCs in response to ultrasound stimulation and chemo-attractants. (A) FAK phosphorylation was examined immediately after ultrasound stimulation showing that the difference of FAK activation became apparent after 5 minutes and significant after 30 minutes, compared to control group. (B and C), Enhanced FAK activation after 24 hours of ultrasound stimulation, 100 nM HMGB1 and 10 nM fMLF and its relative fold increase. LIPUS alone ($p=0.004$) and 10 nM fMLF with ($p=0.003$) and without ultrasound ($p=0.005$) significantly enhanced phosphorylation of FAK respectively, while HMGB1 showed no difference. (-) and (+) represent with or without ultrasound respectively and asterisk represents statistical significant (**$p<0.01$) Error bars represent sample variations (n=4-9).

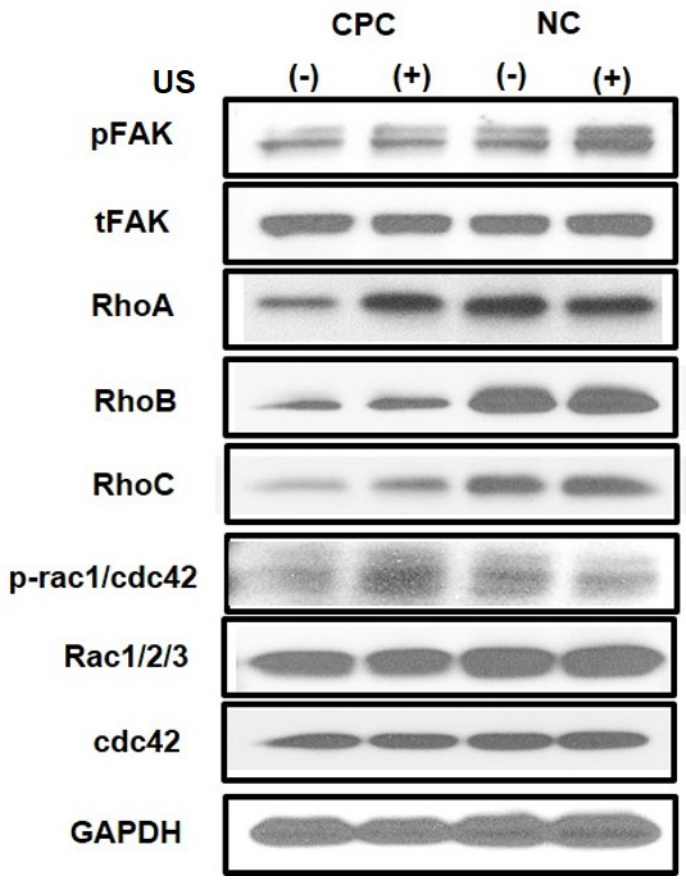

Figure 3.8 Ultrasound stimulation triggered cellular mechanotransductive signaling pathway. The effects of ultrasound stimulation on focal adhesion associated protein activation on NCs and CPCs was examined. CPCs were more sensitive to ultrasound stimulation rather than NCs by western blot analysis. Ultrasound activated FAK, Rho A, B and C, and phosphorylation of rac1 and cdc42 which are known to be associated with stress fiber and focal adhesion formation as well as directional movement of cells.

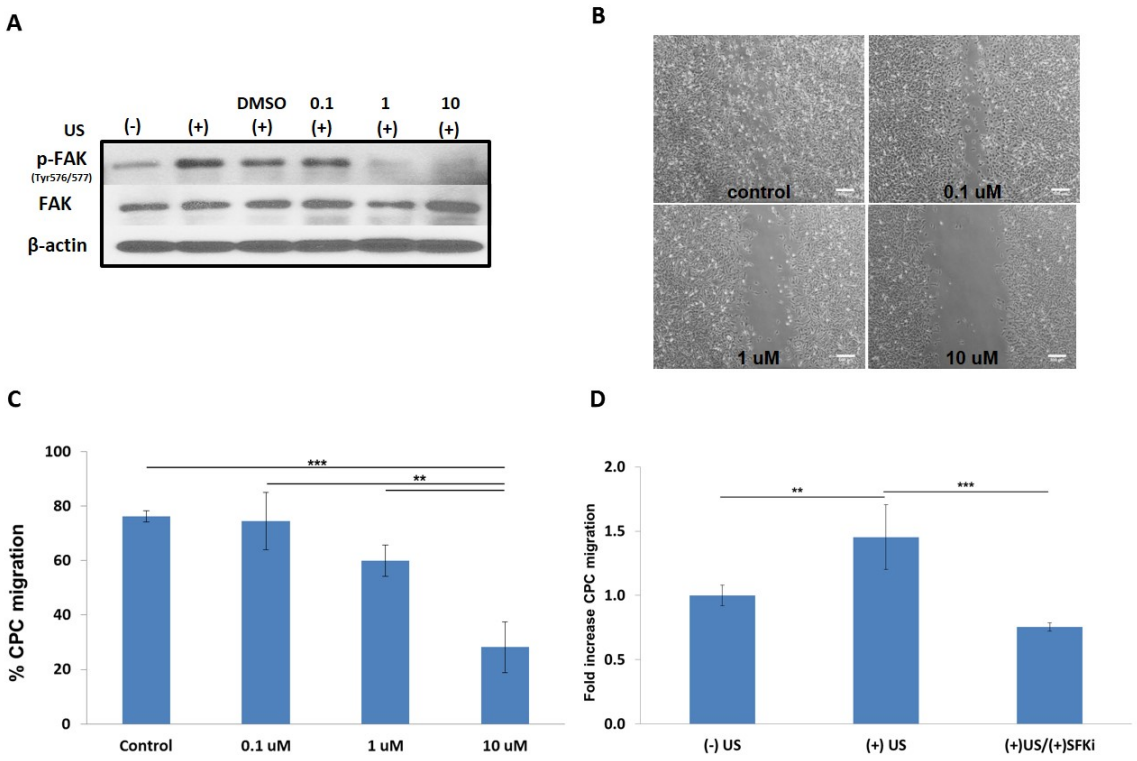

Figure 3.9 Inhibition of cell migration pathway by blocking FAK phosphorylation at tyrosine 576/577 by Src family kinases inhibitor (SFKi). (A) Western blot analysis showed that ultrasound stimulation induced FAK activation at kinase domain (Tyr 576/577) was suppressed by SFK inhibitor in dose-dependent manner. (B and C) The effect of SFK inhibitor on CPC migration in monolayer wound healing assay showed that CPC motility was suppressed by SFK inhibitor in dose-dependent manner. (D) Performance of cell invasion assay kit confirmed that CPC motility was enhanced by ultrasound stimulation ($p<0.001$) and abolished by 10 uM SFKs inhibitor ($p<0.001$). The column indicates the relative fold increase of CPC migration and the data are normalized to ultrasound-untreated control group. (-) and (+) represent with or without ultrasound respectively and asterisk represents statistical significant (**$p< 0.01$, ***$p<0.001$).

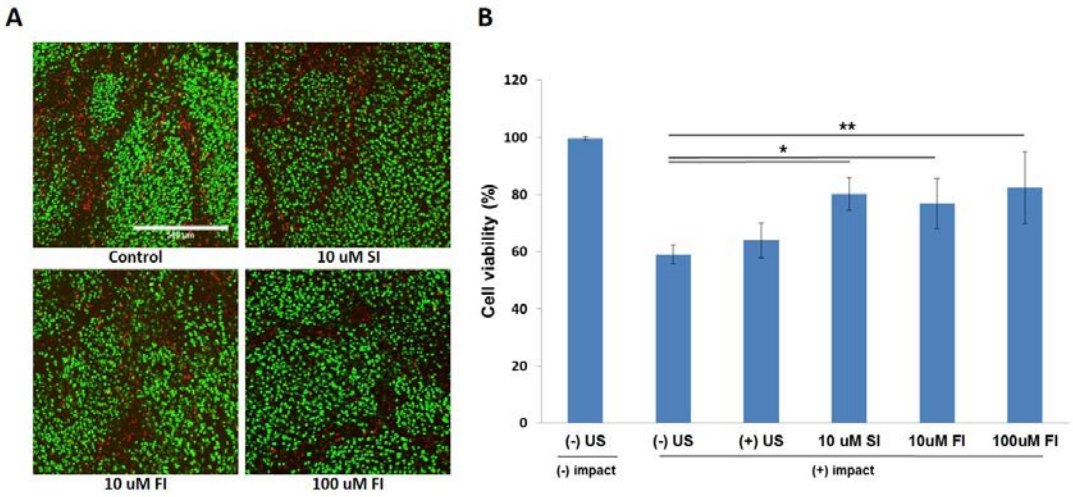

Figure 3.10 The effects of focal adhesion activation and inhibition on instant chondrocyte mortality following an impact induced cartilage injury. (A) Confocal microscopy shows live (green) and dead (red) chondrocytes in an impact site in an un-treated control explant, and in explants treated with 10 µM SFKi and either 10 or 100 µM FAKi. (B) Quantified cell viability revealed that blunt impact declined cell viability to around 60% and FAK activation by pre-ultrasound stimulation did not make any difference. However, focal adhesion inhibition by SFK or FAK inhibitor treatment recovered cell death approximately 80%. Between two tested concentrations, 100 µM FAKi was more effective than 10 µM. bar 500 um. Asterisk represents statistical significant (*p< 0.05, **p<0.01).

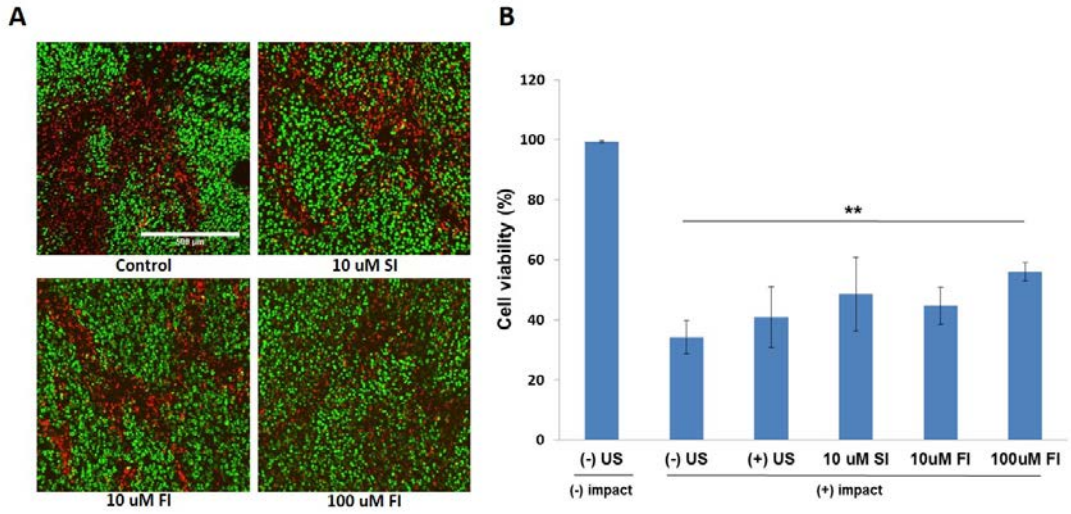

Figure 3.11 The effects of focal adhesion activation and inhibition on chondrocyte mortality at post 24 hours following an impact induced cartilage injury. (A) Confocal microscopy taken 24 hours post-impact shows that live (green) and dead (red) chondrocytes in an un-treated control explant, and in explants treated with 10 µM SFK inhibitor and either 10 or 100 µM FAK inhibitor. (B) Overall cell viability was declined following a cartilage injury, however, 100 uM FAK inhibitor treated group showed the highest chondrocyte viability among tested groups. Statistical analysis revealed that 100 µM FAK inhibitor treatment was the only group that had a statistically significant effect. Asterisk represents statistical significant (**$p<0.01$).

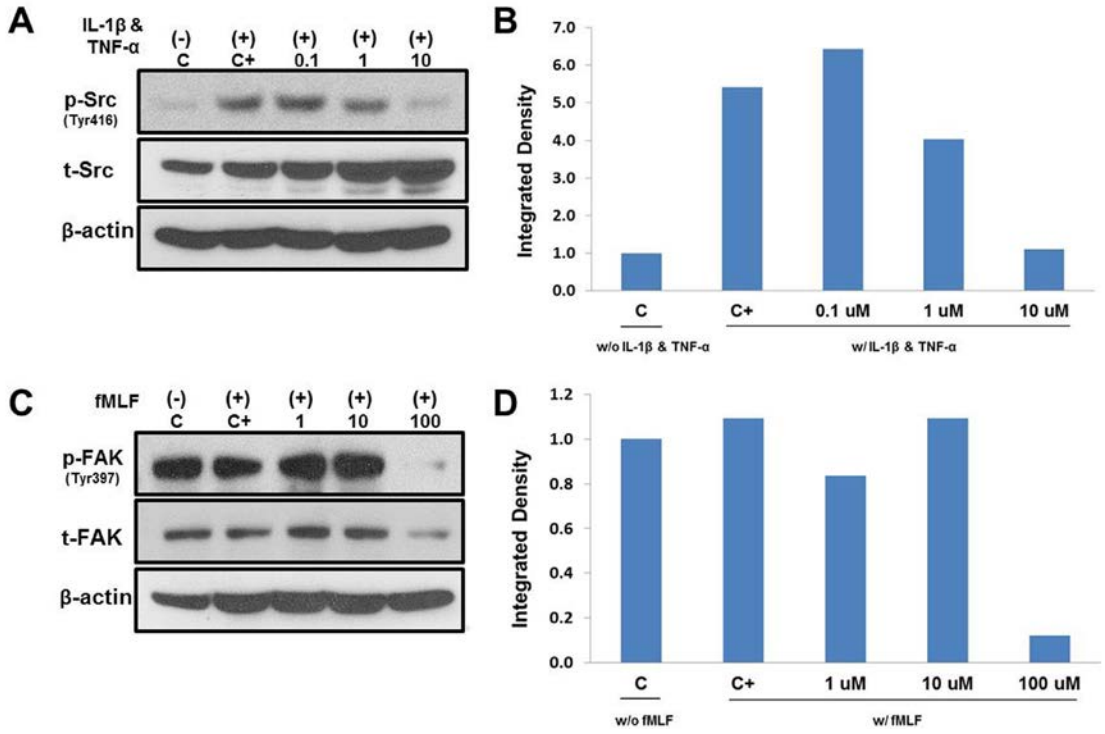

Figure 3.12 Kinetics of FAK and SFK inhibitions by western blot analysis. (A and B) Western blot analysis and its quantification showed that treatment with 10 ng/ml IL-1β and 100 ng/ml TNF-α for 30 min significantly increased SFKs phosphorylation at Tyr 416 and the treatment of SFK inhibitor diminished dose dependently. (C and D) Western blot analysis and its quantification showed that treatment with 100 nM fMLF for 30 min did not enhance FAK phosphorylation at Tyr 397; however 100 μM FAK inhibitor treatment significantly reduced FAK phosphorylation. Analysis of the integrated densities of the bands with the phosphor- to total proteins ratio.

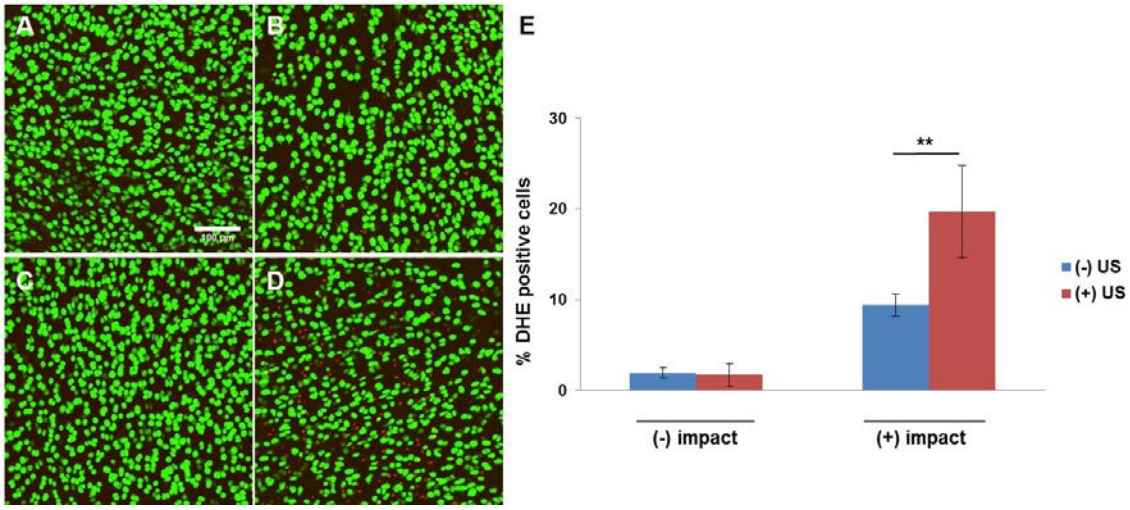

Figure 3.13 The effects of LIPUS stimulation on immediate ROS production following an impact induced cartilage injury. Confocal microscopy taken after LIPUS stimulation showing that live chondrocytes (green) and superoxide (red). Without impact-induced cartilage injury, LIPUS stimulation for 60 minutes did not make any difference (B) with respect to ROS production compared to control (A). However, with impact-induced cartilage injury, LIPUS stimulation for 60 minutes significantly increased ROS production (D) compared to 60 minutes SHAM-operated control (D). (E) Quantification of ROS production revealed that there was no statistical significance in non-impacted group while significantly enhanced superoxide production by LIPUS was found following an impact-induced cartilage injury. Asterisk represents statistical significant (**$p<0.01$).

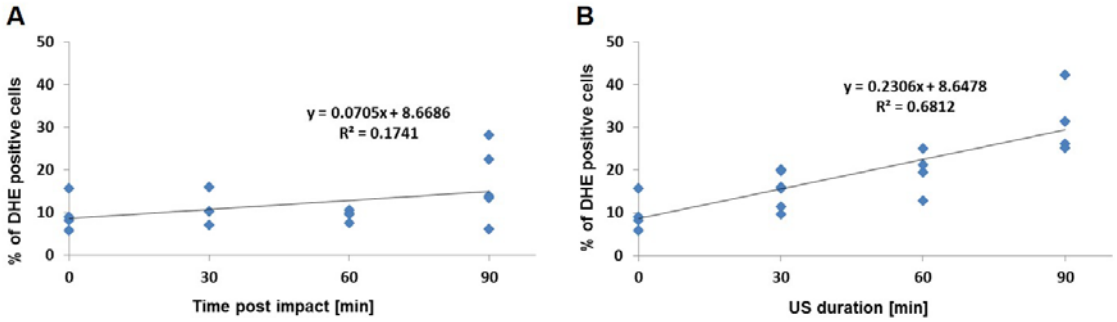

Figure 3.14 Time course of ROS production with or without LIPUS stimulation following an impact-induced cartilage injury. (A) Time course of ROS production following an impact-induced cartilage injury without ROS stimulation showed that the increase of ROS production was little. However, in LIPUS stimulated cartilage, accelerated ROS production was found in response to duration of LIPUS stimulation (B).

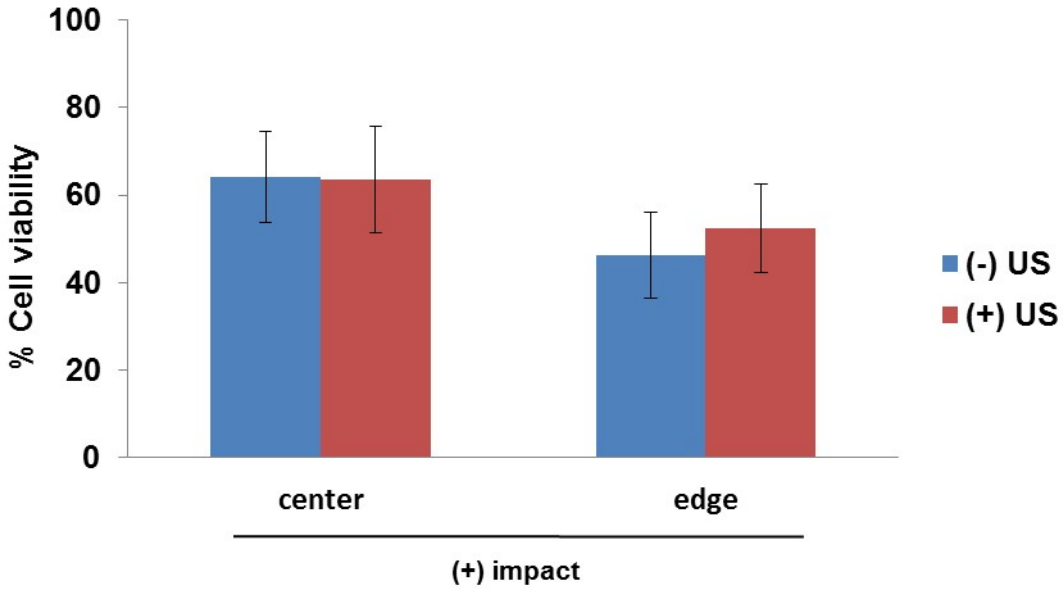

Figure 3.15 The effect of enhanced ROS production by LIPUS stimulation on chondrocyte viability at post 24 hours following an impact induced cartilage injury. Cell viability was examined inside and edge of impact sites in cartilage and the results revealed that there were no considerable cell viability difference between SHAM-operated and LIPUS stimulation for 60 minutes groups.

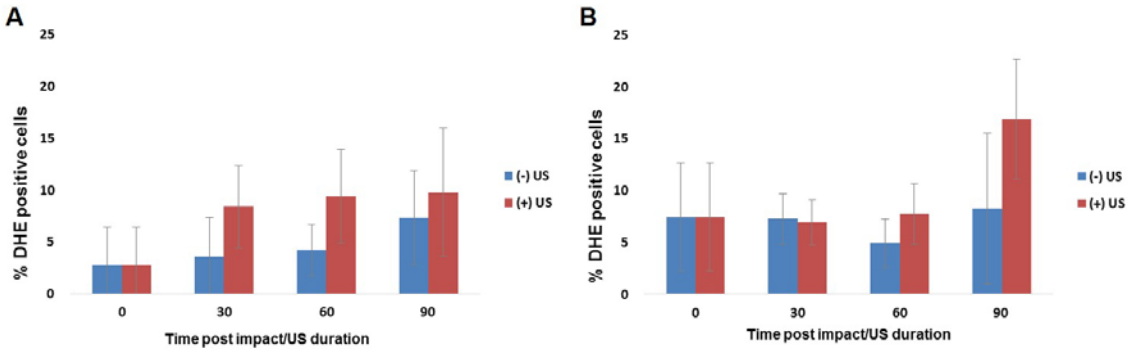

Figure 3.16 Discrimination of the source dependent ROS in chondrocytes induced by LIPUS stimulation following an impact induced cartilage injury. (A) Intracellular ROS production in chondrocytes. LIPUS stimulation accelerated intracellular ROS production with 30 minutes LIPUS duration and this became diminished when the duration went longer. (B) Extracellular ROS production in chondrocytes. There were no considerable difference until 60 minutes; yet the difference became apparent at 90 minutes. There was no statistical significance in all groups.

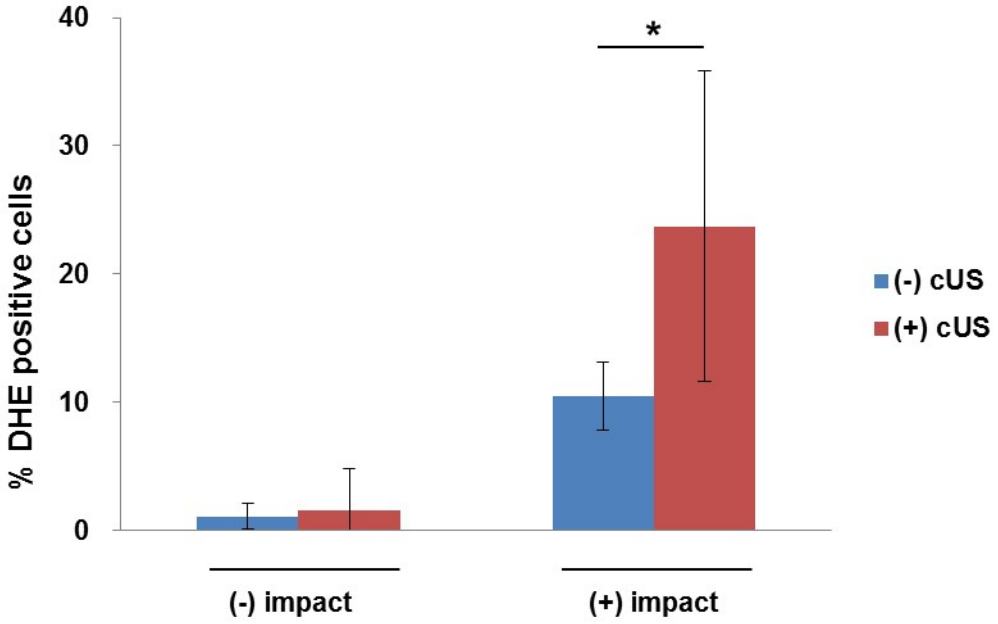

Figure 3.17 The effect of LIUS stimulation on ROS production following an impact induced cartilage injury. In the absence of cartilage injury, LIUS stimulation for 5 minutes had no effect with respect to ROS production compared to control. However, following an impact induced cartilage injury, LIUS stimulation for 5 minutes significantly increased ROS production compared to control. Asterisk represents statistical significant (*$p<0.05$).

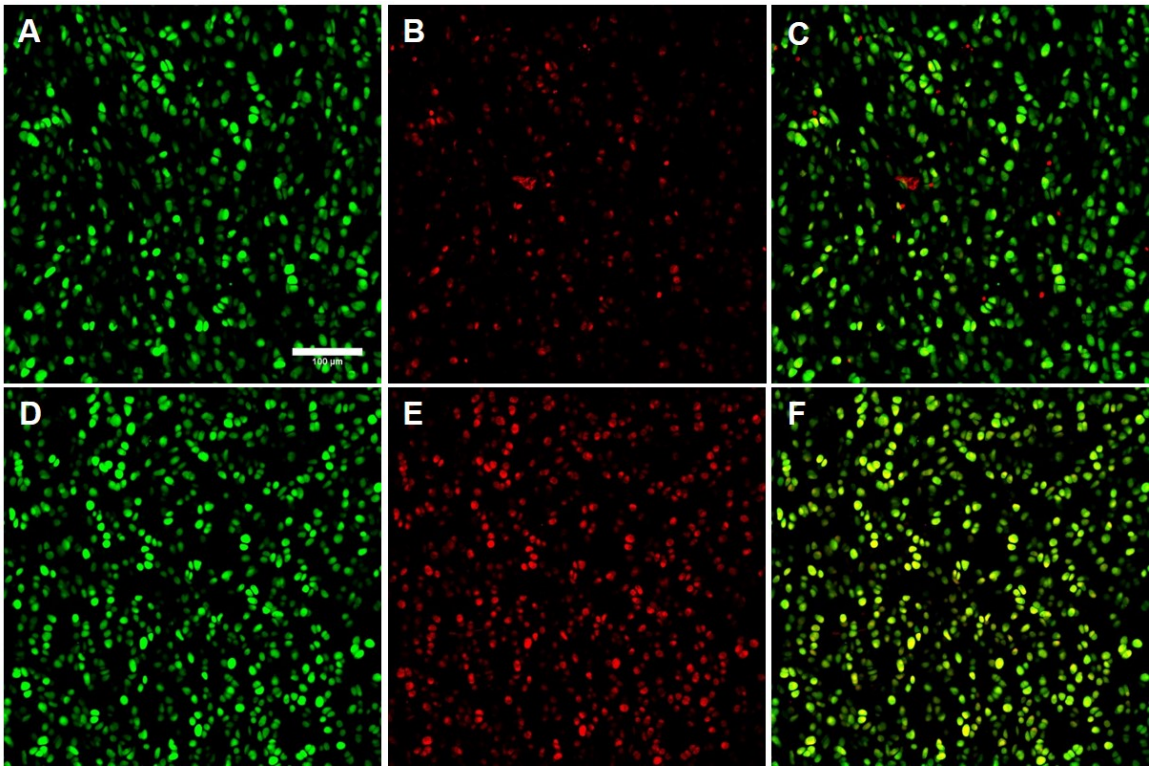

Figure 3.18 The effects of LIPUS on DHE intensity in live chondrocytes. LIPUS exposure significantly enhanced intensity of DHE stains within chondrocytes (D, E and F) compared to control (A, B and C). Live chondrocytes were stained as green (A and D), DHE positive cells were stained as red (B and E), and composited images overlapped DHE-positive cells and live cells (C and F). Bar = 100 µm.

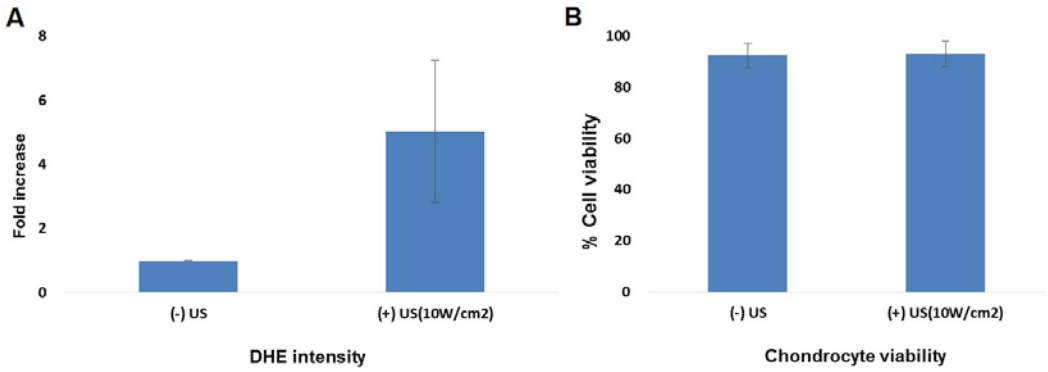

Figure 3.19 Quantitated DHE intensity and the cytotoxicity at post 24 hours following an LIPUS exposure. (A) Confocal microscopy results indicated that LIUS exposure considerably enhanced intensity of DHE stains within live chondrocytes compared to control. (B) Confocal microscopy results indicated that there was no considerable cytotoxicity of tested LIUS intensity, 10 W/cm^2.

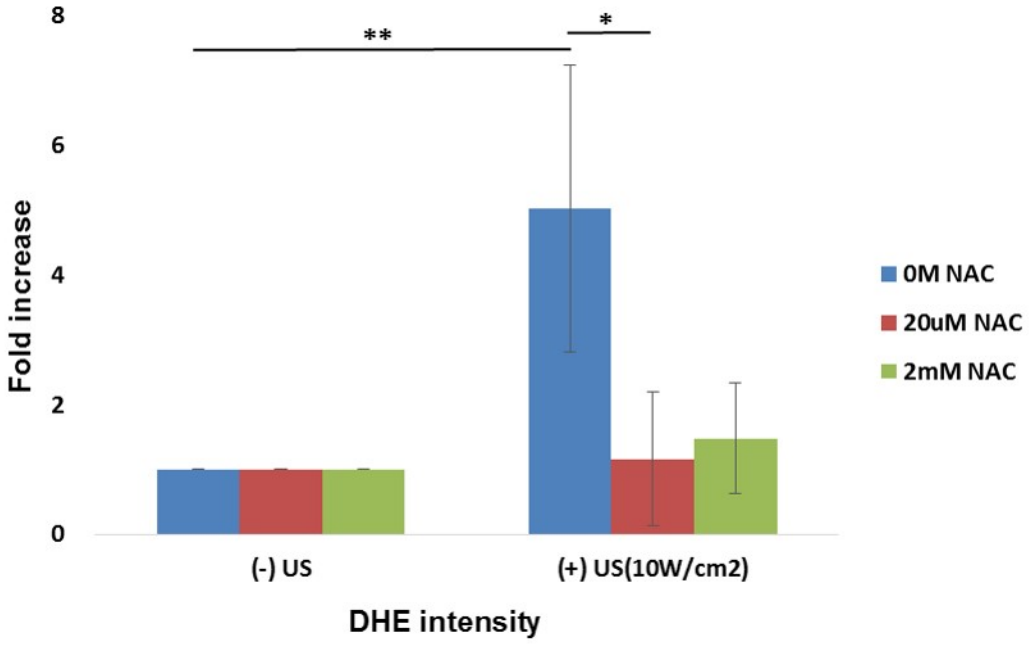

Figure 3.20 The effects of ultrasound therapy and NAC treatment on the suppression of DHE intensity in live chondrocytes. Both tested NAC concentrations of 20 µM and 2 mM significantly suppressed increased DHE intensity within live chondrocytes by ultrasound exposure.

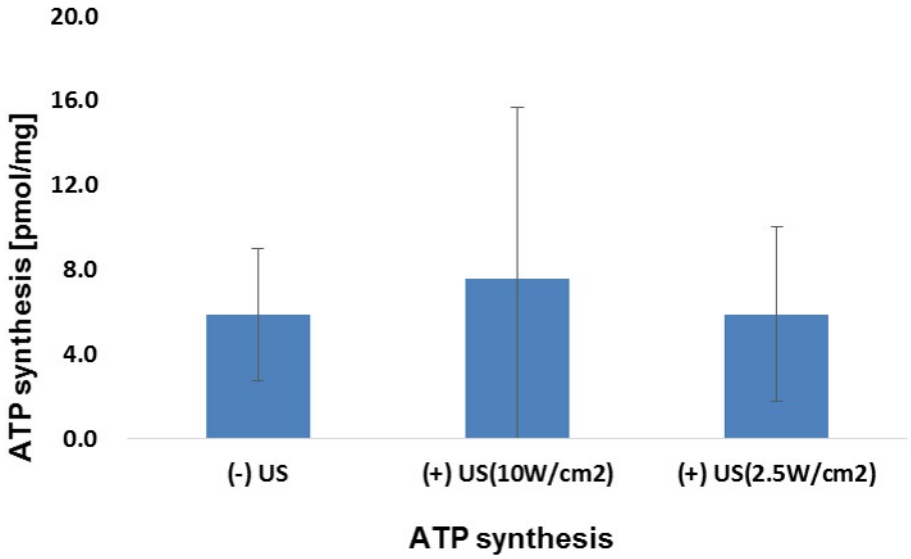

Figure 3.21 The effects of 2.5 and 10 W/cm^2 of ultrasound intensity on the production of ATP by chondrocytes in cartilage. ATP synthesis was normalized by wet weight of cartilage. Two tested ultrasound intensities, 2.5 and 10 W/cm^2, had no effect on ATP synthesis by chondrocytes in cartilage. Error bar indicates standard deviation.

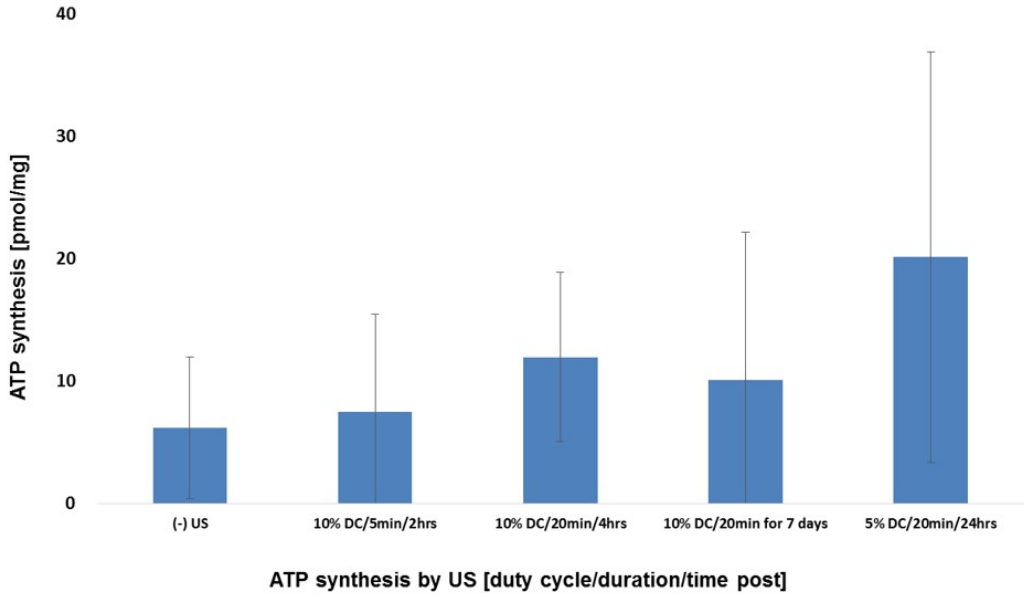

Figure 3.22 The effects of parameter dependent ultrasound stimulation on ATP production in cartilage. ATP synthesis was examined in response to the effect of lower intensity of ultrasound, below 1 W/cm^2, and ultrasound parameters such as duty cycle, ultrasound duration and pulse repetition frequency; however, no difference was found among tested. Error bar indicates standard deviation.

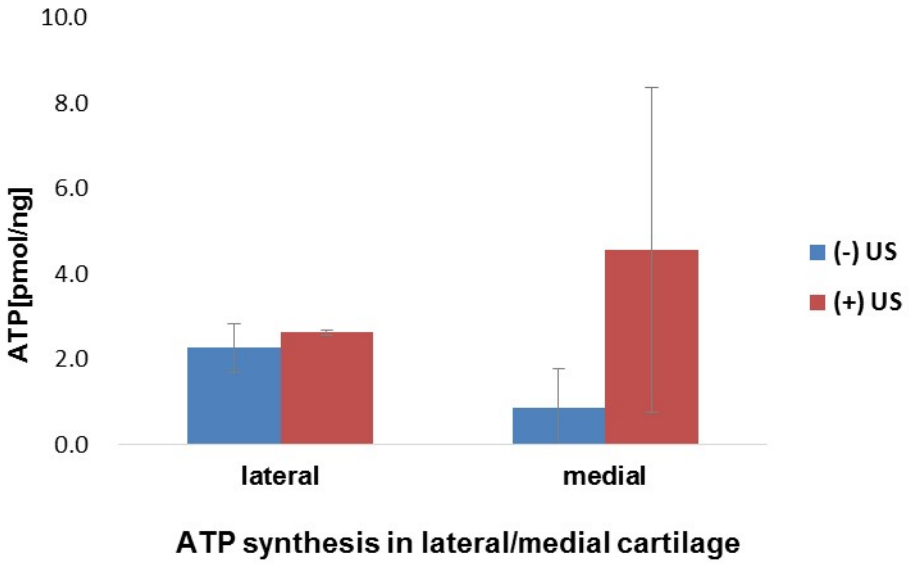

Figure 3.23 Cartilage properties dependent ATP synthesis in response to ultrasound stimulation. No considerable changes of ATP synthesis in lateral cartilage was observed, while ultrasound stimulation enhanced ATP synthesis in medial cartilage. However, there were no statistical significance in both groups.

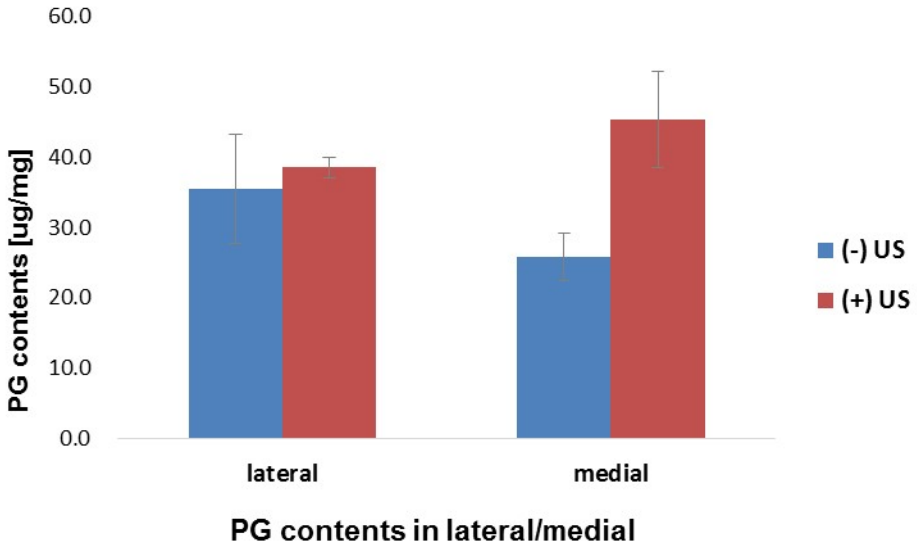

Figure 3.24 Analysis of PG contents in lateral and medial cartilage in response to ultrasound stimulation. No considerable difference was found in cartilage from lateral tibia plateau, while PG contents were slightly higher in cartilage from medial tibia plateau in response to ultrasound stimulation.

CHAPTER 4

MICROBUBBLE-MEDIATED ULTRASOUND THERAPY FOR CANCER TREATMENT

4.1 Background and significance

The biophysical effects of low intensity ultrasound therapy can be classified into thermal and non-thermal effects.(45, 90, 191) Thermal effects can be caused by the conversion of attenuated ultrasound energy into heat in biological tissues. Cavitation, a formation of tiny gas bubbles, is typically considered to be a non-thermal biophysical effect of ultrasound. Tiny gas bubbles are generated by rapid changes in pressure in an ultrasound field and they undergo linear oscillations at low pressure amplitude that change their size and shape, but the bubbles undergo complete destruction by producing shock waves when oscillations become non-linear at higher pressure amplitudes.(45, 90, 192)

Ultrasound contrast agents in the form of gas-filled microbubbles have become popular in medical ultrasound imaging fields since they increase ultrasonic reflection as a result of acoustic impedance mismatches.(193, 194) Typically microbubbles are made of biocompatible materials, which can be as intravenously administered, and the acoustic behavior of microbubbles in the field of ultrasound depends on their size, stability, diffusion, and surface tension. The shell is usually made of albumin, lipid or polymer with the core filled with either air or heavy gases.(99, 100)

Optison, a sterile non-pyrogenic suspension of microspheres of human serum albumin with perfluoropropane (C_3F_8), is one of the commercially

available ultrasound contrast agents typically used for ultrasonography. Since Optison contains plenty of microspheres in suspension, it lowers the threshold of cavitation.(195, 196) Based on its characteristics and the biophysical effects of ultrasound, there have been frequent attempts to cause cancer cell apoptosis and lysis using ultrasound exposure and microbubble destruction. (108, 116, 118)

In low pressure ultrasound fields, microbubbles linearly oscillate, changing shape and size in a manner that is inversely proportional to the ultrasound pressure amplitude; however, microbubbles oscillate non-linearly in high pressure ultrasound fields which may lead to complete fragmentation.(49-51) Microbubble destruction mechanisms also depend on a type of microbubble shells. Lipid or albumin shelled microbubbles oscillate linearly at lower intensities and finally undergo complete destruction as a result of non-linear oscillation at higher intensities ultrasound field. However, polymer shelled microbubbles do not oscillate at lower intensities ultrasound but rather undergo complete destruction all of a sudden at higher intensities (Fig. 4.1).

The induction of microbubble destruction by ultrasound is of interest therapeutically since the fragmented microbubbles serve as cavitation nuclei (Fig. 4.2), which can be used to induce tumor cell death *via* apoptosis and necrosis.(116, 118, 197) Mechanical shock waves produced by ultrasound mediated microbubble destruction (UMMD) have been also been utilized for anti-cancer drug delivery into vascularized tumor. Studies have shown that the growth of tumor was significantly suppressed by UMMD treatment and UMMD transiently increased membrane permeability resulting in increased anti-cancer drug uptake.(49, 112-115) However, treatment of tumors by

UMMD has had limited success since intravenously administered microbubbles have shown results only in vascularized tumors.(125)

Chondrosarcoma, as a well-known type of avascular tumors, can be formed by cells producing cartilage which could be derived from abnormal transformation of mesenchymal stem cells. Primary chondrosarcoma arises *de novo* whereas secondary chondrosarcoma is derived from malignant transformation of benign cartilage-like neoplasms.(198, 199) Chondrosarcoma is more prevalent in adults than younger people and can develop anywhere in the skeleton.(200) Low-grade chondrosarcoma grow slowly over several years asymptomatically, while high-grade chondrosarcoma progress aggressively resulting in pain and disability.(201-203) Therapeutic options are limited to surgical excision since chondrosarcoma is chemo- and radio- resistant as it is avascular. However, surgical excision with wide margins often results in extensive collateral damage to normal tissue.(11, 201, 202, 204-207)

Therefore, it was hypothesized that UMMD has the potential to treat tumors regardless of vascularization by the direct intratumoral delivery of lethal shock waves with or without sustained anti-cancer drug release. Due to the limited availability of avascular tumor samples this hypothesis was tested using *in vitro* model of articular cartilage and chondrocyte pellet cultures, which are similar to chondrosarcoma in matrix composition.(200, 208, 209) The hypothesis was also tested *in vivo* in melanoma tumor bearing mice.

4.2 Specific aims and hypotheses

Developing non-surgical or minimally invasive methods to ablate or shrink surgically inaccessible tumor tissue would have great value for patients. A number of studies have shown that microbubble mediated ultrasound therapy has the potential to suppress tumors by transiently enhancing anti-cancer drug delivery through intravascular injection; however, this method requires that tumors are well vascularized. For this reason, direct intratumoral delivery of lethal shock waves or controlled release of anti-cancer drugs has been investigated using microbubble mediated ultrasound therapy in this study with specific aims and hypotheses as follows.

Specific Aim 1: Determine the effects of low intensity ultrasound mediated Optison microbubble destruction on a suppression of tumor growth.

Hypothesis 1: Ultrasound mediated Optison microbubble destruction produces shock waves that are lethal by rupturing adjacent cell membrane.

Hypothesis 2: Intratumoral delivery of lethal shock waves by Optison microbubble mediated ultrasound therapy has a potential for an *in vivo* tumor suppressive effect.

Specific Aim 2: Determine the effects of low intensity ultrasound mediated PLGA microbubble destruction on controlled drugs or lethal shock waves release.

Hypothesis 1: Ultrasound mediated PLGA microbubble destruction produces shock waves that are lethal by rupturing adjacent cell membrane.

Hypothesis 2: Release of doxorubicin loaded in PLGA microbubbles can be controlled by low intensity ultrasound therapy.

4.3 Material and methods

4.3.1 Cells, cells in pellets cultures and osteochondral explants preparation

Osteochondral explants, 2.5 x 2.5 cm^2, were prepared from mature bovine stifle joints including the central loaded area from the tibial plateau and gently rinsed using Hank's balanced salt solution (HBSS) (Invitrogen Life Technologies, Carlsbad, CA, USA). The explants were then cultured for 2 days in 45% Dulbecco's modified eagle medium (DMEM) and Ham's F-12 (F-12) supplemented with 10% fetal bovine serum (FBS), 100 U/mL penicillin, 100 µg/mL streptomycin, and 2.5 µg/mL amphotericin B at 37ºC, 5% CO_2 and O_2. To generate superficial specific chondrogenic progenitor cells, approximately 0.5-mm-deep scratches were created in the cartilage using a 22-guage needle and cultured for 7 to 10 days as previously described.(31)

Bovine chondrocytes (BCs) were isolated from cartilage tissues harvested from femoral condyle joints by treatment with 0.4% protease and 0.25% collagenase (Sigma-Aldrich, Rochester, NY, USA) dissolved in culture medium. Grade II human chondrosarcoma cells (hCSCs) were donated from the University of Iowa Hospitals and Clinics and cultured in 40% DMEM and MEM-α supplemented with 10% F-12, 10% FBS, 100 U/ml penicillin, 100 µg/ml streptomycin, 2.5 µg/ml amphotericin B, 4 mg/mL insulin, 25 mg/mL ascorbate, and 20 µg/ml hydrocortisone at 37ºC, 5% CO_2 and O_2. Malignant melanoma cell line, B16F10, (B16) was purchased (ATCC, Manassas, VA, USA) and cultured in 90% DMEM supplemented with 10% FBS, 2mM GlutaMAX-1, 10mM HEPES, 50ng/mL Gentamycin and 1mM sodium pyruvate at 37ºC, 5% CO_2 and O_2. Bovine chondrocyte pellets were prepared with 1.5 x 10^6 cells by centrifuging at 500g for 5 minutes at room temperature and cultured under the same culture condition.

4.3.2 Microbubbles preparation

Albumin-shelled commercially available ultrasound contrast agents were purchased (Optison®, GE healthcare, Princeton, NJ, USA) and polymer-shelled poly(lactic-co-glycolic acid) (PLGA) microbubbles were prepared using the double emulsion solvent evaporation method with or without doxorubicin hydrochloride (Sigma-Aldrich, St. Louis, MO, USA).

4.3.3 Low intensity ultrasound therapy system

Versatile sweep function generator (BK Precision, Yorba Linda, CA, USA) was used to modulate sinusoidal continuous and pulsed (burst rate: 1 kHz) waveforms. Input pulses with various duty cycles at 0, 1, 10, 30, 50 and 100% were tested by adjusting number of cycles per each burst: 0% and 100% duty cycles were equivalent to non-ultrasound control and continuous ultrasound respectively. The pulses were amplified using a radio frequency power amplifier (Electronic Navigation Industries Inc., Rochester, NY, USA) and transferred to customized 1 MHz non-focused water-immersible ultrasonic transducer (Ultrasonic S-Lab, Concord, CA, USA). The output power was evaluated by radiation force balance and calculated ultrasound intensity was assumed as spatial averaged and temporal averaged (SATA).(156-158)

4.3.4 Cytotoxicity test of microbubble mediated ultrasound therapy

Cell suspension, either BCs, hCSCs or B16, was prepared in culture medium (0.2 x 10^6 cells/mL) containing 10% (v/v) Optison microbubbles or 1% (w/v) PLGA microbubbles and was exposed to low intensity ultrasound for 10 seconds (Fig. 4.6A). Osteochondral explants were sealed in non-porous polystyrene plastic bag with culture medium containing 10% Optison microbubbles and were exposed to low intensity

continuous ultrasound. Control explants were treated the same way but without ultrasound exposure (Fig. 4.6B). BCs in pellet cultures were suspended in 50 µL of 100% microbubbles (Optison®) and were exposed to low intensity ultrasound for 10 seconds with 10 times repetitions. Control groups were treated the same way but without ultrasound exposure. To examine the effects of UMMD on the release of lactate dehydrogenase (LDH) in BC pellets, the pellets after UMMD treatment were incubated overnight in 500 µL of culture medium and LDH release was evaluated using LDH Cytotoxicity Assay kit (Thermo Fisher Scientific Inc., Rockford, IL, USA) by following manufacturer's instruction. The levels of LDH release were normalized by the contents of DNA in BC pellets and DNA contents were measured using Quant-iT PicoGreen dsDNA Assay Kit (Invitrogen Life Technologies) and a SpectraMax M5 multi-detection microplate reader (Molecular Devices Inc., Sunnyvale, CA, USA). All the groups were then normalized by the non-microbubbles control group.

4.3.5 Cell viability evaluation

After UMMD treatments BCs, hCSCs or B16 were stained with 1µM Calcein-AM, a live cell indicator, and 1µM ethidium homodimer-2 (EthD-2), a dead cell indicator (Invitrogen Life Technologies), and living and dead cells were counted using a hematocytometer with fluorescence microscope (BX60, Olympus, Center Valley, PA, USA). Osteochondral explants was stained with 1µM Calcein-AM/EthD-2 and then scanned to an average depth of 200 µm at 20 µm intervals with a confocal laser scanning microscope (Fluoview 1000, Olympus). A percentage of cell viability was calculated as [(living cells)/(living + dead cells)] x100 [%]. Z-axis projections of confocal scanned images were stacked using ImageJ (rsb.info.nih.gov/ij) and cartilage zone-specific cell

viability in explants was evaluated using a customized automatic cell counting program. Immediately after low intensity ultrasound exposure, BCs in pellet cultures were stained with 1μM Calcein-AM/EthD-2 and then scanned with a confocal laser scanning microscope (Fluoview 1000, Olympus). Z-axis projections of confocal scanned images were stacked using ImageJ (rsb.info.nih.gov/ij).

4.3.6 Histology

Tissues were processed for paraffin histology and were sectioned at 5μm. Sections were stained with safranin-O/ hematoxylin (to reveal matrix proteoglycans and chondrocytes respectively) as previously described.(210)

4.3.7 Confirmation of microbubble destruction by low intensity ultrasound therapy

Two hundred milliliter of culture medium containing 10% (v/v) Optison microbubbles without cells was suspended in polypropylene tubes and exposed to ultrasound with various duty cycles at 0, 1, 10, 30, 50 and 100% for 10 seconds. Immediately after ultrasound exposure, the number of microbubbles in suspension was counted using a hematocytometer.

4.3.8 Morphology of PLGA microbubbles

Before and after UMMD treatments, morphology of PLGA microbubbles were examined using a scanning electron microscopy (Hitachi S-4800, Hitachi High Technologies America, Inc., Schaumburg, IL, USA).

4.3.9 Statistical analysis

Cell viability among tested groups was compared with the statistical analysis software package SPSS (IBM, Armonk, NY, USA). One-way analysis of variance

(ANOVA) with the Tukey *post hoc* test was conducted to test all possible pairwise comparisons. The level of significance was set at $p < 0.05$.

4.4 Results

4.4.1 The mechanisms of ultrasound mediated microbubble destruction

Ultrasound power was evaluated using a radiation force balance technique. As expected the duty cycle was correlated with output ultrasound power. The number of imploded Optison microbubbles in the ultrasound field was significantly enhanced by increasing ultrasound power. In this study, we confirmed that sufficiently higher intensity ultrasound therapy imploded both Optison ad PLGA microbubbles and lethal shock waves were released by rupturing adjacent cell membranes (Fig. 4.3).

4.4.2 Preparation of microbubbles and ultrasound therapy system setup.

Two types of microbubbles, either albumin or PLGA shelled, were tested for whether lethal shock waves are released during destruction in response to ultrasound exposure. Optison microbubbles were purchased (Fig. 4.4) and PLGA microbubbles were synthesized using a double emulsion solvent evaporation method (Fig. 4.5).(211)

To confirm whether microbubbles undergo complete destruction and release lethal shock waves in response to low intensity ultrasound, cells in suspension (0.5×10^6/mL) containing either 10% Optison microbubbles (v/v) or 1% PLGA microbubbles (w/v) were prepared using a eppendorf tube and immediately exposed to ultrasound for approximately 10 seconds (Fig. 4.6A). A same experimental setup was configured for osteochondral explants with the

culture medium containing 10% Optison microbubbles (v/v) to investigate whether released lethal shock waves affect soft tissue cells (Fig. 4.6B).

4.4.3 Cytotoxicity of ultrasound mediated Optison microbubble destruction

A viability of cells, BCs, hCSCs and B16, in suspension containing 10% Optison microbubbles was over 95% without exposure to low intensity ultrasound exposure, and remained the same with a 0.5% duty cycle of ultrasound exposure (n=3-9). However, viability gradually declined in a manner that was inversely proportional to the pulse duty cycle: viability was around 75% at 5% duty cycle (n=3-6), 70% at 10% duty cycle (n=3), 60% at 30% duty cycle (n=3), 20% at 50% duty cycle (n=3), and 30% when exposed to 100% duty cycle (n=3-5). There were no statistically significant differences between hCSC and BC viability at any of the duty cycles tested (Fig. 4.7 A and B) confirming that BCs or any type of cells are an appropriate surrogate for studying UMMD effects since there was no difference in sensitivity to UMMD.

Treatment with 2 mM N-acetylcysteine (NAC), a free radical scavenger, in the suspension containing 10% microbubbles had no effect with respect to hCSC death. Viability immediately after ultrasound exposure was around 95% at 0% duty cycle (n=9), 70% at 10% duty cycle (n=3) and 25% at 50% duty cycle (n=3) respectively for both hCSC groups with or without NAC treatment (Fig. 4.8A). After 6 hours, overall cell viability declined compared to immediately after UMMD. Ultrasound exposure alone, without microbubbles and NAC, did not contribute to cell death; the viability was around 80 to 90% irrespective of all tested duty cycles (n=3). hCSC viability was not affected by NAC treatment and UMMD and the viability pattern was similar compared to the viability immediately after UMMD; viability was around 80% at 0 (n=3) and 1% duty

cycle (n=3), 50% at 10% duty cycle (n=3), around 20% at 30 (n=3), 50 and 100% duty cycle (n=3) (Fig. 4.8B).

4.4.4 Demonstration of Optison microbubble destruction by ultrasound therapy

The number of microbubbles remaining after ultrasound exposure was evaluated using a hematocytometer. The results showed that the number of microbubbles remaining was inversely proportional to the ultrasound duty cycle (Fig. 4.9A, B and C). When compared to the untreated control group (n=8) (0% duty cycle), 60% of microbubbles remained after exposure to a 1% duty cycle (n=9), 40% of microbubbles remained after exposure to a 5% duty cycle (n=6), and cell viability gradually declined from 40 to 20% between 5 and 100% duty cycle (n=4-10) (Fig. 4.9D). Radiation force balance measurements revealed that ultrasound intensity, or power, increased with increased pulse duty cycle. Spatially and temporally averaged intensity of ultrasound was equivalent to 26.8 mW/cm^2 at 10% duty cycle, 144 mW/cm^2 at 50 %, and 267 mW/cm^2 at 100% duty cycle (Fig. 4.9E).

4.4.5 The cytotoxicity of ultrasound mediated Optison microbubble destruction on cells in pellet cultures

In the absence of microbubbles, ultrasound exposure at 100% duty cycle did little damage to BCs in pellet cultures (Fig. 4.10B and G) compared to the control group (Fig. 4.10A and F). Microbubbles alone without ultrasound exposure had no significant effect on viability (Fig. 4.10C and H) compared to other groups without microbubbles. Ultrasound exposure at 50% duty cycle significantly enhanced cell death (Fig. 4.10D and I) and almost all cells were killed after ultrasound exposure at 100% duty cycle (Fig. 4.10E and J).

4.4.6 Histologic similarity of extracellular matrix of chondrosarcoma, bovine articular cartilage and bovine chondrocytes in pellet culture

Safranin-O histology shows similar proteoglycan densities in the extracellular matrix of chondrosarcoma, bovine articular cartilage and bovine chondrocytes in pellet culture (Fig. 4.11).

4.4.7 LDH release in cells in pellet cultures

The cytotoxicity of ultrasound exposure in combination with or without Optison microbubbles was determined by lactate dehydrogenase (LDH) release, which was normalized to the DNA content of the pellet cultures. All groups were normalized to the control group without Optison microbubbles. Statistical analysis revealed that ultrasound exposure significantly increased LDH release from cell pellets in both groups irrespective of Optison microbubbles. Control groups, with or without Optison microbubbles, showed no difference from each other (Fig. 4.12).

4.4.8 The cytotoxicity of ultrasound mediated Optison microbubble destruction in articular cartilage

Fibroblast-like chondrogenic progenitor cells (CPCs), which respond to cartilage injury, were seen on cartilage surfaces after 7 to 10 days post-injury. Immediately after UMMD treatments, most of CPCs was disappeared in cartilage (n=2) (Fig. 4.13C and D, G and H with higher magnification respectively). Yet, the numbers of CPCs remained unchanged in the control group (n=2) (Fig. 4.13A and B, E and F with higher magnification respectively).

To examine the depth-dependent cytotoxicity of UMMD in articular cartilage, osteochondral explants were sealed in a non-porous polystyrene plastic bag filled with

culture medium containing 10% Optison microbubbles and low intensity continuous ultrasound therapy was immediately applied. A sham control group was treated the same way but without ultrasound exposure. Confocal microscopy showed abundant dead cells in cartilage treated with UMMD (n=2) (Fig. 4.14B) whereas there was very little cell death in the control group (n=2) (Fig. 4.14A). Zonal analysis of cell viability revealed that cell death was most significant in the superficial zone and diminished through the deep zone of cartilage; however, cell viability in the control group remained around 100% in superficial and deep zones in cartilage (Fig. 4.14C).

4.4.9 Ultrasound mediated PLGA microbubble destruction

In the absence of 1% (w/v) PLGA microbubbles, no noticeable cell death was found in response to ultrasound exposure; cell viability remained around 95% (n=3-5). However, cell viability rapidly declined to 40% in the presence of PLGA microbubbles after exposure to a 50% duty cycle of ultrasound and further declined to around 2% with 100% duty cycle. These data confirmed that PLGA microbubbles, similarly to Optison microbubbles, also undergo complete destruction by releasing lethal shock waves in response to ultrasound exposure.

4.4.10 Morphology of PLGA microbubbles in response to low intensity ultrasound therapy

Scanning electron microscopy (SEM) was performed to examine the morphology of PLGA microbubbles in response to ultrasound exposure. The SEM images showed intact and smooth surfaces in non-treated control PLGA microbubble groups, but ultrasound exposure created cracks and holes in the surface of PLGA microbubbles (Fig. 4.16).

4.4.11 Doxorubicin cytotoxicity test

To examine to the cytotoxicity of doxorubicin, a lethal dose at 50% (LD_{50}) of doxorubicin with B16 melanoma cancer cells was evaluated. The results showed that dose-dependent cytotoxicity of doxorubicin in monolayer cultured B16 cells for 24 hours. LD_{50} was determined as 0.29 µg/mL (Fig. 4.17).

4.4.12 Controlled release of doxorubicin in PLGA by low intensity ultrasound therapy

To determine the relationship between low intensity ultrasound therapy and doxorubicin release through PLGA microbubble degradation, the amount of doxorubicin released was examined. The results revealed that UMMD treatments increased the release rate of doxorubicin showing ultrasound duty cycle-dependent kinetics (Fig. 4.18).

4.4.13 *In vivo* tumor suppressive effects of microbubble mediated low intensity ultrasound therapy

Melanoma tumors became noticeable in mice approximately 7 days after subcutaneous melanoma cancer cells injection. Optison microbubbles were intratumorally injected and low intensity ultrasound therapy was immediately followed through a coupling gel (Fig. 4.19). The control groups received same amount of PBS instead of microbubbles. Tumor volume was measured every day using a digital caliper and mice were euthanized when the tumor reached 20 mm in width or length and 10 mm in height. In PBS treated control mice showed that melanoma tumors become noticeable through the flank in mice at day 7 and the tumor started growing exponentially. Lethal shock waves produced by ultrasound

mediated Optison microbubble destruction were delivered to the tumor on day 7, 8, 9, 11 and 13 and the growth of melanoma tumors was significantly suppressed until at day 20 (Fig. 4.20). The actual size of the melanoma tumors was compared after euthanizing the mice and the results confirmed the measurements by a digital caliper (Fig. 4.21).

4.5 Discussion and conclusions

Over the past few decades, the use of gas-filled microbubbles has been extended from imaging contrast agents in diagnostic ultrasonography to a localized anti-cancer drug delivery vehicle for the treatment of *in vivo* cancer cells or tumors.(212, 213) The mechanical behavior of the microbubbles in the field of ultrasound is exceptionally dynamic. Under the lower peak negative ultrasound pressure, microbubbles stably oscillate, changing in size and shape and possibly producing microstreaming adjacent to cells. However, at higher peak negative ultrasound pressures microbubbles oscillate non-linearly, which can result in their destruction. Fragmented microbubbles are likely to contribute to the formation of inertial cavitation that produces mechanical shock waves, elevated temperature, and free radical formation.(102, 118, 213) Collapsing microbubbles may trigger intracellular signaling, sonoporation, apoptosis or instant cell necrosis.(110, 214) Therefore, the effects of low intensity ultrasound therapy mediated microbubble destruction on the treatment of tumors were investigated regardless of tumor vascularization.

Lejbkowicz et al. demonstrated that malignant cells are more sensitive to ultrasonic irradiation than normal cells.(215) For this reason, the sensitivity of normal and malignant cells to ultrasonic irradiation was first examined using bovine

chondrocytes (BCs) and human chondrosarcoma cells (hCSCs) in suspension containing 10% Optison microbubbles. However, the results revealed no differences in sensitivity between BCs and hCSCs to UMMD with Optison microbubbles. The basis of this inconsistency with previous observations remains unclear; however, it may indicate that the mechanical shock waves produced by collapsing microbubbles were strong enough to physically rupture cell membranes.

Immediately after the exposure of Optison microbubble mediated low intensity ultrasound therapy with 100% duty cycle for 10 seconds, cell viability in suspension was around 30%. This was not different to the results after 10 minutes exposure (data not shown). This strongly suggests that the destruction of microbubbles takes place immediately under the ultrasound field and cellular necrosis also happened within a few seconds. Cell viability gradually declined under UMMD when the duty cycle increased suggesting that the more lethal mechanical shock waves were produced adjacent to cells by increased microbubble destruction in the stronger ultrasound field. This trend is somewhat similar to previous findings that cell viability was reduced by increasing ultrasound intensity: 100% at 0 W/cm^2, 80% at 1 W/cm^2, 60% at 2 W/cm^2 and 40% at 4 W/cm^2 in the presence of microbubbles. However, in this study we confirmed that even lower ultrasound intensity below 50 mW/cm^2 also resulted in significant cell.(118) This difference might be attributable to different microbubble concentrations, ultrasound setup, or duration of ultrasound exposure.

Analysis of the number of Optison microbubbles remaining after ultrasound exposure showed that the amount of microbubble destruction was dependent on duty cycle or ultrasound power. Since intensity of ultrasound was evaluated by radiation force

balance, specific ultrasonic pressure profiles or a mechanical index are not available. However, there was an obvious linear relationship between the duty cycle and ultrasound power. The data agree with previous findings that higher intensity ultrasound killed more cells in the presence of microbubbles. This suggests that the lethal shock waves produced by UMMD play a critical role in ultrasound power-dependent cell death.(118)

Antioxidants including N-acetylcysteine (NAC), superoxide dismutase and vitamin E have been shown to prevent mechanical stress-associated chondrocyte death, indicating reactive oxygen species play a role in chondrocyte death.(30, 216, 217) Recent evidence also confirms that treatment with NAC prevented oxidative stress can induce cellular apoptosis.(30, 218, 219) Thus, cell death pathways were examined weather it was through mechanical stress involved apoptosis or direct cell necrosis by adding NAC during UMMD treatments, even though it has been previously suggested that cellular death is associated with both instant necrosis and apoptosis.(116-118) In this study, no NAC effect on cell viability was observed either immediately after or 6 hours after UMMD. Although apoptotic activity beyond 6 hours is possible, we presume that in this experimental setup necrosis was the principle mechanism of cellular death.

Previously superficial zone specific chondrogenic progenitor cells (CPCs) have been observed in response to cartilage injury.(31) It has been reasoned that UMMD could be used to selectively kill cells behaving similarly to CPCs as if migrating metastatic cancer cells on the surfaces of tumors. The confocal microscopy results revealed that the CPCs disappeared after UMMD, and zonal cell viability analysis confirmed that the lethal effect of UMMD diminished rapidly below the cartilage surface. This may indicate that the most of the shock wave energy was absorbed by extracellular matrix, resulting in

protection of chondrocytes in deeper zone of cartilage. Alternatively, microbubble penetration may have been limited to the superficial zone. Given the similarities in matrix composition between cartilage and chondrosarcoma these results indicate that a similar depth limitation is likely to be encountered when treating tumors. Thus, multiple UMMD exposures may be necessary to radically shrink large tumor masses.

To assess the potential of UMMD for the treatment of tumors *in vivo*, the cytotoxicity of UMMD with 100% Optison suspension on BCs in pellet cultures was evaluated. Ultrasound exposure was applied using a contact-type transducer with coupling gel into cell pellets. The results revealed that cell death was again duty cycle-dependent and a 100% duty cycle with microbubbles killed almost all cells. A lactate dehydrogenase (LDH) assay was performed to confirm the cytotoxicity of UMMD on BC pellets. Analysis of LDH release by cells showed somewhat inconsistent when it was compared to confocal microscopy results. Ultrasound alone considerably increased LDH release into culture media and the amount released was similar in the presence or absence of microbubbles. The reason why ultrasound alone without microbubbles enhanced LDH release remains unclear; however, it could be that cavitation produced by ultrasound resulted in transient increases in cellular membrane permeability that were not lethal.(220) We expected LDH release from cells with ultrasound exposure in the presence of microbubbles to be a lot greater than we observed. This may be due to the fact that most of the released LDH was flushed out during 10 times ultrasound exposure by replacing microbubbles and there were the few cells to release LDH into the culture media as almost all cells were dead already.

Characteristics of polymer shelled PLGA microbubbles with respect to their destruction, degradation and drug releases in response to low intensity ultrasound therapy were evaluates. The use of PLGA microbubbles would have more advantages over Optison microbubbles as drugs could be securely loaded and its release could be controlled by ultrasound exposure. To confirm that PLGA microbubbles undergo complete destruction and release lethal shock waves similarly to Optison microbubbles in response to low intensity ultrasound therapy, cytotoxicity of ultrasound mediated PLGA microbubble destruction on B16 cells in suspension was evaluated. The results showed that PLGA microbubbles also underwent complete destruction and released lethal shock waves in response to ultrasound exposure leading to B16 cell death. Morphology of PLGA microbubbles was examined using a scanning electron microscopy (SEM) and a number of cracks and holes in the surface of PLGA microbubbles were found in the ultrasound exposed group but not in the control group suggesting that some of the PLGA microbubbles underwent complete destruction and the rest of the PLGA microbubbles were in the transition to destruction as supporting previous study.(49) Since the PLGA microbubbles were imploded and were degraded by ultrasound exposure, it was reasonable to hypothesize that the release kinetics of drugs loaded in PLGA microbubbles show ultrasound power-dependent. To test this hypothesis, doxorubicin, an anti-cancer drug, was loaded in PLGA microbubbles and suspended in PBS. And power-dependent ultrasound was exposed and the concentration of doxorubicin in PBS was evaluated. The results indicated that the doxorubicin release rate depended on duty cycle suggesting stronger ultrasound energy resulted in more doxorubicin release by accelerating PLGA microbubbles degradation. It would have great potential for the treatment of tumors if

tumors are treated by lethal shock waves, then followed by sustained release of doxorubicin.

Due to the limited availability of avascular tumor model we evaluated the anti-cancer effects of UMMD on mice bearing melanoma tumors. In first batch of experiments, lethal shock waves were directly delivered into melanoma tumors at day 11 and the tumor growth was temporarily suppressed for 3 days when it was compared to PBS injected control mice. However, the tumor was relapsed back to grow and additional lethal shock waves deliveries at day 14 and 16 were no longer effective. This result may indicate that the tumor suppressive effect by lethal shock waves was more effective in gradual tumor growth phase than exponential phase where cytotoxicity of UMMD was not able to overwhelm the tumors in exponential growth phase. For this reason, we tested the effect of more intensive UMMD treatment on the tumor growth starting earlier at day 7 with 2 fold higher concentrated Optison microbubble concentration. Intensive UMMD treatment was performed at day 7, 8, 9, 11 and 13 and the results showed that the tumor growth was suppressed until day 19 or 20 while PBS injected control group had no effect on tumor growth. Mice in each group were euthanized at day 15 and actual melanoma tumors were harvested to compare their actual size. The results confirmed that the actual melanoma size in the mouse treated with UMMD was strikingly smaller than the one treated with PBS. However, the tumors were relapsed back to grow in the end. This may indicate that UMMD treatments killed most of cells in tumor but failed to kill all cells completely resulting in the tumors relapsing back to grow in the end. Provided that the tumors are treated with lethal shock waves followed by sustained release of anti-cancer drugs, there might have much stronger tumor suppressive effects.

There have been extensive attempts to use UMMD for drug delivery and its effect has proven to be promising. However, this method is successful only when tumors are vascularized, which are not the case with many avascular tumors, such as chondrosarcomas.(112, 113, 115, 221-223) In conclusion, tumors regardless of tumor types, vascularization and surgical accessibility can be treated with minimal- or non–invasive intratumoral lethal shock waves delivery by microbubble mediated low intensity ultrasound therapy.

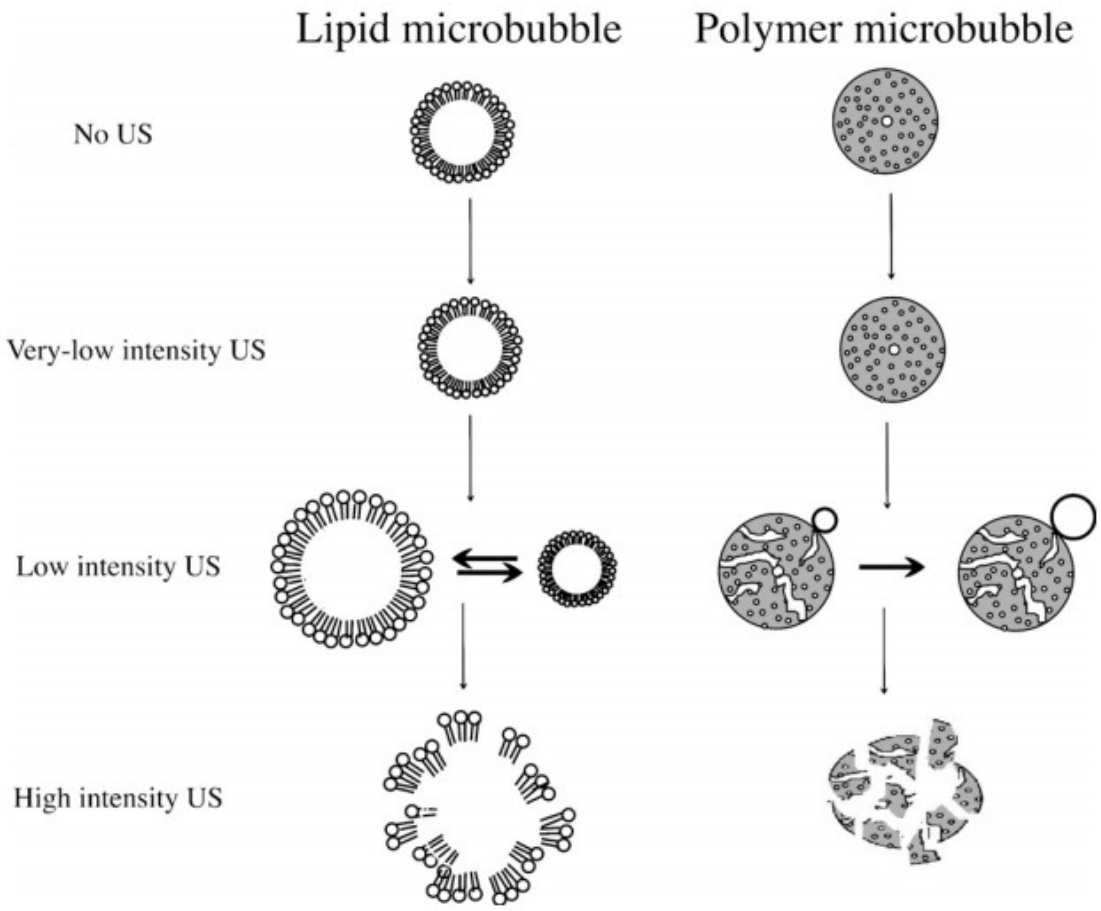

Figure 4.1 The shell-type dependent destructive mechanisms of microbubbles in response to ultrasound. Lipid shelled microbubbles undergo linear oscillation in a lower intensity of ultrasound and complete destruction in a higher intensity of ultrasound. However, polymer shelled microbubbles do not undergo linear oscillation in a lower intensity of ultrasound but undergo complete destruction all of a sudden in a higher ultrasound intensity.(49)

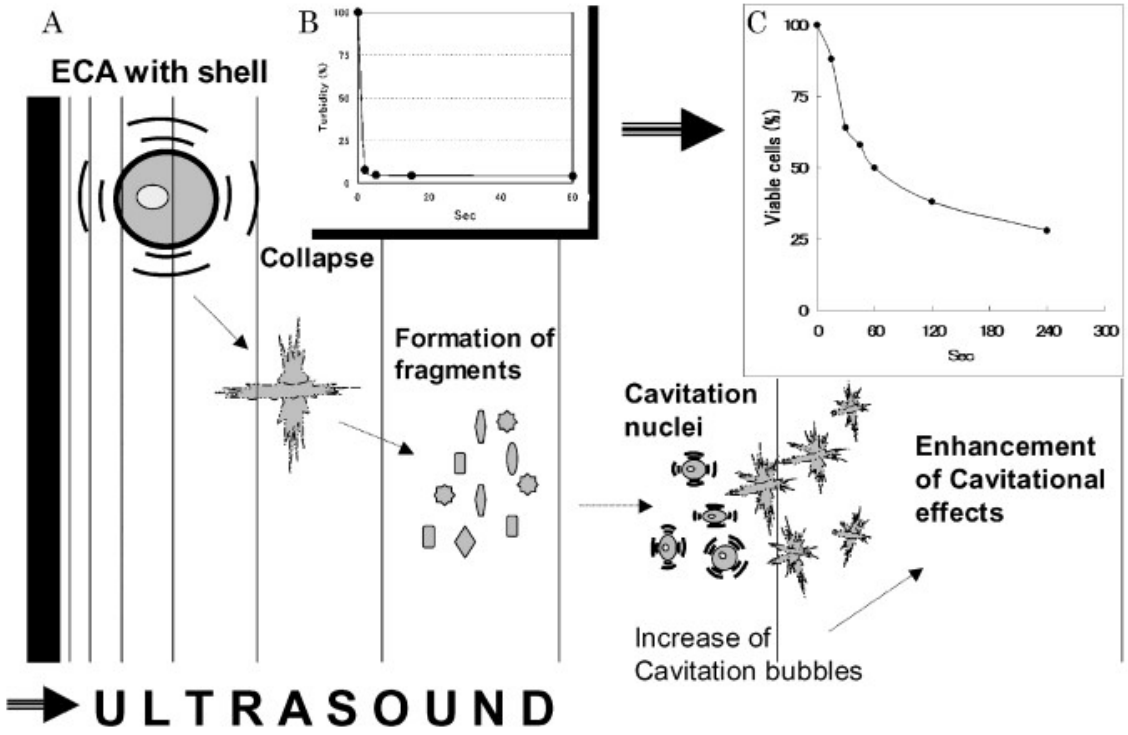

Figure 4.2 Enhanced cavitation effects by ultrasound mediated microbubble destruction. Microbubble destruction was in close correlation with the duration of ultrasound exposure which results in cell death suggesting that fragments as a result of microbubble destruction may serve as cavitation nuclei for cavitational effects.(117)

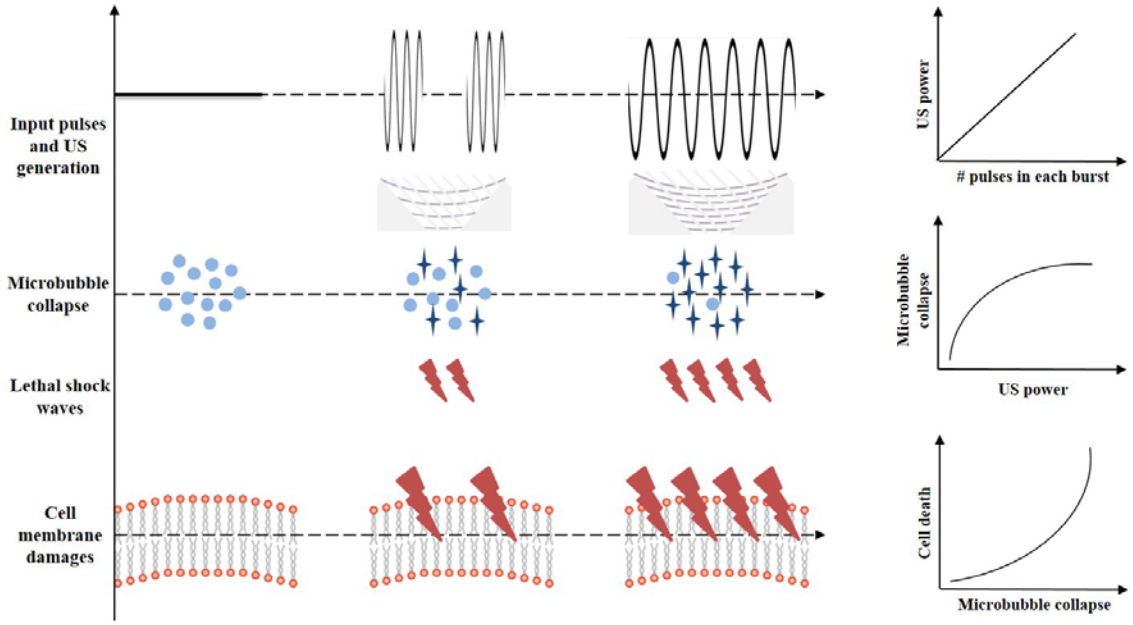

Figure 4.3 Schematic illustration of lethal shock waves release by ultrasound mediated microbubble destruction. The number of pulses in each burst, or duty cycle, is linearly proportional to ultrasound power which has close correlation with microbubble destruction. The lethal shock waves are released from imploding microbubbles which lead to rupture cytoplasmic membrane.

Figure 4.4 Commercially available ultrasound contrast agents, Optison. Optison microbubbles are diagnostic agents intended for contrast enhancement during ultrasonography which made of human albumin with infusion of octafluoropropane (C_3F_8) with molecular weight of 188.02 g/mol.

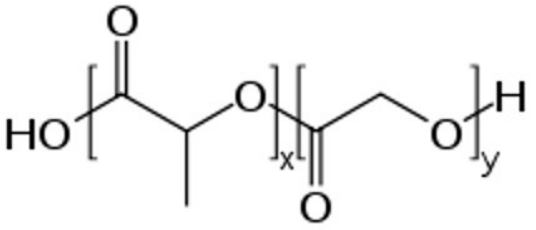

PLGA (poly(lactic-co-glycolic acid))

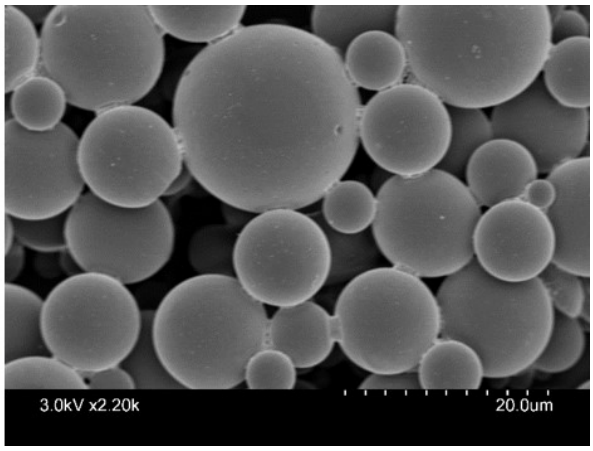

Figure 4.5 Morphology of synthesized PLGA shelled microbubbles. PLGA shelled microbubbles were synthesized using a double emulsion solvent evaporation method and size dependent separation was performed by rotation speed dependent centrifugation. Scanning electron microscopy shows that PLGA microbubble has smooth intact surface with distinct size distribution.

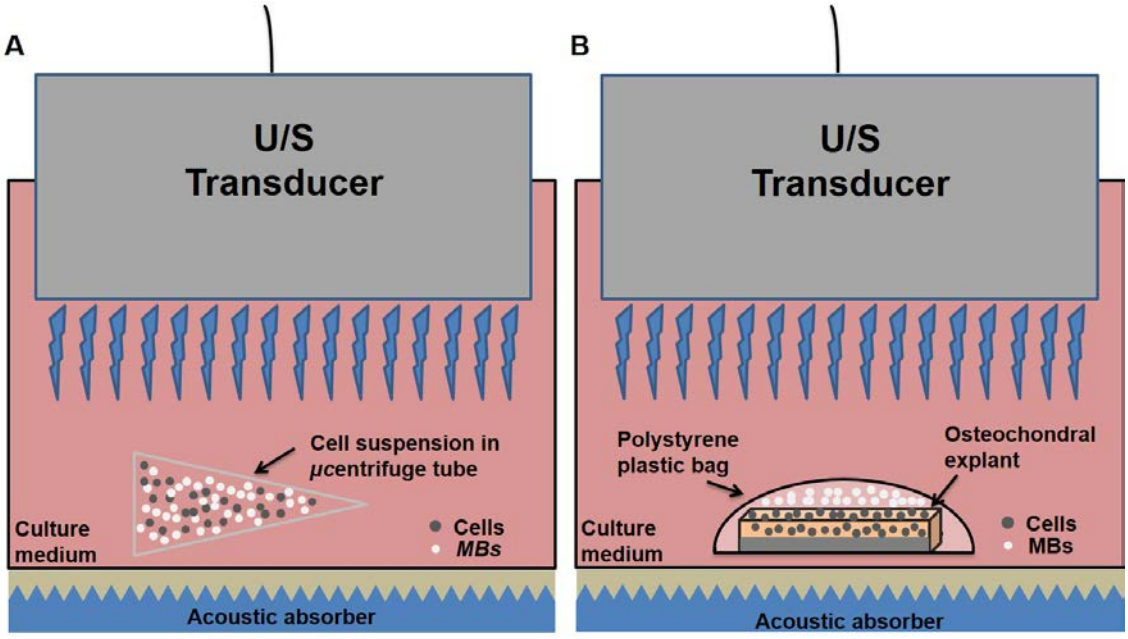

Figure 4.6 Configuration of ultrasound exposure for *in vitro* cytotoxicity test of UMMD. Versatile function generator is used to produce various duty cycle adjusted waveforms either continuous or pulsed waves. Radio frequency power amplifier amplifies waves from function generator and ultrasonic transducer converts the electric pulses to mechanical ultrasounds.

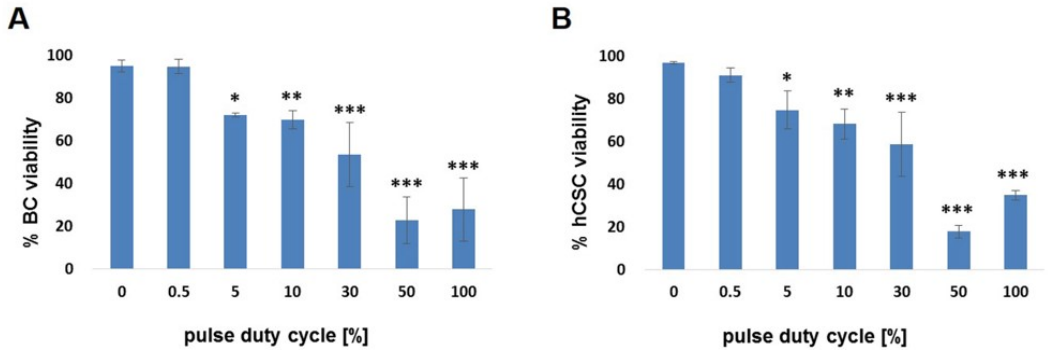

Figure 4.7 The *in vitro* cytotoxicity of UMMD in suspension. Cell viability of BCs and hCSCs in suspension containing 10% Optison microbubbles was dependent on duty cycle of ultrasound. Cell viability was declined with increasing duty cycle of ultrasound and there was no different effect of UMMD on both BC and hCSC viability (A and B). Asterisk represents statistical significance (*p< 0.05, **p<0.01 and ***p<0.001) and error bars represent sample variations (n=3-9).

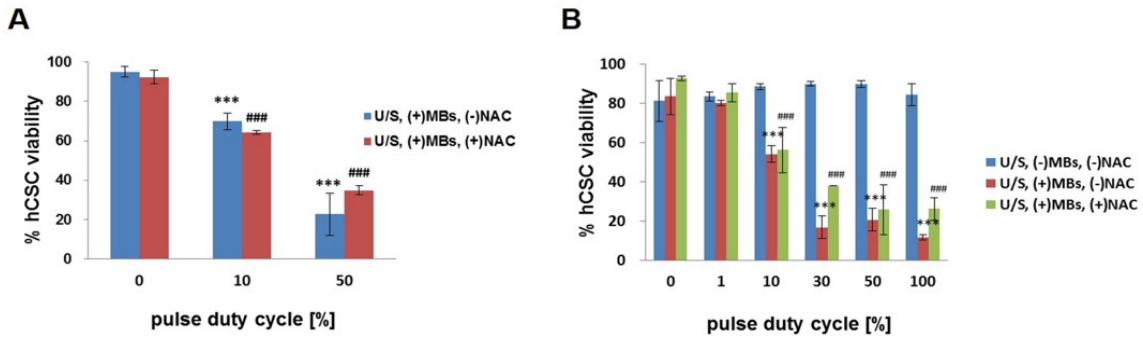

Figure 4.8 The effects of NAC treatments on cytotoxicity of UMMD in suspension. When applied immediately after UMMD, 2mM NAC had no effect on cell viability (n=3-9) (A). Six hours after UMMD, no significant cell viability difference was observed between NAC untreated and treated group. Also, ultrasound itself did not contribute to cell death (n=3) (B). Statistical significance was set at $p < 0.05$ (***$p<0.001$, $^{###}p<0.001$) and error bars represent sample variations.

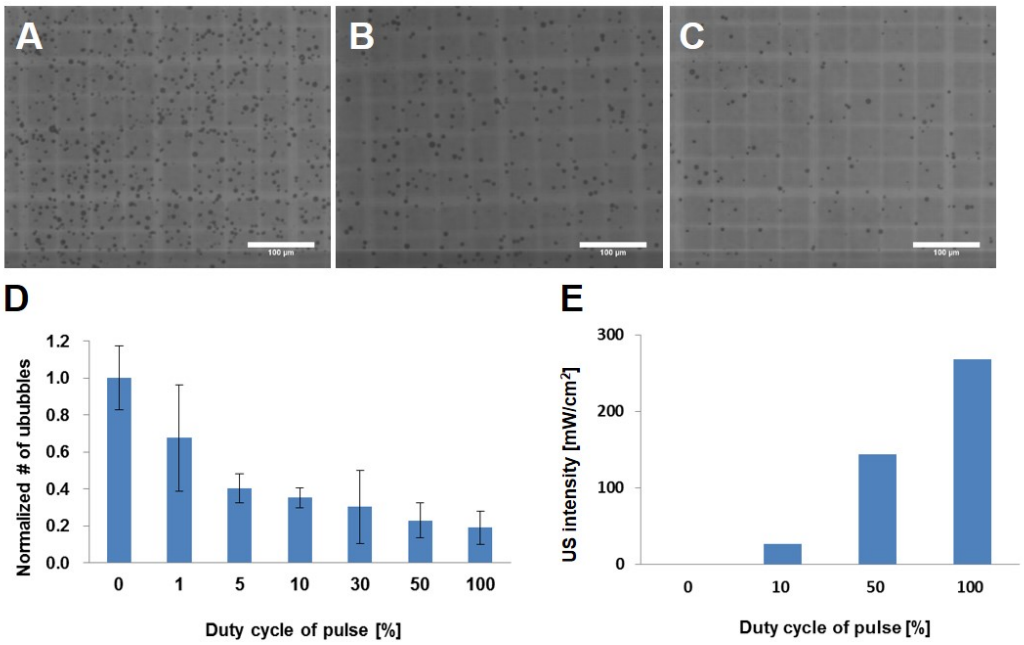

Figure 4.9 The analysis of remaining microbubbles after UMMD. The effect of ultrasound on Optison microbubbles was assessed using a hematocytometer. The results showed that the number of intact Optison microbubbles declined with increasing duty cycle of ultrasound (A, B and C). Normalized percentage of remained Optison microbubbles revealed that 60% of Optison microbubbles were left at 1% duty cycle of ultrasound and became decreased from 40% to 20% at above 5% duty cycles of ultrasound (D). Ultrasound intensity was evaluated and confirmed that linear relationship between intensity and percentage of duty cycles (n=4-10) (E). Bars = 100 µm.

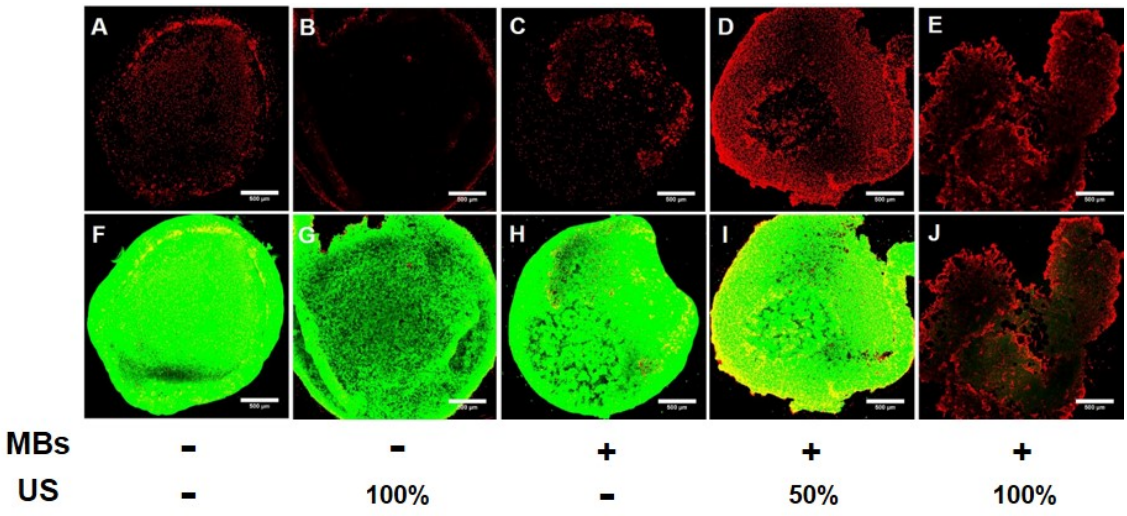

Figure 4.10 The effects of UMMD on cell death in chondrocyte pellets. Z-axis stacked confocal microscopic images showing dead cells (red) and composite images with live cells (green) in full thickness of chondrocyte pellets. In the absence of Optison microbubbles, a few dead cells were observed after ultrasound exposure; however, most of cells were alive for both groups (A and F: without ultrasound, B and G: with ultrasound). In the presence of Optison microbubbles, dead cells increased with 50% duty cycle and was further enhanced with 100% duty cycle (C and H: without ultrasound, D and I: 50% duty cycle, E and J: 100% duty cycle). Bars = 500 µm.

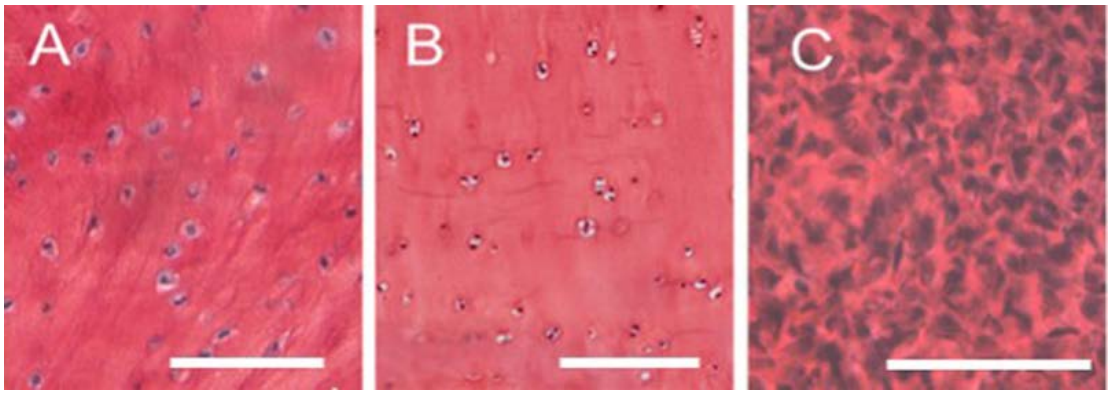

Figure 4.11 Histologic similarities between chondrosarcoma, articular cartilage, and BCs in pellet cultures. Paraffin sections of a chondrosarcoma (A), bovine articular cartilage (B), and bovine chondrocyte pellet culture (C) were stained with safranin-O (Red) to reveal matrix proteoglycans. The similar intensity of the stain indicates similar proteoglycan density. Bars = 100 µm.

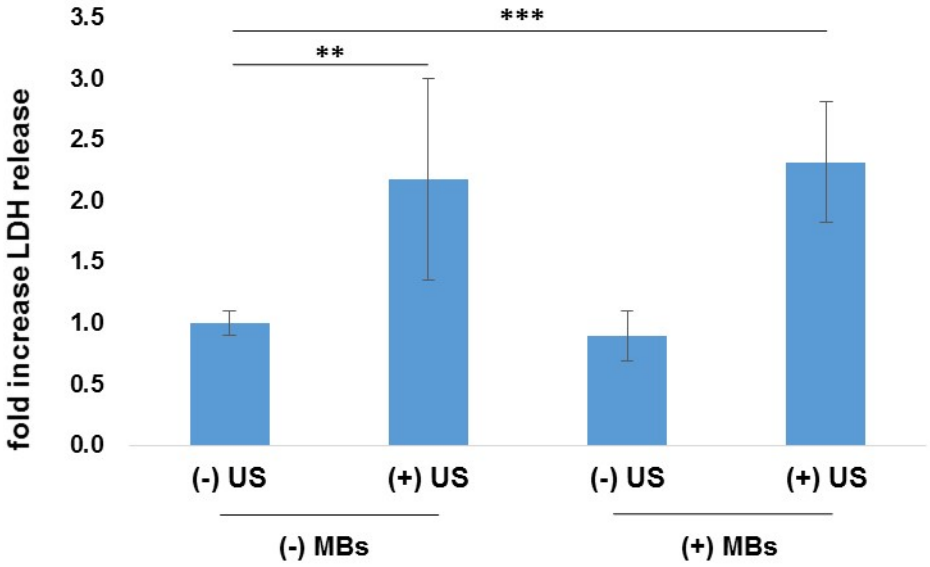

Figure 4.12 The effects of UMMD on LDH release in chondrocyte pellets. Released LDH was measured in culture media post 24 hours of UMMD. All groups were normalized to control (ultrasound in the absence of Optison microbubbles). Optison microbubbles alone did not contribute to LDH release; however, ultrasound exposure significantly enhanced LDH release in both the presence and absence of Optison microbubbles. Statistical significance was set at $p < 0.05$ (**p<0.01, ***p<0.001) and error bars represent sample variations (n=6).

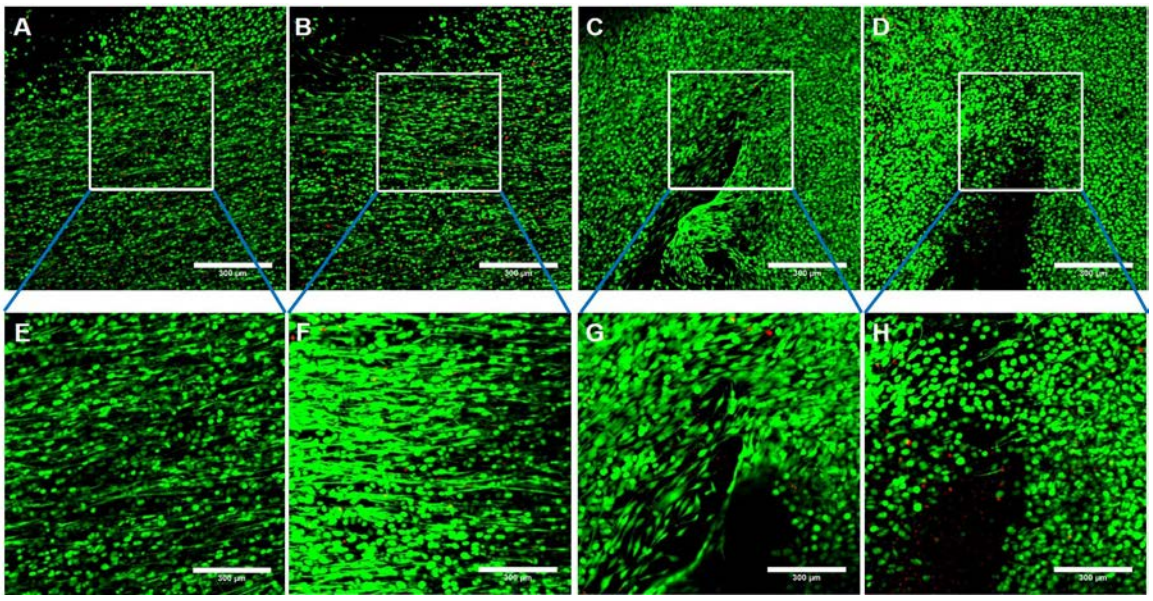

Figure 4.13 The effects of UMMD on surface migrating chondrogenic progenitor cell death. After 7 to 10 days of cartilage injury, elongated chondrogenic progenitor cells were emerged and these cells morphologically differ from bovine chondrocytes which are round in shape. In control group, the numbers of elongated, fibroblast-like progenitor cells remained same before and after SHAM-operation without ultrasound exposure (A and B: before and after, E and F: higher magnification of A and B respectively). However, ultrasound exposure treated group with microbubbles, the progenitor cells disappeared after UMMD (C and D: before and after, G and H: higher magnification of C and D respectively) (n=2). Bars = 300 µm in A, B, C and D. Bars = 100 µm in E, F, G and H.

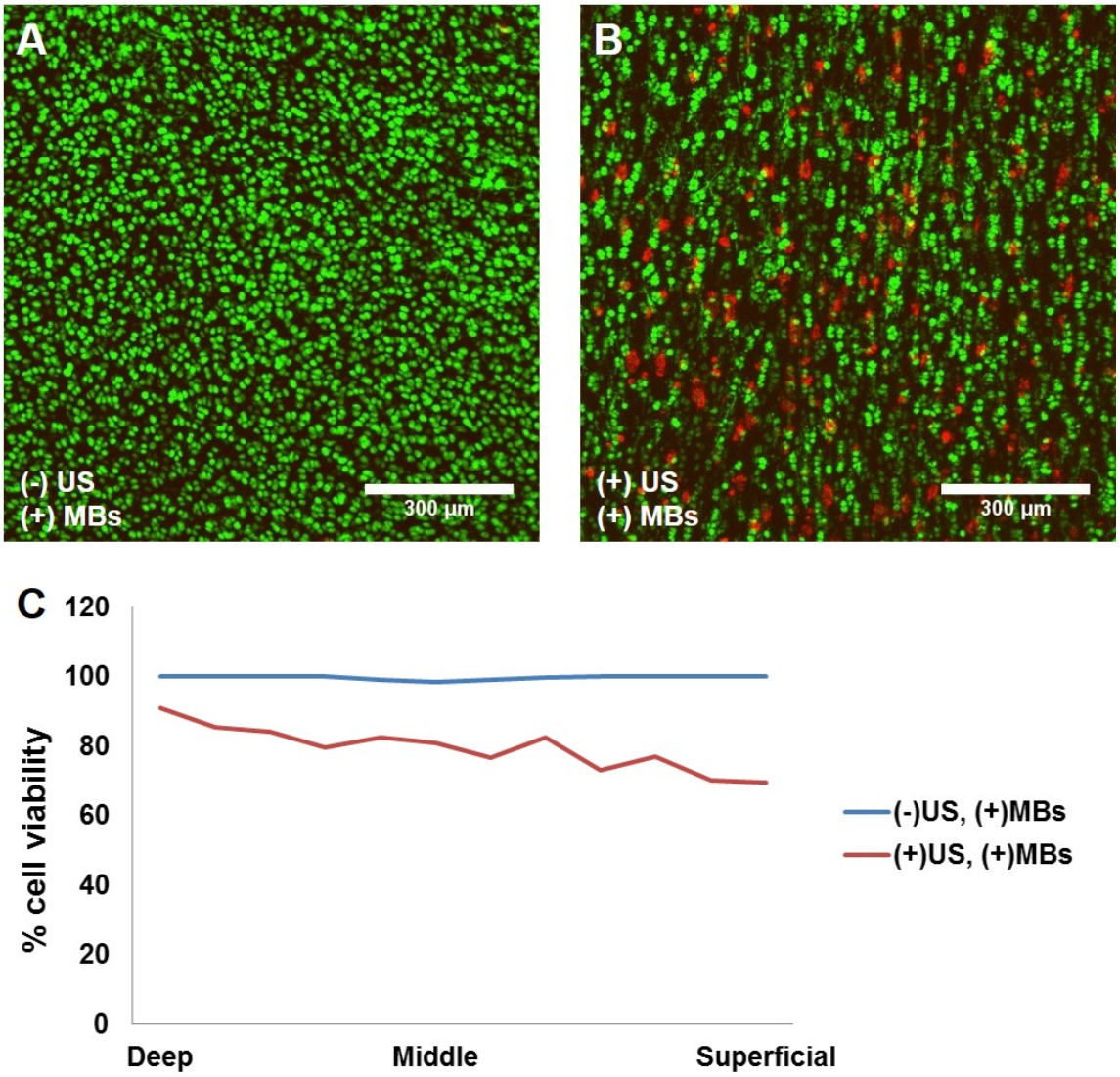

Figure 4.14 The effects of UMMD on chondrocyte death in zonal dependent articular cartilage. Z-axis stacked confocal microscopic images showing live cells (green) and dead cells (red) in full thickness cartilage defects. No considerable cell death was observed in control group without ultrasound exposure (A); however, significantly enhanced cell death was observed in cartilage after ultrasound mediated Optison microbubble destruction (B). Zonal analysis of cell viability revealed that the cell death was the most significant in superficial zone and it became reduced in deeper zone in cartilage (n=2) (C). Bars = 300 µm.

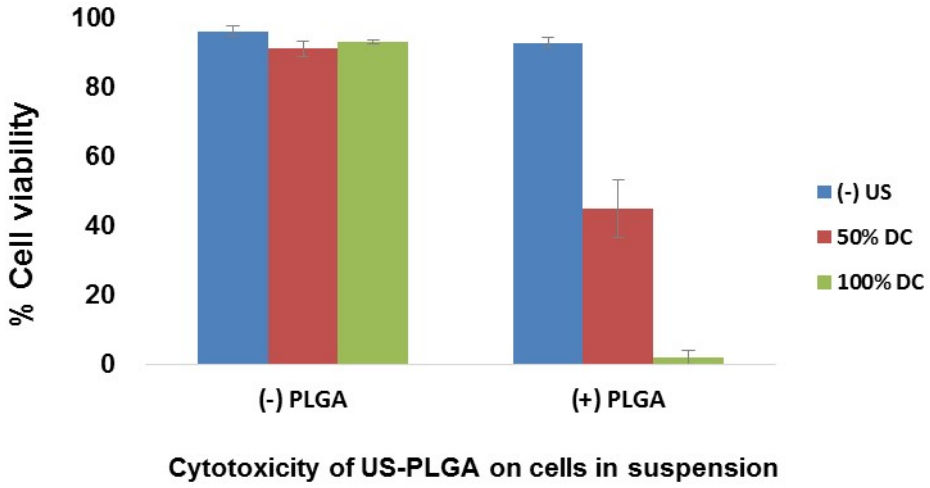

Figure 4.15 The *in vitro* cytotoxicity of ultrasound mediated PLGA microbubble destruction in suspension. Cell viability was similar to ultrasound mediated Optison microbubble destruction that cell death was gradually increased when duty cycles are increased. In the absence of PLGA microbubbles there were no considerable cell death with or without ultrasound exposure.

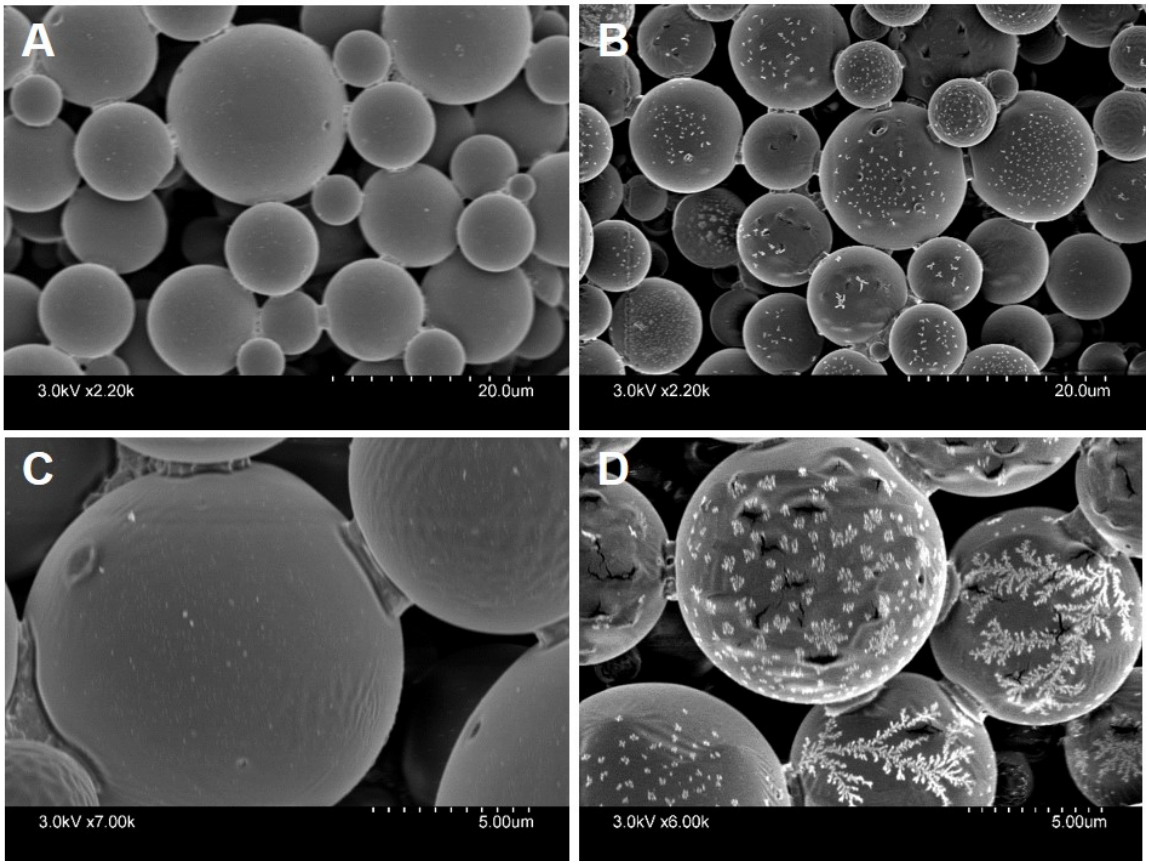

Figure 4.16 The morphology of PLGA microbubbles after ultrasound therapy. (A) Morphology of untreated PLGA microbubbles showing intact and smooth surfaces. (C) Higher magnification PLGA microbubbles without ultrasound exposure. (B) Morphology of ultrasound exposed PLGA microbubbles showing degradation or cracking in the surface. (D) Higher magnification of PLGA microbubbles in response to ultrasound exposure.

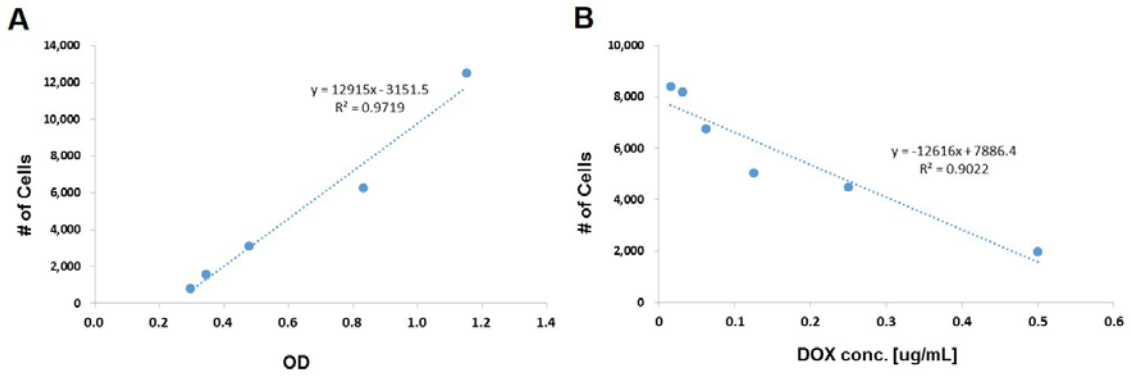

Figure 4.17 The cytotoxicity of doxorubicin after 24 hours in monolayer cultured B16 melanoma cells. (A) Standard curve representing observance density is linearly correlated with the number of cells. (B) Cell viability was gradually reduced with increased doxorubicin concentration and the lethal death at 50% was 0.29 µg/mL.

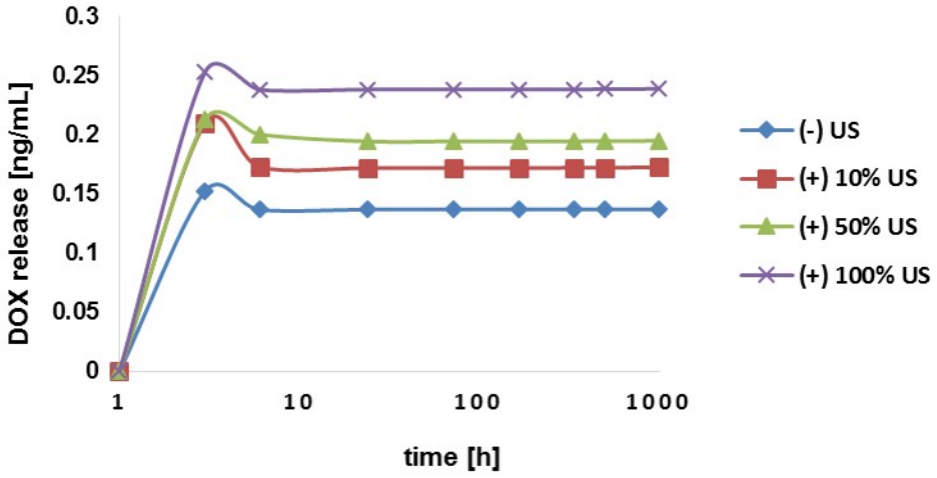

Figure 4.18 The accelerated doxorubicin release in PLGA microbubbles in response to ultrasound therapy. Doxorubicin release was increased by ultrasound exposure and the enhancement showed in kinetics of ultrasound duty cycles.

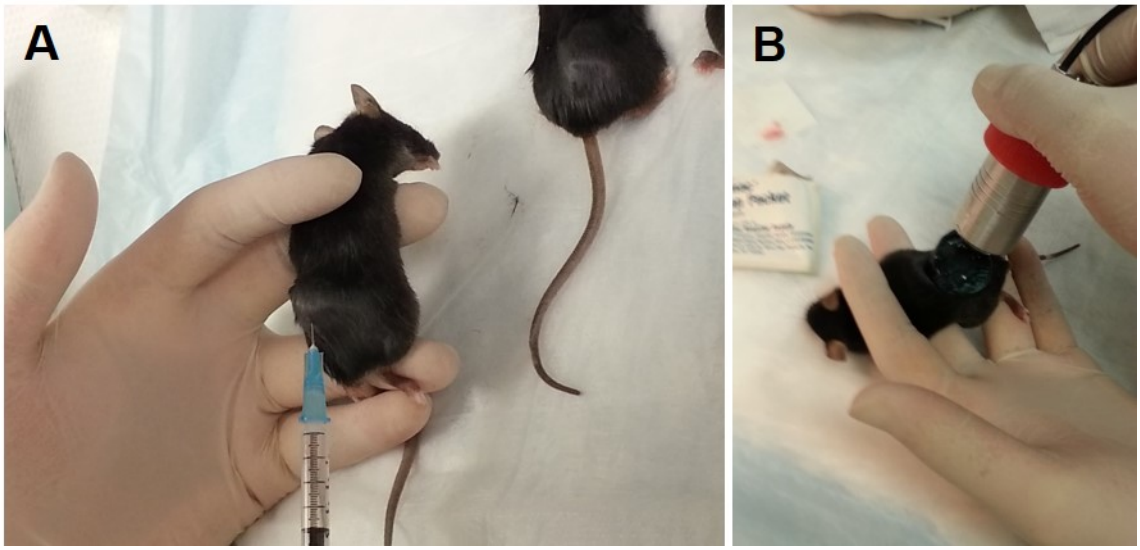

Figure 4.19 The *in vivo* procedures of microbubble mediated ultrasound therapy with mice bearing melanoma tumors. (A) After 7 days of B16 melanoma cancer cell injection, microbubbles were intratumorally injected. (B) After microbubbles injection, ultrasound exposure was immediately followed through coupling gel.

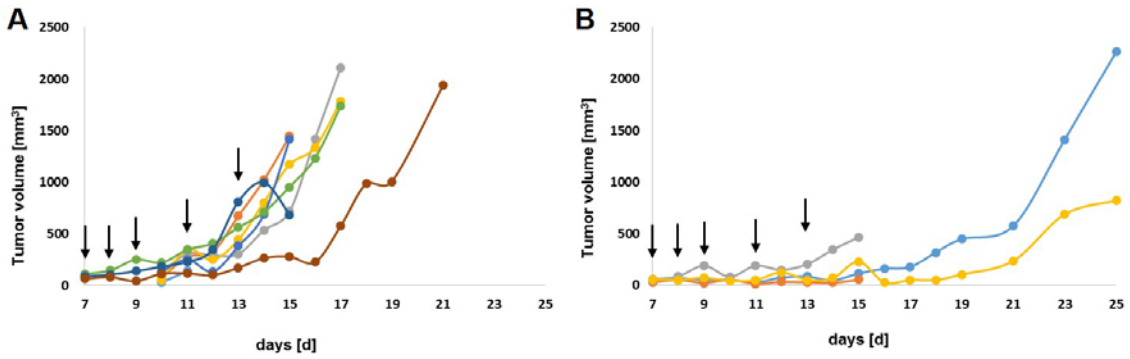

Figure 4.20 The effects of UMMD treatment on *in vivo* tumor suppression in mice bearing melanoma tumors. (A) PBS injected mice show gradually increases of melanoma tumor volume until at day 11 and exponential growth from at day 12. (B) UMMD treatment revealed that tumor growth was significantly suppressed at earlier time point. Arrows indicate the day of treatment either PBS or UMMD.

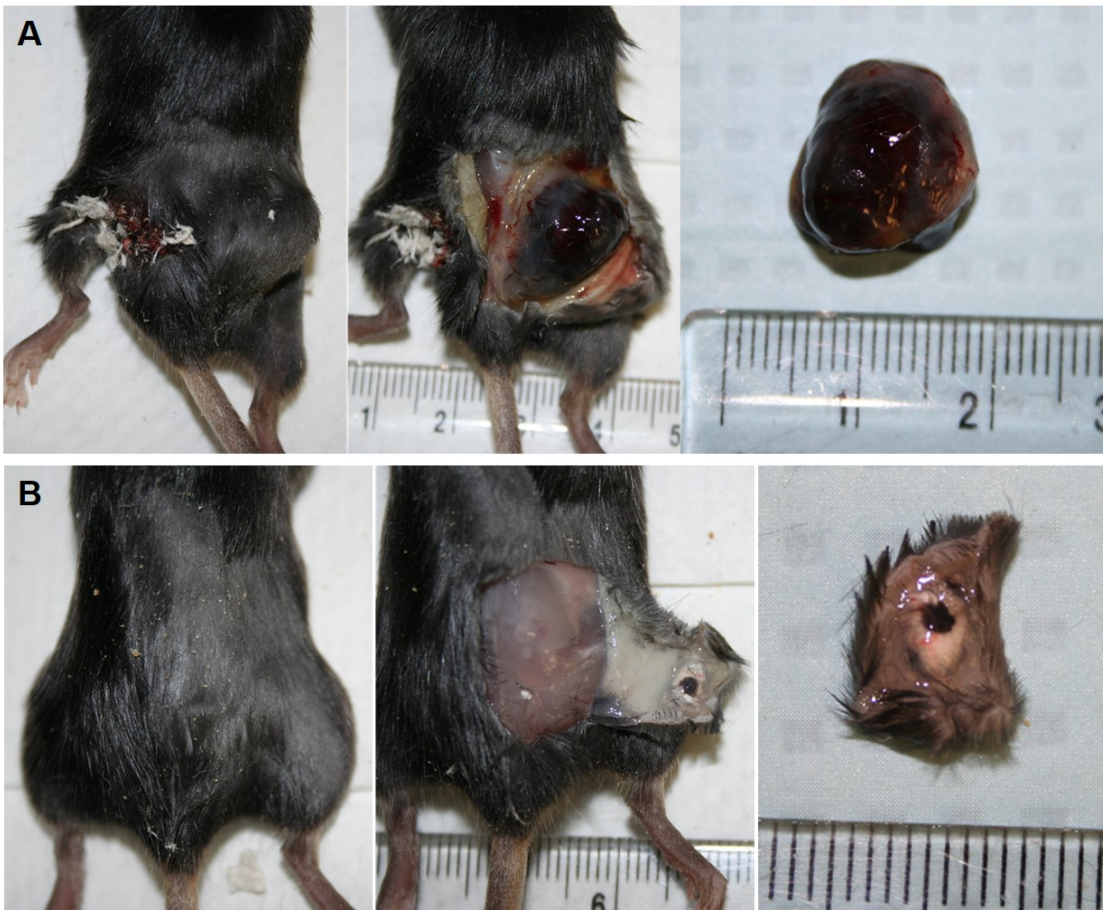

Figure 4.21 The actual melanoma tumor size comparison at day 15 in untreated control and UMMD treated mice. (A) Melanoma tumor in PBS injected control mouse at day 15. (B) Melanoma tumor in ultrasound mediated Optison microbubble treated mouse at day 15.

CHAPTER 5

DISCUSSION AND CONCLUSIONS

There have been frequent attempts to use low intensity ultrasound to stimulate cartilage repair. Studies have proven that ultrasound stimulates cartilage anabolism by enhancing the production of matrix molecules, attenuating the progression of cartilage degradation and increasing chondrogenesis of mesenchymal stem cells (MSCs). However, progress in understanding the mechanism of the benefits has been slow. Elucidation of biologically detailed mechanisms is necessary to fully understand and utilize the ultrasound as an anabolic stimulator.

Previously, it was found that chondrogenic progenitor cells (CPCs) emerge and tend to home toward injured sites in response to cartilage injury that may result in faster cartilage repair. It has been hypothesized that low intensity ultrasound therapy, a form of mechanical energy that can be non-invasively transferred into human body, triggers mechanotransductive cell signaling pathways as physically applied mechanical loading does. We found that low intensity ultrasound therapy significantly accelerated the homing of CPCs toward injured sited in cartilage suggesting that accelerated CPC homing in response to ultrasound therapy may speed up the return to normal cellularity in injured cartilage resulting in faster cartilage matrix repair. Since dynamic regulation of focal adhesions between cells and extracellular matrix (ECM) is critical for cell motility, it was hypothesized that low intensity ultrasound therapy triggers integrins associated cell migration signaling pathways. Direct focal adhesion associated protein tyrosine kinases such as FAK and Src family kinases (SFKs) were examined and further downstream

factors, the rho family of GTPases, were investigated. The results demonstrated that low intensity ultrasound stimulation increased FAK phosphorylation that is closely involved in cell motility signaling pathways. Inhibition of SFKs diminished ultrasound-activated CPC motility. The rho family of GTPases, which are known to be associated with actin polymerization and directional movement of cells, was also activated by low intensity ultrasound therapy in CPCs while normal chondrocytes were less responsive. In conclusion, low intensity ultrasound therapy accelerates homing ability of CPCs toward injured sites *via* triggering mechanotransductive cell signaling pathways and this can be considered as one of the biologic mechanisms of low intensity ultrasound therapy in cartilage repair.

Low intensity ultrasound therapy has proven to be beneficial for cartilage repair by synthesizing ECM molecules in which chondrocytes require sufficient metabolic energy such as ATP. However, little has been discovered about the role of low intensity ultrasound therapy in chondrocyte energy modulation. Thus, we investigated ATP production in response to low intensity ultrasound therapy. Recent findings suggest that mechanical loading enhanced ATP synthesis *via* induced ROS production in articular cartilage. For this reason, we hypothesized that ultrasound therapy may have a potential to synthesize ATP *via* modest levels of ROS production as mechanical stimulation does. The results revealed that ultrasound therapy enhanced ROS production in both injured and intact cartilage without any noticeable chondrocyte death. However, there was no considerable correlation between produced ROS and ATP synthesis. The effects of enhanced ROS by ultrasound therapy still remain unknown.

Over the past few decades, the use of gas-filled microbubbles has been extended from ultrasound contrast agents used in diagnostic ultrasonography to facilitating local anti-cancer drug delivery for the treatment of cancer cells or tumors. Under the lower peak negative ultrasound pressure, microbubbles stably oscillate, changing in size and shape and possibly producing microstreaming adjacent to cells. However, at higher peak negative ultrasound pressures microbubbles oscillate non-linearly, which can result in complete destruction of microbubbles. Fragmented microbubbles are likely to contribute to the formation of inertial cavitation that produces mechanical shock waves, elevated temperature, and free radical formation. Based on these findings, it was hypothesized that ultrasound mediated microbubble destruction could be used for the treatment of tumors regardless of vascularization and controlled release of drug delivery. The response of albumin shelled Optison microbubbles and polymer shelled PLGA microbubbles to ultrasound therapy was evaluated. The results demonstrated that low intensity ultrasound therapy imploded both types of microbubbles and lethal shock waves were released resulting in rupturing adjacent cell membranes. *In vitro* cytotoxicity test revealed that most of cells were dead *via* necrosis rather than apoptosis and there was no ultrasound sensitivity for both normal and malignant cells. Cell death was proportional to the ultrasound power and all of chondrocytes in pellet cultures were also killed. Similarly to albumin shelled Optison microbubbles, polymer shelled PLGA microbubbles also underwent complete destruction by releasing lethal shock waves that led B16 cell death in response to low intensity ultrasound therapy. Morphologic examination using a scanning electron microscopy showed that a number of cracks and holes in the surface PLGA microbubbles were created in response to low intensity ultrasound therapy. This

may indicated that the part of PLGA microbubbles underwent complete destruction and the rest of them were in transition of destruction. The release rate of doxorubicin from the PLGA microbubbles in response to ultrasound exposure revealed that the release kinetics were ultrasound duty cycle-dependent suggesting that stronger ultrasound energy resulted in more doxorubicin release by accelerating PLGA microbubbles degradation. To demonstrate the *in vivo* anti-cancer effects of lethal shock waves produced during ultrasound mediated Optison microbubble destruction, C57BL/6J mice were inoculated with B16 melanoma cancer cells. The mice group delivered with intratumoral lethal shock waves showed that the growth of tumors was significantly suppressed compared to the PBS injected control group. In conclusion, direct delivery of intratumoral lethal shock waves have potentials for overcoming current limitations of intravascularly administered microbubble mediated ultrasound therapy by reducing potential side effects of high concentrations of anti-cancer drugs at the site where the life of microbubbles ends during systemic circulation. In addition, intratumoral lethal shock waves delivery followed by sustained anti-cancer drug release could have significant clinical value as a non- or minimal-invasive tumor treatment method regardless of tumor types, vascularization and surgical accessibility.

REFERENCES

1. Buckwalter JA, Mankin HJ, Grodzinsky AJ. Articular cartilage and osteoarthritis. Instructional course lectures. 2005;54:465-80.
2. Nishimuta JF, Levenston ME. Response of cartilage and meniscus tissue explants to in vitro compressive overload. Osteoarthritis and cartilage / OARS, Osteoarthritis Research Society. 2012;20(5):422-9.
3. Borrelli J, Jr., Silva MJ, Zaegel MA, Franz C, Sandell LJ. Single high-energy impact load causes posttraumatic OA in young rabbits via a decrease in cellular metabolism. Journal of orthopaedic research : official publication of the Orthopaedic Research Society. 2009;27(3):347-52.
4. Brown TD, Johnston RC, Saltzman CL, Marsh JL, Buckwalter JA. Posttraumatic osteoarthritis: a first estimate of incidence, prevalence, and burden of disease. Journal of orthopaedic trauma. 2006;20(10):739-44.
5. Buckwalter JA, Brown TD. Joint injury, repair, and remodeling: roles in post-traumatic osteoarthritis. Clinical orthopaedics and related research. 2004(423):7-16.
6. O'Reilly SC, Muir KR, Doherty M. Effectiveness of home exercise on pain and disability from osteoarthritis of the knee: a randomised controlled trial. Annals of the rheumatic diseases. 1999;58(1):15-9.
7. Leong DJ, Hardin JA, Cobelli NJ, Sun HB. Mechanotransduction and cartilage integrity. Annals of the New York Academy of Sciences. 2011;1240:32-7.
8. Ikenoue T, Trindade MC, Lee MS, Lin EY, Schurman DJ, Goodman SB, et al. Mechanoregulation of human articular chondrocyte aggrecan and type II collagen expression by intermittent hydrostatic pressure in vitro. Journal of orthopaedic research : official publication of the Orthopaedic Research Society. 2003;21(1):110-6.
9. Martin JA, Buckwalter JA. Aging, articular cartilage chondrocyte senescence and osteoarthritis. Biogerontology. 2002;3(5):257-64.
10. Martin JA, Buckwalter JA. The role of chondrocyte senescence in the pathogenesis of osteoarthritis and in limiting cartilage repair. The Journal of bone and joint surgery American volume. 2003;85-A Suppl 2:106-10.
11. Buckwalter JA, Mankin HJ. Articular cartilage: degeneration and osteoarthritis, repair, regeneration, and transplantation. Instructional course lectures. 1998;47:487-504.
12. Hjelle K, Solheim E, Strand T, Muri R, Brittberg M. Articular cartilage defects in 1,000 knee arthroscopies. Arthroscopy : the journal of arthroscopic & related surgery : official publication of the Arthroscopy Association of North America and the International Arthroscopy Association. 2002;18(7):730-4.
13. Hunziker EB. Articular cartilage repair: basic science and clinical progress. A review of the current status and prospects. Osteoarthritis and cartilage / OARS, Osteoarthritis Research Society. 2002;10(6):432-63.
14. Laupattarakasem W, Laopaiboon M, Laupattarakasem P, Sumananont C. Arthroscopic debridement for knee osteoarthritis. The Cochrane database of systematic reviews. 2008(1):CD005118.
15. Jackson RW, Dieterichs C. The results of arthroscopic lavage and debridement of osteoarthritic knees based on the severity of degeneration: a 4- to 6-year symptomatic follow-up. Arthroscopy : the journal of arthroscopic & related surgery : official publication of the Arthroscopy Association of North America and the International Arthroscopy Association. 2003;19(1):13-20.

16. Hubbard MJ. Articular debridement versus washout for degeneration of the medial femoral condyle. A five-year study. The Journal of bone and joint surgery British volume. 1996;78(2):217-9.
17. Blevins FT, Steadman JR, Rodrigo JJ, Silliman J. Treatment of articular cartilage defects in athletes: an analysis of functional outcome and lesion appearance. Orthopedics. 1998;21(7):761-7; discussion 7-8.
18. Browne JE, Branch TP. Surgical alternatives for treatment of articular cartilage lesions. The Journal of the American Academy of Orthopaedic Surgeons. 2000;8(3):180-9.
19. Fond J, Rodin D, Ahmad S, Nirschl RP. Arthroscopic debridement for the treatment of osteoarthritis of the knee: 2- and 5-year results. Arthroscopy : the journal of arthroscopic & related surgery : official publication of the Arthroscopy Association of North America and the International Arthroscopy Association. 2002;18(8):829-34.
20. Ibarra-Ponce de Leon JC, Cabrales-Pontigo M, Crisostomo-Martinez JF, Almazan-Diaz A, Cruz-Lopez F, Encalada-Diaz MI, et al. [Results of arthroscopic debridement and lavage in patients with knee osteoarthritis]. Acta ortopedica mexicana. 2009;23(2):85-9.
21. Johnson LL. Arthroscopic abrasion arthroplasty: a review. Clinical orthopaedics and related research. 2001(391 Suppl):S306-17.
22. Saw KY, Anz A, Merican S, Tay YG, Ragavanaidu K, Jee CSY, et al. Articular Cartilage Regeneration With Autologous Peripheral Blood Progenitor Cells and Hyaluronic Acid After Arthroscopic Subchondral Drilling: A Report of 5 Cases With Histology. Arthroscopy-the Journal of Arthroscopic and Related Surgery. 2011;27(4):493-506.
23. Steadman JR, Briggs KK, Rodrigo JJ, Kocher MS, Gill TJ, Rodkey WG. Outcomes of microfracture for traumatic chondral defects of the knee: Average 11-year follow-up. Arthroscopy-the Journal of Arthroscopic and Related Surgery. 2003;19(5):477-84.
24. Dirschl DR, Marsh JL, Buckwalter JA, Gelberman R, Olson SA, Brown TD, et al. Articular fractures. J Am Acad Orthop Sur. 2004;12(6):416-23.
25. Kurz B, Lemke AK, Fay J, Pufe T, Grodzinsky AJ, Schunke M. Pathomechanisms of cartilage destruction by mechanical injury. Annals of anatomy = Anatomischer Anzeiger : official organ of the Anatomische Gesellschaft. 2005;187(5-6):473-85.
26. Chen CT, Burton-Wurster N, Borden C, Hueffer K, Bloom SE, Lust G. Chondrocyte necrosis and apoptosis in impact damaged articular cartilage. Journal of orthopaedic research : official publication of the Orthopaedic Research Society. 2001;19(4):703-11.
27. Chen CT, Burton-Wurster N, Lust G, Bank RA, Tekoppele JM. Compositional and metabolic changes in damaged cartilage are peak-stress, stress-rate, and loading-duration dependent. Journal of orthopaedic research : official publication of the Orthopaedic Research Society. 1999;17(6):870-9.
28. Borrelli J, Jr., Tinsley K, Ricci WM, Burns M, Karl IE, Hotchkiss R. Induction of chondrocyte apoptosis following impact load. Journal of orthopaedic trauma. 2003;17(9):635-41.
29. Goodwin W, McCabe D, Sauter E, Reese E, Walter M, Buckwalter JA, et al. Rotenone prevents impact-induced chondrocyte death. Journal of orthopaedic research : official publication of the Orthopaedic Research Society. 2010;28(8):1057-63.

30. Martin JA, McCabe D, Walter M, Buckwalter JA, McKinley TO. N-acetylcysteine inhibits post-impact chondrocyte death in osteochondral explants. J Bone Joint Surg Am. 2009;91(8):1890-7.
31. Seol D, McCabe DJ, Choe H, Zheng HJ, Yu Y, Jang K, et al. Chondrogenic progenitor cells respond to cartilage injury. Arthritis Rheum-Us. 2012;64(11):3626-37.
32. Parvizi J, Wu CC, Lewallen DG, Greenleaf JF, Bolander ME. Low-intensity ultrasound stimulates proteoglycan synthesis in rat chondrocytes by increasing aggrecan gene expression. Journal of orthopaedic research : official publication of the Orthopaedic Research Society. 1999;17(4):488-94.
33. Zhang ZJ, Huckle J, Francomano CA, Spencer RGS. The effects of pulsed low-intensity ultrasound on chondrocyte viability, proliferation, gene expression and matrix production. Ultrasound Med Biol. 2003;29(11):1645-51.
34. Zhang ZJ, Huckle J, Francomano CA, Spencer RGS. The influence of pulsed low-intensity ultrasound on matrix production of chondrocytes at different stages of differentiation: an explant study (vol 28, pg 1547, 2002). Ultrasound Med Biol. 2003;29(8):1223-.
35. Korstjens CM, van der Rijt RH, Albers GH, Semeins CM, Klein-Nulend J. Low-intensity pulsed ultrasound affects human articular chondrocytes in vitro. Medical & biological engineering & computing. 2008;46(12):1263-70.
36. Khanna A, Nelmes RT, Gougoulias N, Maffulli N, Gray J. The effects of LIPUS on soft-tissue healing: a review of literature. British medical bulletin. 2009;89:169-82.
37. Naito K, Watari T, Muta T, Furuhata A, Iwase H, Igarashi M, et al. Low-intensity pulsed ultrasound (LIPUS) increases the articular cartilage type II collagen in a rat osteoarthritis model. Journal of orthopaedic research : official publication of the Orthopaedic Research Society. 2010;28(3):361-9.
38. Ebisawa K, Hata K, Okada K, Kimata K, Ueda M, Torii S, et al. Ultrasound enhances transforming growth factor beta-mediated chondrocyte differentiation of human mesenchymal stem cells. Tissue engineering. 2004;10(5-6):921-9.
39. Schumann D, Kujat R, Zellner J, Angele MK, Nerlich M, Mayr E, et al. Treatment of human mesenchymal stem cells with pulsed low intensity ultrasound enhances the chondrogenic phenotype in vitro. Biorheology. 2006;43(3-4):431-43.
40. Cui JH, Park SR, Park K, Choi BH, Min BH. Preconditioning of mesenchymal stem cells with low-intensity ultrasound for cartilage formation in vivo. Tissue engineering. 2007;13(2):351-60.
41. Park SR, Choi BH, Min BH. Low-Intensity Ultrasound (LIUS) as an Innovative Tool for Chondrogenesis of Mesenchymal Stem Cells (MSCs). Organogenesis. 2007;3(2):74-8.
42. Gurkan I, Ranganathan A, Yang X, Horton WE, Jr., Todman M, Huckle J, et al. Modification of osteoarthritis in the guinea pig with pulsed low-intensity ultrasound treatment. Osteoarthritis and cartilage / OARS, Osteoarthritis Research Society. 2010;18(5):724-33.
43. Lai CH, Chen SC, Chiu LH, Yang CB, Tsai YH, Zuo CS, et al. Effects of low-intensity pulsed ultrasound, dexamethasone/TGF-beta1 and/or BMP-2 on the transcriptional expression of genes in human mesenchymal stem cells: chondrogenic vs. osteogenic differentiation. Ultrasound Med Biol. 2010;36(6):1022-33.
44. Zhou S, Schmelz A, Seufferlein T, Li Y, Zhao J, Bachem MG. Molecular mechanisms of low intensity pulsed ultrasound in human skin fibroblasts. The Journal of biological chemistry. 2004;279(52):54463-9.

45. ter Haar G. Ultrasound bioeffects and safety. Proceedings of the Institution of Mechanical Engineers Part H, Journal of engineering in medicine. 2010;224(2):363-73.
46. O'Brien WD, Jr. Ultrasound-biophysics mechanisms. Progress in biophysics and molecular biology. 2007;93(1-3):212-55.
47. Ahmadi F, McLoughlin IV, Chauhan S, ter-Haar G. Bio-effects and safety of low-intensity, low-frequency ultrasonic exposure. Progress in biophysics and molecular biology. 2012;108(3):119-38.
48. Miller DL, Smith NB, Bailey MR, Czarnota GJ, Hynynen K, Makin IR, et al. Overview of therapeutic ultrasound applications and safety considerations. Journal of ultrasound in medicine : official journal of the American Institute of Ultrasound in Medicine. 2012;31(4):623-34.
49. Hernot S, Klibanov AL. Microbubbles in ultrasound-triggered drug and gene delivery. Advanced drug delivery reviews. 2008;60(10):1153-66.
50. Chomas JE, Dayton P, Allen J, Morgan K, Ferrara KW. Mechanisms of contrast agent destruction. IEEE transactions on ultrasonics, ferroelectrics, and frequency control. 2001;48(1):232-48.
51. Chomas JE, Dayton PA, May D, Allen J, Klibanov A, Ferrara K. Optical observation of contrast agent destruction. Appl Phys Lett. 2000;77(7):1056-8.
52. Fox AJS, Bedi A, Rodeo SA. The Basic Science of Articular Cartilage. Sports Health. 2009

;1(6):461-8.
53. Aydelotte MB, Greenhill RR, Kuettner KE. Differences between Sub-Populations of Cultured Bovine Articular Chondrocytes .2. Proteoglycan Metabolism. Connect Tissue Res. 1988;18(3):223-34.
54. Aydelotte MB, Kuettner KE. Differences between Sub-Populations of Cultured Bovine Articular Chondrocytes .1. Morphology and Cartilage Matrix Production. Connect Tissue Res. 1988;18(3):205-22.
55. Buckwalter JA, Mankin HJ. Articular cartilage .1. Tissue design and chondrocyte-matrix interactions. Journal of Bone and Joint Surgery-American Volume. 1997;79A(4):600-11.
56. Weiss C, Rosenber.L, Helfet AJ. An Ultrastructural Study of Normal Young Adult Human Articular Cartilage. Journal of Bone and Joint Surgery-American Volume. 1968;A 50(4):663-&.
57. Bhosale AM, Richardson JB. Articular cartilage: structure, injuries and review of management. British medical bulletin. 2008;87(1):77-95.
58. Brower TD, Hsu WY. Normal Articular Cartilage. Clinical orthopaedics and related research. 1969(64):9-&.
59. Stockwell RA. Chondrocytes. Journal of clinical pathology Supplement. 1978;12:7-13.
60. Stockwell RA. The cell density of human articular and costal cartilage. Journal of anatomy. 1967;101(Pt 4):753-63.
61. Muir H. The Chondrocyte, Architect of Cartilage - Biomechanics, Structure, Function and Molecular-Biology of Cartilage Matrix Macromolecules. Bioessays. 1995;17(12):1039-48.
62. Burrage PS, Mix KS, Brinckerhoff CE. Matrix metalloproteinases: Role in arthritis. Front Biosci. 2006;11:529-43.

63. Nesic D, Whiteside R, Brittberg M, Wendt D, Martin I, Mainil-Varlet P. Cartilage tissue engineering for degenerative joint disease. Adv Drug Deliver Rev. 2006;58(2):300-22.
64. Ding L, Heying E, Nicholson N, Stroud NJ, Homandberg GA, Buckwalter JA, et al. Mechanical impact induces cartilage degradation via mitogen activated protein kinases. Osteoarthr Cartilage. 2010;18(11):1509-17.
65. Martin JA, Buckwalter JA. Roles of articular cartilage aging and chondrocyte senescence in the pathogenesis of osteoarthritis. The Iowa orthopaedic journal. 2001;21:1-7.
66. Buckwalter JA, Martin JA. Osteoarthritis. Adv Drug Deliv Rev. 2006;58(2):150-67.
67. Lawrence RC, Helmick CG, Arnett FC, Deyo RA, Felson DT, Giannini EH, et al. Estimates of the prevalence of arthritis and selected musculoskeletal disorders in the United States. Arthritis Rheum. 1998;41(5):778-99.
68. Helmick CG, Felson DT, Lawrence RC, Gabriel S, Hirsch R, Kwoh CK, et al. Estimates of the prevalence of arthritis and other rheumatic conditions in the United States. Part I. Arthritis Rheum. 2008;58(1):15-25.
69. Gabriel SE, Crowson CS, Campion ME, O'Fallon WM. Direct medical costs unique to people with arthritis. The Journal of rheumatology. 1997;24(4):719-25.
70. Centers for Disease Control and Prevention, http://www.cdc.gov/.
71. World Health Organization (WHO), http://www.who.int/en/.
72. Saklatvala J. Tumour necrosis factor alpha stimulates resorption and inhibits synthesis of proteoglycan in cartilage. Nature. 1986;322(6079):547-9.
73. Jang KW, Buckwalter JA, Martin JA. Inhibition of cell-matrix adhesions prevents cartilage chondrocyte death following impact injury. Journal of orthopaedic research : official publication of the Orthopaedic Research Society. 2014;32(3):448-54.
74. Sauter E, Buckwalter JA, McKinley TO, Martin JA. Cytoskeletal dissolution blocks oxidant release and cell death in injured cartilage. Journal of orthopaedic research : official publication of the Orthopaedic Research Society. 2012;30(4):593-8.
75. Mithoefer K, Williams RJ, 3rd, Warren RF, Potter HG, Spock CR, Jones EC, et al. Chondral resurfacing of articular cartilage defects in the knee with the microfracture technique. Surgical technique. The Journal of bone and joint surgery American volume. 2006;88 Suppl 1 Pt 2:294-304.
76. Mithoefer K, Williams RJ, 3rd, Warren RF, Potter HG, Spock CR, Jones EC, et al. The microfracture technique for the treatment of articular cartilage lesions in the knee. A prospective cohort study. The Journal of bone and joint surgery American volume. 2005;87(9):1911-20.
77. Steadman JR, Briggs KK, Rodrigo JJ, Kocher MS, Gill TJ, Rodkey WG. Outcomes of microfracture for traumatic chondral defects of the knee: average 11-year follow-up. Arthroscopy : the journal of arthroscopic & related surgery : official publication of the Arthroscopy Association of North America and the International Arthroscopy Association. 2003;19(5):477-84.
78. Smith GD, Richardson JB, Brittberg M, Erggelet C, Verdonk R, Knutsen G, et al. Autologous chondrocyte implantation and osteochondral cylinder transplantation in cartilage repair of the knee joint. The Journal of bone and joint surgery American volume. 2003;85-A(12):2487-8; author reply 8.
79. Brittberg M, Lindahl A, Nilsson A, Ohlsson C, Isaksson O, Peterson L. Treatment of deep cartilage defects in the knee with autologous chondrocyte transplantation. The New England journal of medicine. 1994;331(14):889-95.

80. Brittberg M. Autologous chondrocyte transplantation. Clinical orthopaedics and related research. 1999(367 Suppl):S147-55.
81. Pittenger MF, Mackay AM, Beck SC, Jaiswal RK, Douglas R, Mosca JD, et al. Multilineage potential of adult human mesenchymal stem cells. Science. 1999;284(5411):143-7.
82. Richter W. Cell-based cartilage repair: illusion or solution for osteoarthritis. Current opinion in rheumatology. 2007;19(5):451-6.
83. Hangody L, Rathonyi GK, Duska Z, Vasarhelyi G, Fules P, Modis L. Autologous osteochondral mosaicplasty. Surgical technique. The Journal of bone and joint surgery American volume. 2004;86-A Suppl 1:65-72.
84. Kitchen SS PC. A review of therapeutic ultrasound, part 1: background and physiological effects. Physiotherapy. 1990;76.
85. Parvizi J, Parpura V, Greenleaf JF, Bolander ME. Calcium signaling is required for ultrasound-stimulated aggrecan synthesis by rat chondrocytes. J Orthopaed Res. 2002;20(1):51-7.
86. Wu JR, Du GH. Temperature Elevation in Tissues Generated by Finite-Amplitude Tone Bursts of Ultrasound. J Acoust Soc Am. 1990;88(3):1562-77.
87. Jang K.W RPS, Buckwalter J.A., Martin J.A. Low-Intensity Continuous Ultrasound (LIUS) Enhances Reactive Oxygen Species Production Following A Blunt Impact Injury In Articular Cartilage. Transactions of the 59th Annual Meeting of the Orthopaedic Research Society. 2014.
88. ter Haar G. Biological effects of ultrasound in clinical applications. In: Suslick KS, ed Ultrasound: Its Chemical, Physical, and Biological Effects New York, NY: VCH Publishers Inc. 1988:305-20.
89. Ogurtan Z, Celik I, Izci C, Boydak M, Alkan F, Yilmaz K. Effect of experimental therapeutic ultrasound on the distal antebrachial growth plates in one-month-old rabbits. Veterinary journal. 2002;164(3):280-7.
90. Dalecki D. Mechanical bioeffects of ultrasound. Annual review of biomedical engineering. 2004;6:229-48.
91. Fowlkes JB, Bioeffects Committee of the American Institute of Ultrasound in M. American Institute of Ultrasound in Medicine consensus report on potential bioeffects of diagnostic ultrasound: executive summary. Journal of ultrasound in medicine : official journal of the American Institute of Ultrasound in Medicine. 2008;27(4):503-15.
92. Santos HM, Lodeiro, C. and Capelo-Martínez, J.-L. . The Power of Ultrasound, in Ultrasound in Chemistry: Analytical Applications. 2009.
93. Pellaumail B, Dewailly V, Watrin A, Loeuille D, Netter P, Berger G, et al. Attenuation coefficient and speed of sound in immature and mature rat cartilage: a study in the 30-70 MHz frequency range. Ultrason. 1999:1361-4.
94. Nieminen HJ, Saarakkala S, Laasanen MS, Hirvonen J, Jurvelin JS, Toyras J. Ultrasound attenuation in normal and spontaneously degenerated articular cartilage. Ultrasound Med Biol. 2004;30(4):493-500.
95. Cook SD, Salkeld SL, Popich-Patron LS, Ryaby JP, Jones DG, Barrack RL. Improved cartilage repair after treatment with low-intensity pulsed ultrasound. Clinical orthopaedics and related research. 2001(391 Suppl):S231-43.
96. Min BH, Woo JI, Cho HS, Choi BH, Park SJ, Choi MJ, et al. Effects of low-intensity ultrasound (LIUS) stimulation on human cartilage explants. Scand J Rheumatol. 2006;35(4):305-11.

97. Lee HJ, Choi BH, Min BH, Son YS, Park SR. Low-intensity ultrasound stimulation enhances chondrogenic differentiation in alginate culture of mesenchymal stem cells. Artif Organs. 2006;30(9):707-15.
98. Jang KW, Ding L, Seol D, Lim TH, Buckwalter JA, Martin JA. Low-intensity pulsed ultrasound promotes chondrogenic progenitor cell migration via focal adhesion kinase pathway. Ultrasound Med Biol. 2014;40(6):1177-86.
99. Lindner JR. Microbubbles in medical imaging: current applications and future directions. Nature reviews Drug discovery. 2004;3(6):527-32.
100. McCulloch M, Gresser C, Moos S, Odabashian J, Jasper S, Bednarz J, et al. Ultrasound contrast physics: A series on contrast echocardiography, article 3. Journal of the American Society of Echocardiography : official publication of the American Society of Echocardiography. 2000;13(10):959-67.
101. Gramiak R, Shah PM. Echocardiography of the aortic root. Investigative radiology. 1968;3(5):356-66.
102. Dijkmans PA, Juffermans LJ, Musters RJ, van Wamel A, ten Cate FJ, van Gilst W, et al. Microbubbles and ultrasound: from diagnosis to therapy. European journal of echocardiography : the journal of the Working Group on Echocardiography of the European Society of Cardiology. 2004;5(4):245-56.
103. Unger EC, Hersh E, Vannan M, Matsunaga TO, McCreery M. Local drug and gene delivery through microbubbles. Prog Cardiovasc Dis. 2001;44(1):45-54.
104. Unger EC, Matsunaga TO, McCreery T, Schumann P, Sweitzer R, Quigley R. Therapeutic applications of microbubbles. Eur J Radiol. 2002;42(2):160-8.
105. Lindner JR, Kaul S. Delivery of drugs with ultrasound. Echocardiogr-J Card. 2001;18(4):329-37.
106. Porter TR, Xie F. Therapeutic ultrasound for gene delivery. Echocardiogr-J Card. 2001;18(4):349-53.
107. van Wamel A, Kooiman K, Harteveld M, Emmer M, ten Cate FJ, Versluis M, et al. Vibrating microbubbles poking individual cells: Drug transfer into cells via sonoporation. J Control Release. 2006;112(2):149-55.
108. Ward M, Wu JR, Chiu JF. Ultrasound-induced cell lysis and sonoporation enhanced by contrast agents. J Acoust Soc Am. 1999;105(5):2951-7.
109. Birnbaum Y, Luo H, Nagai T, Fishbein MC, Peterson TM, Li SP, et al. Noninvasive in vivo clot dissolution without a thrombolytic drug - Recanalization of thrombosed iliofemoral arteries by transcutaneous ultrasound combined with intravenous infusion of microbubbles. Circulation. 1998;97(2):130-4.
110. Forbes MM, Steinberg RL, O'Brien WD. Examination of Inertial Cavitation of Optison in Producing Sonoporation of Chinese Hamster Ovary Cells. Ultrasound Med Biol. 2008;34(12):2009-18.
111. Datta S, Coussios CC, Ammi AY, Mast TD, de Courten-Myers GM, Holland CK. Ultrasound-enhanced thrombolysis using Definity (R) as a cavitation nucleation agent. Ultrasound Med Biol. 2008;34(9):1421-33.
112. Liu H, Chang S, Sun J, Zhu S, Pu C, Zhu Y, et al. Ultrasound-mediated destruction of LHRHa-targeted and paclitaxel-loaded lipid microbubbles induces proliferation inhibition and apoptosis in ovarian cancer cells. Molecular pharmaceutics. 2014;11(1):40-8.
113. Pu C, Chang S, Sun J, Zhu S, Liu H, Zhu Y, et al. Ultrasound-mediated destruction of LHRHa-targeted and paclitaxel-loaded lipid microbubbles for the treatment of intraperitoneal ovarian cancer xenografts. Molecular pharmaceutics. 2014;11(1):49-58.

114. Du J, Du LF, Li FH, Zheng XZ, Li HL, Shi QS, et al. Ultrasound targeted microbubble destruction-mediated gene delivery system: application to therapy for ocular disease. Asian Biomed. 2011;5(5):577-87.
115. Pitt WG, Husseini GA, Staples BJ. Ultrasonic drug delivery--a general review. Expert opinion on drug delivery. 2004;1(1):37-56.
116. Feng Y, Tian ZM, Wan MX. Bioeffects of Low-Intensity Ultrasound In Vitro Apoptosis, Protein Profile Alteration, and Potential Molecular Mechanism. J Ultras Med. 2010;29(6):963-74.
117. Feril LB, Jr., Kondo T. Biological effects of low intensity ultrasound: the mechanism involved, and its implications on therapy and on biosafety of ultrasound. Journal of radiation research. 2004;45(4):479-89.
118. Feril LB, Kondo T, Zhao QL, Ogawa R, Tachibana K, Kudo N, et al. Enhancement of ultrasound-induced apoptosis and cell lysis by echo-contrast agents. Ultrasound in Medicine and Biology. 2003;29(2):331-7.
119. Kodama T, Tomita Y, Koshiyama KI, Blomley MJK. Transfection effect of microbubbles on cells in superposed ultrasound waves and behavior of cavitation bubble. Ultrasound in Medicine and Biology. 2006;32(6):905-14.
120. Chen ZY, Wang YX, Zhao YZ, Yang F, Liu JB, Lin Y, et al. Apoptosis induction by ultrasound and microbubble mediated drug delivery and gene therapy. Current molecular medicine. 2014;14(6):723-36.
121. Gao R, Zhou X, Yang Y, Wang Z. Transfection of wtp53 and Rb94 genes into retinoblastomas of nude mice by ultrasound-targeted microbubble destruction. Ultrasound Med Biol. 2014;40(11):2662-70.
122. Wu S, Li L, Wang G, Shen W, Xu Y, Liu Z, et al. Ultrasound-targeted stromal cell-derived factor-1-loaded microbubble destruction promotes mesenchymal stem cell homing to kidneys in diabetic nephropathy rats. International journal of nanomedicine. 2014;9:5639-51.
123. Zhu F, Jiang Y, Luo F, Li P. Effectiveness of localized ultrasound-targeted microbubble destruction with doxorubicin liposomes in H22 mouse hepatocellular carcinoma model. Journal of drug targeting. 2015:1-12.
124. Liu Y, Li L, Su Q, Liu T, Ma Z, Yang H. Ultrasound-Targeted Microbubble Destruction Enhances Gene Expression of microRNA-21 in Swine Heart via Intracoronary Delivery. Echocardiography. 2015.
125. Tang CH. Molecular mechanisms of chondrosarcoma metastasis. BioMedicine. 2012;2(3):92-8.
126. Anatomy of knee joint. ePainAssistcom.
127. Articular cartilage in knee joint. Houston Methodist Orthopedics & Sports Medicine
128. Osteoarthritis of the Knee. Dreamstimecom.
129. Microfracture. Orthoinforaaosorg.
130. Noth U, Steinert AF, Tuan RS. Technology insight: adult mesenchymal stem cells for osteoarthritis therapy. Nature clinical practice Rheumatology. 2008;4(7):371-80.
131. Osteochondral transplantation. BoneandSpinecom.
132. UTMD. http://spot.colorado.edu/~mabo4929/research pages/therapy.html.
133. Wang Y, Ding C, Wluka AE, Davis S, Ebeling PR, Jones G, et al. Factors affecting progression of knee cartilage defects in normal subjects over 2 years. Rheumatology. 2006;45(1):79-84.

134. Zhang ZJ, Huckle J, Francomano CA, Spencer RGS. The influence of pulsed low-intensity ultrasound on matrix production of chondrocytes at different stages of differentiation: An explant study. Ultrasound Med Biol. 2002;28(11-12):1547-53.
135. Huveneers S, Danen EHJ. Adhesion signaling - crosstalk between integrins, Src and Rho. J Cell Sci. 2009;122(8):1059-69.
136. Aplin AE, Howe A, Alahari SK, Juliano RL. Signal transduction and signal modulation by cell adhesion receptors: the role of integrins, cadherins, immunoglobulin-cell adhesion molecules, and selectins. Pharmacological reviews. 1998;50(2):197-263.
137. Howe A, Aplin AE, Alahari SK, Juliano RL. Integrin signaling and cell growth control. Current opinion in cell biology. 1998;10(2):220-31.
138. Clark EA, Brugge JS. Integrins and signal transduction pathways: the road taken. Science. 1995;268(5208):233-9.
139. Lauffenburger DA, Horwitz AF. Cell migration: a physically integrated molecular process. Cell. 1996;84(3):359-69.
140. Parsons JT. Focal adhesion kinase: the first ten years. J Cell Sci. 2003;116(Pt 8):1409-16.
141. Hanks SK, Calalb MB, Harper MC, Patel SK. Focal adhesion protein-tyrosine kinase phosphorylated in response to cell attachment to fibronectin. Proceedings of the National Academy of Sciences of the United States of America. 1992;89(18):8487-91.
142. Ilic D, Furuta Y, Kanazawa S, Takeda N, Sobue K, Nakatsuji N, et al. Reduced cell motility and enhanced focal adhesion contact formation in cells from FAK-deficient mice. Nature. 1995;377(6549):539-44.
143. Cary LA, Chang JF, Guan JL. Stimulation of cell migration by overexpression of focal adhesion kinase and its association with Src and Fyn. J Cell Sci. 1996;109 (Pt 7):1787-94.
144. Sieg DJ, Hauck CR, Schlaepfer DD. Required role of focal adhesion kinase (FAK) for integrin-stimulated cell migration. J Cell Sci. 1999;112 (Pt 16):2677-91.
145. Sieg DJ, Hauck CR, Ilic D, Klingbeil CK, Schaefer E, Damsky CH, et al. FAK integrates growth-factor and integrin signals to promote cell migration. Nature cell biology. 2000;2(5):249-56.
146. Calalb MB, Zhang XE, Polte TR, Hanks SK. Focal adhesion kinase tyrosine-861 is a major site of phosphorylation by Src. Biochem Bioph Res Co. 1996;228(3):662-8.
147. Chaturvedi LS, Gayer CP, Marsh HM, Basson MD. Repetitive deformation activates Src-independent FAK-dependent ERK motogenic signals in human Caco-2 intestinal epithelial cells. Am J Physiol-Cell Ph. 2008;294(6):C1350-C61.
148. Green TP, Fennell M, Whittaker R, Curwen J, Jacobs V, Allen J, et al. Preclinical anticancer activity of the potent, oral Src inhibitor AZD0530. Mol Oncol. 2009;3(3):248-61.
149. Grimshaw MJ, Mason RM. Bovine articular chondrocyte function in vitro depends upon oxygen tension. Osteoarthr Cartilage. 2000;8(5):386-92.
150. Zhou SD, Cui ZF, Urban JPG. Factors influencing the oxygen concentration gradient from the synovial surface of articular cartilage to the cartilage-bone interface - A modeling study. Arthritis Rheum-Us. 2004;50(12):3915-24.
151. Lane JM, Brighton CT, Menkowitz BJ. Anaerobic and Aerobic Metabolism in Articular-Cartilage. Journal of Rheumatology. 1977;4(4):334-42.
152. Otte P. Basic Cell-Metabolism of Articular-Cartilage - Manometric Studies. Z Rheumatol. 1991;50(5):304-12.
153. Lee RB, Urban JPG. Evidence for a negative Pasteur effect in articular cartilage. Biochem J. 1997;321:95-102.

154. Wolff KJ, Ramakrishnan PS, Brouillette MJ, Journot BJ, McKinley TO, Buckwalter JA, et al. Mechanical stress and ATP synthesis are coupled by mitochondrial oxidants in articular cartilage. Journal of orthopaedic research : official publication of the Orthopaedic Research Society. 2013;31(2):191-6.
155. Martin JA, Martini A, Molinari A, Morgan W, Ramalingam W, Buckwalter JA, et al. Mitochondrial electron transport and glycolysis are coupled in articular cartilage. Osteoarthritis and cartilage / OARS, Osteoarthritis Research Society. 2012;20(4):323-9.
156. Zeqiri B, Bickley CJ. A new anechoic material for medical ultrasonic applications. Ultrasound Med Biol. 2000;26(3):481-5.
157. Preston RC. Measurement and Characterization of the Acoustic Output of Medical Ultrasonic Equipment .1. Medical & biological engineering & computing. 1986;24(2):113-20.
158. Preston RC. Measurement and Characterization of the Acoustic Output of Medical Ultrasonic Equipment .2. Medical & biological engineering & computing. 1986;24(3):225-34.
159. Hood JD, Cheresh DA. Role of integrins in cell invasion and migration. Nature reviews Cancer. 2002;2(2):91-100.
160. Amano M, Chihara K, Kimura K, Fukata Y, Nakamura N, Matsuura Y, et al. Formation of actin stress fibers and focal adhesions enhanced by Rho-kinase. Science. 1997;275(5304):1308-11.
161. Lim ST, Longley RL, Couchman JR, Woods A. Direct binding of syndecan-4 cytoplasmic domain to the catalytic domain of protein kinase C alpha (PKC alpha) increases focal adhesion localization of PKC alpha. Journal of Biological Chemistry. 2003;278(16):13795-802.
162. Merlot S, Firtel RA. Leading the way: directional sensing through phosphatidylinositol 3-kinase and other signaling pathways. J Cell Sci. 2003;116(17):3471-8.
163. Humphries JD, Wang P, Streuli C, Geiger B, Humphries MJ, Ballestrem C. Vinculin controls focal adhesion formation by direct interactions with talin and actin. The Journal of cell biology. 2007;179(5):1043-57.
164. Choi CK, Vicente-Manzanares M, Zareno J, Whitmore LA, Mogilner A, Horwitz AR. Actin and alpha-actinin orchestrate the assembly and maturation of nascent adhesions in a myosin II motor-independent manner. Nature cell biology. 2008;10(9):1039-50.
165. Critchley DR, Gingras AR. Talin at a glance. J Cell Sci. 2008;121(9):1345-7.
166. Schaller MD. Cellular functions of FAK kinases: insight into molecular mechanisms and novel functions. J Cell Sci. 2010;123(7):1007-13.
167. Giancotti FG, Ruoslahti E. Integrin signaling. Science. 1999;285(5430):1028-32.
168. Mitra SK, Hanson DA, Schlaepfer DD. Focal adhesion kinase: in command and control of cell motility. Nature reviews Molecular cell biology. 2005;6(1):56-68.
169. Zhao X, Guan JL. Focal adhesion kinase and its signaling pathways in cell migration and angiogenesis. Adv Drug Deliv Rev. 2011;63(8):610-5.
170. Cabrita MA, Jones LM, Quizi JL, Sabourin LA, McKay BC, Addison CL. Focal adhesion kinase inhibitors are potent anti-angiogenic agents. Mol Oncol. 2011;5(6):517-26.
171. Sanchez-Bailon MP, Calcabrini A, Gomez-Dominguez D, Morte B, Martin-Forero E, Gomez-Lopez G, et al. Src kinases catalytic activity regulates proliferation, migration and invasiveness of MDA-MB-231 breast cancer cells. Cellular signalling. 2012;24(6):1276-86.

172. Degryse B, Bonaldi T, Scaffidi P, Muller S, Resnati M, Sanvito F, et al. The high mobility group (HMG) boxes of the nuclear protein HMG1 induce chemotaxis and cytoskeleton reorganization in rat smooth muscle cells. The Journal of cell biology. 2001;152(6):1197-206.
173. Carrigan SO, Pink DB, Stadnyk AW. Neutrophil transepithelial migration in response to the chemoattractant fMLP but not C5a is phospholipase D-dependent and related to the use of CD11b/CD18. Journal of leukocyte biology. 2007;82(6):1575-84.
174. Palumbo R, De Marchis F, Pusterla T, Conti A, Alessio M, Bianchi ME. Src family kinases are necessary for cell migration induced by extracellular HMGB1. Journal of leukocyte biology. 2009;86(3):617-23.
175. Filaferro M, Novi C, Ruggieri V, Genedani S, Alboni S, Malagoli D, et al. Neuropeptide S stimulates human monocyte chemotaxis via NPS receptor activation. Peptides. 2013;39:16-20.
176. Hauck CR, Sieg DJ, Hsia DA, Loftus JC, Gaarde WA, Monia BP, et al. Inhibition of focal adhesion kinase expression or activity disrupts epidermal growth factor-stimulated signaling promoting the migration of invasive human carcinoma cells. Cancer Res. 2001;61(19):7079-90.
177. Ciccimaro E, Hanks SK, Blair IA. Quantification of Focal Adhesion Kinase Activation Loop Phosphorylation as a Biomarker of Src Activity. Mol Pharmacol. 2009;75(3):658-66.
178. Anderson DD, Chubinskaya S, Guilak F, Martin JA, Oegema TR, Olson SA, et al. Post-traumatic osteoarthritis: improved understanding and opportunities for early intervention. Journal of orthopaedic research : official publication of the Orthopaedic Research Society. 2011;29(6):802-9.
179. Ramakrishnan P, Hecht BA, Pedersen DR, Lavery MR, Maynard J, Buckwalter JA, et al. Oxidant conditioning protects cartilage from mechanically induced damage. Journal of orthopaedic research : official publication of the Orthopaedic Research Society. 2010;28(7):914-20.
180. Mofrad MR, Golji J, Abdul Rahim NA, Kamm RD. Force-induced unfolding of the focal adhesion targeting domain and the influence of paxillin binding. Mechanics & chemistry of biosystems : MCB. 2004;1(4):253-65.
181. Hall JE, Fu W, Schaller MD. Focal Adhesion Kinase: Exploring Fak Structure to Gain Insight into Function. Int Rev Cel Mol Bio. 2011;288:185-225.
182. Parsons JT, Martin KH, Slack JK, Taylor JM, Weed SA. Focal adhesion kinase: a regulator of focal adhesion dynamics and cell movement. Oncogene. 2000;19(49):5606-13.
183. Seufferlein T, Rozengurt E. Sphingosine induces p125FAK and paxillin tyrosine phosphorylation, actin stress fiber formation, and focal contact assembly in Swiss 3T3 cells. The Journal of biological chemistry. 1994;269(44):27610-7.
184. Galbraith CG, Yamada KM, Sheetz MP. The relationship between force and focal complex development. Journal of Cell Biology. 2002;159(4):695-705.
185. Quinn TM, Allen RG, Schalet BJ, Perumbuli P, Hunziker EB. Matrix and cell injury due to sub-impact loading of adult bovine articular cartilage explants: effects of strain rate and peak stress. J Orthopaed Res. 2001;19(2):242-9.
186. Burgin LV, Aspden RM. A drop tower for controlled impact testing of biological tissues. Medical engineering & physics. 2007;29(4):525-30.
187. Hochwald SN, Nyberg C, Zheng M, Zheng D, Wood C, Massoll NA, et al. A novel small molecule inhibitor of FAK decreases growth of human pancreatic cancer. Cell cycle. 2009;8(15):2435-43.

188. Golubovskaya VM, Nyberg C, Zheng M, Kweh F, Magis A, Ostrov D, et al. A small molecule inhibitor, 1,2,4,5-benzenetetraamine tetrahydrochloride, targeting the y397 site of focal adhesion kinase decreases tumor growth. Journal of medicinal chemistry. 2008;51(23):7405-16.
189. Wu Z, Chang PC, Yang JC, Chu CY, Wang LY, Chen NT, et al. Autophagy Blockade Sensitizes Prostate Cancer Cells towards Src Family Kinase Inhibitors. Genes & cancer. 2010;1(1):40-9.
190. Dong M, Rice L, Lepler S, Pampo C, Siemann DW. Impact of the Src inhibitor saracatinib on the metastatic phenotype of a fibrosarcoma (KHT) tumor model. Anticancer research. 2010;30(11):4405-13.
191. Speed CA. Therapeutic ultrasound in soft tissue lesions. Rheumatology. 2001;40(12):1331-6.
192. Church CC. Frequency, pulse length, and the mechanical index. Acoust Res Lett Onl. 2005;6(3):162-8.
193. Blomley MJ, Cooke JC, Unger EC, Monaghan MJ, Cosgrove DO. Microbubble contrast agents: a new era in ultrasound. Bmj. 2001;322(7296):1222-5.
194. Miwa H, Numata K, Tanabe T, Koh R, Kaneko T, Sugimori K, et al. Differential Diagnosis of Solid Pancreatic Lesions by Using Three-Dimensional Contrast Enhanced Ultrasonography With High Mechanical Index Mode. Gastroenterology. 2012;142(5):S617-S.
195. Kobayashi N, Yasu T, Yamada S, Kudo N, Kuroki M, Kawakami M, et al. Endothelial cell injury in venule and capillary induced by contrast ultrasonography. Ultrasound Med Biol. 2002;28(7):949-56.
196. Kobayashi N, Yasu T, Yamada S, Kudo N, Kuroki M, Miyatake K, et al. Influence of contrast ultrasonography with perflutren lipid microspheres on microvessel injury. Circulation journal : official journal of the Japanese Circulation Society. 2003;67(7):630-6.
197. Hassan MA, Feril LB, Jr., Suzuki K, Kudo N, Tachibana K, Kondo T. Evaluation and comparison of three novel microbubbles: enhancement of ultrasound-induced cell death and free radicals production. Ultrasonics sonochemistry. 2009;16(3):372-8.
198. Altay M, Bayrakci K, Yildiz Y, Erekul S, Saglik Y. Secondary chondrosarcoma in cartilage bone tumors: report of 32 patients. Journal of orthopaedic science : official journal of the Japanese Orthopaedic Association. 2007;12(5):415-23.
199. Gelderblom H, Hogendoorn PC, Dijkstra SD, van Rijswijk CS, Krol AD, Taminiau AH, et al. The clinical approach towards chondrosarcoma. The oncologist. 2008;13(3):320-9.
200. Buckwalter JA. The structure of human chondrosarcoma proteoglycans. J Bone Joint Surg Am. 1983;65(7):958-74.
201. Gitelis S, Bertoni F, Picci P, Campanacci M. Chondrosarcoma of bone. The experience at the Istituto Ortopedico Rizzoli. J Bone Joint Surg Am. 1981;63(8):1248-57.
202. Marco RA, Gitelis S, Brebach GT, Healey JH. Cartilage tumors: evaluation and treatment. The Journal of the American Academy of Orthopaedic Surgeons. 2000;8(5):292-304.
203. Martin JA, Forest E, Block JA, Klingelhutz AJ, Whited B, Gitelis S, et al. Malignant transformation in human chondrosarcoma cells supported by telomerase activation and tumor suppressor inactivation. Cell growth & differentiation : the molecular biology journal of the American Association for Cancer Research. 2002;13(9):397-407.
204. Pritchard DJ, Lunke RJ, Taylor WF, Dahlin DC, Medley BE. Chondrosarcoma: a clinicopathologic and statistical analysis. Cancer. 1980;45(1):149-57.

205. Bauer HC, Brosjo O, Kreicbergs A, Lindholm J. Low risk of recurrence of enchondroma and low-grade chondrosarcoma in extremities. 80 patients followed for 2-25 years. Acta orthopaedica Scandinavica. 1995;66(3):283-8.
206. Terek RM, Schwartz GK, Devaney K, Glantz L, Mak S, Healey JH, et al. Chemotherapy and P-glycoprotein expression in chondrosarcoma. Journal of orthopaedic research : official publication of the Orthopaedic Research Society. 1998;16(5):585-90.
207. Buckwalter JA. Osteoarthritis and articular cartilage use, disuse, and abuse: experimental studies. The Journal of rheumatology Supplement. 1995;43:13-5.
208. Lichtenstein L, Jaffe HL. Chondrosarcoma of Bone. The American journal of pathology. 1943;19(4):553-89.
209. O'Neal LW, Ackerman LV. Chondrosarcoma of bone. Cancer. 1952;5(3):551-77.
210. Rosenberg L. Chemical basis for the histological use of safranin O in the study of articular cartilage. J Bone Joint Surg Am. 1971;53(1):69-82.
211. Joshi VB, Geary SM, Salem AK. Biodegradable Particles as Vaccine Delivery Systems: Size Matters. Aaps J. 2013;15(1):85-94.
212. Mayer CR, Geis NA, Katus HA, Bekeredjian R. Ultrasound targeted microbubble destruction for drug and gene delivery. Expert opinion on drug delivery. 2008;5(10):1121-38.
213. Kodama T, Tomita Y, Koshiyama K, Blomley MJ. Transfection effect of microbubbles on cells in superposed ultrasound waves and behavior of cavitation bubble. Ultrasound Med Biol. 2006;32(6):905-14.
214. Qin P, Xu L, Zhong W, Yu AC. Ultrasound-microbubble mediated cavitation of plant cells: effects on morphology and viability. Ultrasound in medicine & biology. 2012;38(6):1085-96.
215. Lejbkowicz F, Salzberg S. Distinct sensitivity of normal and malignant cells to ultrasound in vitro. Environmental health perspectives. 1997;105 Suppl 6:1575-8.
216. Beecher BR, Martin JA, Pedersen DR, Heiner AD, Buckwalter JA. Antioxidants block cyclic loading induced chondrocyte death. The Iowa orthopaedic journal. 2007;27:1-8.
217. Kurz B, Lemke A, Kehn M, Domm C, Patwari P, Frank EH, et al. Influence of tissue maturation and antioxidants on the apoptotic response of articular cartilage after injurious compression. Arthritis and rheumatism. 2004;50(1):123-30.
218. Aggarwal A, Misro MM, Maheshwari A, Sehgal N, Nandan D. N-acetylcysteine counteracts oxidative stress and prevents hCG-induced apoptosis in rat Leydig cells through down regulation of caspase-8 and JNK. Molecular reproduction and development. 2010;77(10):900-9.
219. Erkkila K, Hirvonen V, Wuokko E, Parvinen M, Dunkel L. N-acetyl-L-cysteine inhibits apoptosis in human male germ cells in vitro. The Journal of clinical endocrinology and metabolism. 1998;83(7):2523-31.
220. Wippel C, Fortsch C, Hupp S, Maier E, Benz R, Ma J, et al. Extracellular calcium reduction strongly increases the lytic capacity of pneumolysin from streptococcus pneumoniae in brain tissue. The Journal of infectious diseases. 2011;204(6):930-6.
221. Terek RM. Angiogenesis in chondrosarcoma. Current Opinion in Orthopaedics. 2002;13(6):449-53.
222. Ryzewicz M, Manaster BJ, Naar E, Lindeque B. Low-grade cartilage tumors: Diagnosis and treatment. Orthopedics. 2007;30(1):35-46.
223. McGough RL, Lin C, Meitner P, Aswad BI, Terek RM. Angiogenic cytokines in cartilage tumors. Clinical orthopaedics and related research. 2002(397):62-9.